Electronic Supplementary Information for

Construction of Isostructural Hydrogen-bonded Organic Frameworks: Limitations and Possibilities of Pore Expansion

Yuto Suzuki,[a] Mario Gutiérrez,[b] Senri Tanaka,[c] Eduardo Gomez,[b] Norimitsu Tohnai,[d] Nobuhiro Yasuda,[e] Nobuyuki Matubayasi,[c]* Abderrazzak Douhal,[b]* Ichiro Hisaki[a]*

[a] Division of Chemistry, Graduate School of Engineering Science, Osaka University, 1-3 Machikaneyama, Toyonaka, Osaka 560-8531, Japan.

[b] Departamento de Química Física, Facultad de Ciencias Ambientales y Bioquímica, INAMOL, Universidad de Castilla-La Mancha, Avenida Carlos III, S/N, 45071 Toledo, Spain.

[c] Division of Chemical Engineering, Graduate School of Engineering Science, Osaka University, 1-3 Machikaneyama, Toyonaka, Osaka 560-8531, Japan.

[d] Division of Applied Chemistry, Graduate School of Engineering, Osaka University, 2-1 Yamadaoka, Suita, Osaka 565-7891, Japan.

[e] JASRI, 1-1-1 Kouto, Sayo-cho, Sayo-gun, Hyogo 679-5198, Japan.

Table of contents

1. General

All reagents and solvents were used as received from commercial suppliers. ^{1}H and ^{13}C NMR spectra were measured on a JEOL 400 YH (400 MHz) spectrometer or Bruker AV400M (400 MHz) spectrometer. Residual proton and carbon of deuterated solvents were used as internal standards for the measurements: δ = 7.26 ppm ($CDCl_3$), δ = 2.50 ppm (DMSO-d_6), δ = 5.50 ppm (NMP-d_9) for ^{1}H NMR, δ = 77.00 ppm ($CDCl_3$), δ = 39.50 ppm (DMSO-d_6) for ^{13}C NMR. HR-MS analyses were conducted on a JEOL JMS-700 instrument or autoflex III Bruker. Thermo gravimetric (TG) analyses were performed on Rigaku TG8120 under an N_2 purge (100 mL/min) at a heating rate of 5 K min^{-1}.

Powder X-ray diffraction (PXRD) data were collected on a Rigaku Ultima-IV (40 kV, 44 mA) using Cu-Kα1 radiation (λ = 1.54056 Å) at room temperature and with a scan rate of 2.0° min^{-1}. Variable temperature PXRD (VT-PXRD) data were collected on same apparatus as PXRD with a temperature control unit. For VT-PXRD, the HOF powders were placed on an aluminum substrate, and the measurements were conducted in atmospheric conditions. The temperature of the sample was increased from room temperature to 360 °C with a rate of 0.5°min^{-1} or 1.0°min^{-1}. PXRD scan of each measurements were collected with a difference in the temperature of ca. 5.1 °C [**TolHAT-1(TMB)**, **TolHAT-1aIV**, and **ThiaHAT-1a**] or ca. 2.6 °C [**ThiaHAT-1**].

Single crystal X-ray measurement and analysis. Diffraction data of **TolHAT-1** and **ThiaHAT-1** were collected at Spring-8 (BL40XU) with synchrotron radiation (λ = 0.81106 Å), and **BPTp-1** was collected with a two-dimensional X-ray detector (PILATUS 200K/R) equipped on a Rigaku XtaLAB P200 diffractometer by using Cu-Kα radiation monochromated with multilayer mirror (λ=1.54187 Å). Diffraction Data collection, cell refinement, and data reduction were carried out with CrysAlis PRO.[S1] SHELXT[S2] was used for the structure solution of the crystals. These calculations were performed with the observed reflections [$I > 2\sigma(I)$] with the program CrystalStructure crystallographic software or OLEX-2 crystallographic software.[S3] Structural refinement was performed by SHELXL.[S4] All non-hydrogen atoms were refined with anisotropic displacement parameters, and hydrogen atoms were placed in idealized positions and refined as rigid atoms with the relative isotropic displacement parameters. SQUEEZE function equipped in the PLATON program was used to treat severely disordered solvent molecules in voids. [S5]

Gas sorption. The activated bulk samples of **TPHAT-a**, **TolHAT-1a*N*** (*N*=I–IV), and **ThiaHAT-1a** were used for gas sorption measurements, which were performed on BELSORP-max (BEL, Japan). The adsorption isotherms of N_2, CO_2, O_2, and H_2 were corrected at 77K, 195 K, 77 K and 77 K, respectively. Brunauer–Emmett–Teller (BET) specific surface area: $S_{A(BET)}$ and non–local density functional (NLDFT) pore diameters were based on N_2 absorption isotherms.

2. Synthesis of building block molecules

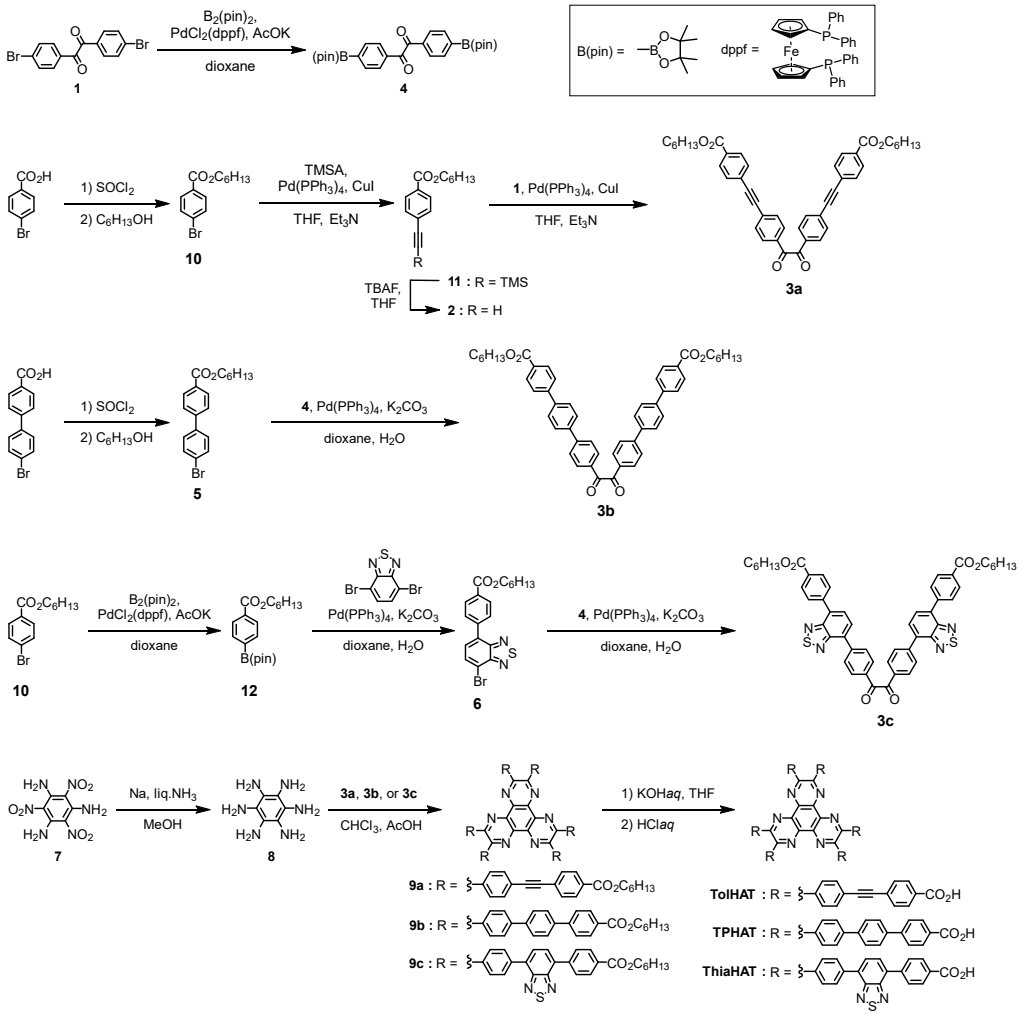

Scheme S1. Synthesis of HAT derivatives **TPHAT**, **TolHAT**, and **ThiaHAT**.

2-1. HAT derivatives

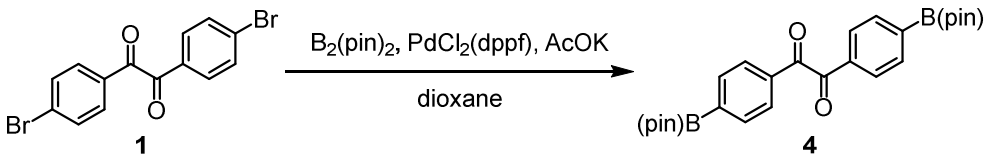

Synthesis of 4. Compound **4** was synthesized according to the literature procedure.[S6] A 200 mL three-necked flask was charged with 4,4'-dibromobenzene (**1**) (2.04 g, 5.43 mmol), bis(pinacolato)diboron (4.14 g, 16.3 mmol, 3 eq.), AcOK (4.30 g, 43.8 mmol, 8 eq.), and $PdCl_2$(dppf) (0.200 g, 0.0273 mmol, 0.05 eq.) under nitrogen. Then degassed dioxane (50 mL)

were added and the reaction mixture was stirred at 80 °C for 17 h. After cooling to room temperature, the product was extracted with CH_2Cl_2. The organic phase was combined and washed with water and brine, dried with anhydrous $MgSO_4$, and filtered. The crude product was purified with column chromatography (silica gel, MeOH in CH_2Cl_2 0% to 5%) to give **4** (2.09 g, 4.53 mmol, 70%) as a pale yellow solid.

^{1}H NMR (400 MHz, $CDCl_3$): δ 7.93 (s, 8H), 1.35 (s, 24H) ppm.

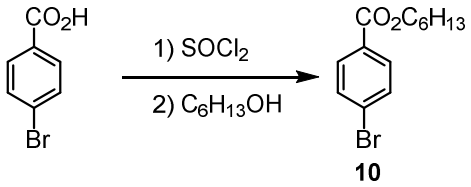

10

Synthesis of 10. A 300 mL three-necked flask was charged with 4-bromobenzoic acid (12.1 g, 60.0 mmol) in dehydrated CH_2Cl_2 (100 mL) under nitrogen. Then $SOCl_2$ (10.0 mL, 60.0 mmol) were added dropwise at 0 °C and dehydrated DMF (0.5 mL) at r.t. The mixture was refluxed for 4 h. After cooling to room temperature, solvent was removed by vacuum and dissolved dehydrated CH_2Cl_2. Then dehydrated *n*-hexanol (11.0 mL) and pyridine (5.0 mL) was added and stirred at r.t. for 18 h. The product was extracted with CH_2Cl_2, washed with water and brine, dried with anhydrous $MgSO_4$, and filtered. The crude product was purified with column chromatography (silica gel, $CHCl_3$/hexane = 1/7 to 1/1) and passed through charcoal to give **10** (16.4 g, 57.8 mmol, 96%) as a pale-yellow oil.

^{1}H NMR (400 MHz, $CDCl_3$): δ 7.89 (d, 2H, J = 8.4 Hz), 7.57 (d, 2H, J = 8.0 Hz), 4.30 (t, 2H, J = 6.4 Hz), 1.70–1.80 (m, 2H), 1.27–1.50 (m, 6H), 0.898 (t, 3H, J = 7.2 Hz) ppm. ^{13}C NMR (100 MHz, $CDCl_3$): δ 165.9, 131.6, 131.0, 129.4, 127.8, 65.4, 31.4, 28.6, 25.6, 22.5, 14.0 ppm. HR-MS (EI^+): calcd. For $C_{13}H_{17}BrO_2$ $[M]^+$ 284.0412; found: 284.0410.

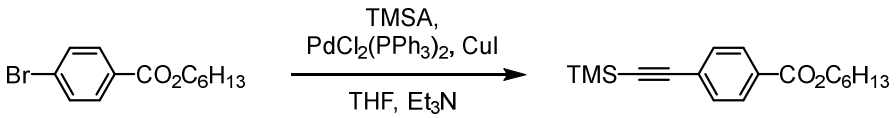

10 **11**

Synthesis of 11. A 100 mL three-necked flask was charged with compound **10** (4.00 g, 14.0 mmol), $PdCl_2(PPh_3)_2$ (0.490 g, 0.700 mmol), CuI (0.266 g, 1.40 mmol) in degassed THF (30 mL) under nitrogen. Then degassed Et_3N (10 mL) and TMSA (4.20 mL, 29.7 mmol) were added and the reaction mixture was heated at 40 °C for 5 h. After cooling to r.t., the solvent was removed under

vacuum. The product was purified with column chromatography (silica gel, CH_2Cl_2/hexane = 1/5) to give **3** (3.53 g, 11.7 mmol, 83%) as a pale yellow oil.

^{1}H NMR (400 MHz, $CDCl_3$): δ 7.97 (d, 2H, *J* = 8.8 Hz), 7.51 (d, 2H, *J* = 8.4 Hz), 4.30 (t, 2H, *J* = 7.2 Hz), 1.70–1.80 (m, 2H), 1.25–1.52 (m, 6H), 0.901 (s, 3H), 0.261 (s, 9H) ppm. ^{13}C NMR (100 MHz, $CDCl_3$): δ 166.1, 131.8, 130.1, 129.3, 127.6, 104.1, 97.5, 65.3, 31.4, 28.6, 25.7, 22.5, 14.0, -0.17 ppm. HR-MS (FAB): calcd. For $C_{18}H_{27}O_2Si$ $[M+H]^+$ 303.1780; found: 303.1779

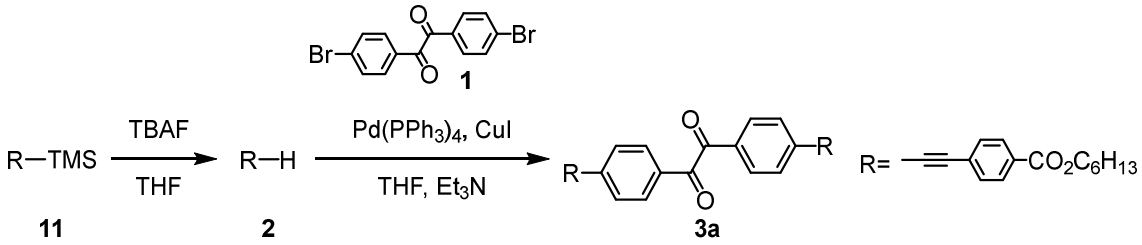

Synthesis of 3a. A 100 mL three-necked flask was charged with compound **11** (4.00 g, 14.0 mmol) in degassed THF (5 mL) under nitrogen. Then 1M tetrabutylammonium fluoride THF solution (5.5 mL, 5.5 mmol) was added dropwise at 0 °C and the reaction mixture was stirred for 15 min. After removing solvent under vacuum, the product was extracted with CH_2Cl_2. The organic phase was combined and washed with water and brine, dried with anhydrous $MgSO_4$, and filtered, to give **2** as a brown solid (1.30 g), which was immediately used in the following reaction without further purification.

A 100 mL three-necked flask was charged with above-synthesized **2** (1.30 g), 4,4'-dibromobenzil (**1**) (0.456 g, 1.24 mmol), $Pd(PPh_3)_4$ (0.106 g, 0.0924 mmol), CuI (0.0180 g, 0.0945 mmol) in degassed THF (30 mL) and degassed Et_3N (5 mL) under nitrogen. Then the reaction mixture was heated at 30 °C for 14h. After cooling to r.t., the solvent was removed under vacuum. The product was thoroughly washed with acetone to give **3a** as a pale blown solid (0.410 g, 0.615 mmol, 25% from **11** in 2 steps).

m.p. 178.5 °C. ^{1}H NMR (400 MHz, $CDCl_3$): δ 8.05 (d, 2H, *J* = 8.8 Hz), 7.99 (d, 2H, *J* = 8.4 Hz), 7.68 (d, 4H, *J* = 8.8 Hz), 7.61 (d, 4H, *J* = 8.4 Hz), 4.33 (t, 4H, *J* = 6.8 Hz), 1.73–1.83 (m, 4H), 1.27–1.50 (m, 12H), 0.909 (t, 6H, *J* = 7.2 Hz) ppm. ^{13}C NMR (100 MHz, $CDCl_3$): δ 193.0, 166.0, 132.23, 132.21, 131.72, 130.6, 129.9, 129.60, 129.57, 126.8, 93.2, 90.9, 65.5, 31.4, 28.6, 25.7, 22.5, 14.0 ppm. HR-MS (FAB): calcd. For $C_{44}H_{43}O_6$ [M+H] 667.3060; found: 677.3073.

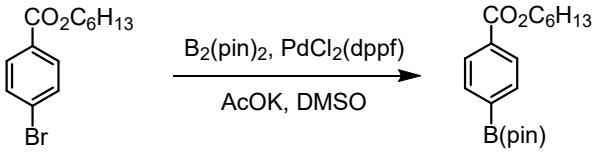

10 **12**

Synthesis of 12. A 100 mL three-necked flask was charged with **10** (6.09 g, 21.4 mmol), $(Bpin)_2$ (5.67 g, 22.5 mmol), AcOK (5.89 g, 60.0 mmol), and $PdCl_2(dppf)$ (0.521 g, 0.641 mmol) under nitrogen. Then degassed DMSO (20 mL) were added and vacuumed at r.t. for 15 min. The reaction mixture was stirred at 80 °C for 17 h. After cooled to r.t., the reaction mixture was poured into water. The precipitate was extracted with AcOEt. The organic phase were combined and washed with water, dried with anhydrous $MgSO_4$, and filtered. The crude product was purified with column chromatography (silica gel, AcOEt/hexane = 1/7) to give **12** (5.58 g, 16.8 mmol, 79%) as a pale yellow oil.

^{1}H NMR (400 MHz, $CDCl_3$): δ 8.02 (d, 2H, J = 8.0 Hz), 7.86 (d, 2H, J = 8.0 Hz), 4.32 (t, 2H, J = 6.6 Hz), 1.72–1.82 (m, 2H), 1.30–1.52 (m, 18H), 0.900 (t, 3H, J = 5.6 Hz) ppm. ^{13}C NMR (100 MHz, $CDCl_3$): δ 166.7, 134.6, 132.7, 130.1, 131.7, 128.5, 127.2, 84.13, 65.20, 31.44, 28.66, 25.68, 24.68, 22.52, 13.96 ppm. HR-MS (EI^+): calcd. For $C_{19}H_{29}O_4B$ $[M]^+$ 332.2159; found: 332.2153

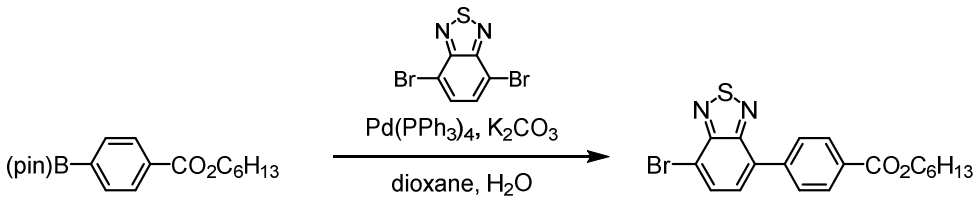

12 **6**

Synthesis of 6. A 200 mL three-necked flask was charged with 4,7-dibromo-2,1,3-thiadiazol (8.24 g, 28.0 mmol), **12** (4.66 g, 14.0 mmol), K_2CO_3 (3.80 g, 28.1 mmol) in degassed dioxane (45 mL) under nitrogen and heated at 80 °C. Then $Pd(PPh_3)_4$ (0.880 g, 0.762 mmol) was added and stirred for 8 h. To promote the reaction, degassed water (10 mL) and $Pd(PPh_3)_4$ (0.220 g, 0.190 mmol) were added and the reaction mixture was stirred at 80 °C for 80 h and at 110 °C for 8 h. After solvent was removed under vacuum, the remained solid was rinsed with $CHCl_3$ three times. Then the product was purified with column chromatography (silica gel, $CHCl_3$/hexane = 1/1 to 1/2) to give **6** (3.99 g, 9.51 mmol, 68%) as a pale yellow solid.

M.p. 68.1 °C. ^{1}H NMR (400 MHz, $CDCl_3$): δ 8.20 (d, 2H, J = 8.0 Hz), 7.92–8.00 (m, 3H), 7.57–7.69 (m, 1H), 4.36 (t, 2H, J = 6.8 Hz), 1.74–1.84 (m, 2H), 1.30–1.52 (m, 6H), 0.916 (t, 3H, J = 6.8 Hz) ppm. ^{13}C NMR (100 MHz, $CDCl_3$): δ 166.3, 153.9, 152.9, 140.8, 132.9, 132.2, 130.5, 130.0, 129.1, 129.7, 114.2, 65.3, 31.5, 28.7, 25.7, 22.6, 14.0 ppm. HR-MS (FAB+): calcd. For

$C_{19}H_{20}N_2O_2SBr$ $[M+H]^+$ 419.0429; found: 419.0423.

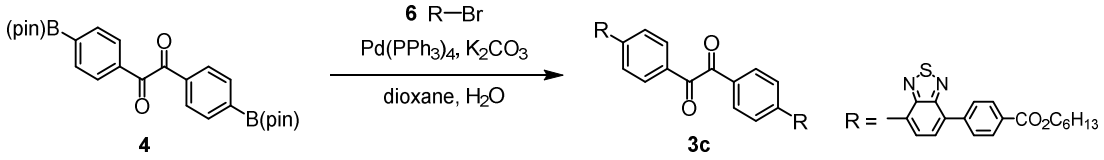

Synthesis of 3c. A 200 mL three-necked flask was charged with **4** (1.62 g, 3.50 mmol), **6** (3.00 g, 7.15 mmol), K_2CO_3 (2.03 g, 15.0 mmol), and $Pd(PPh_3)_4$ (0.406 g, 0.398 mmol) in degassed dioxane (30 mL) and degassed water (5 mL) under nitrogen. Then the reaction mixture was refluxed for 17 h. After cooling to r.t., water (70 mL) was added and the precipitate was collected by filtration, rinsed with water (50 mL) and acetone (100 mL). The product was purified by careful washing with acetone and AcOEt to give **3c** (2.96 g, 3.33 mmol, 95%) as a green solid.
M.p. 226.1 °C. ^{1}H NMR (400 MHz, $CDCl_3$): δ 8.16–8.25 (m, 12H), 8.07 (d, 4H, J = 8.0 Hz), 7.88–7.93 (m, 4H), 4.37 (t, 4H J = 6.8 Hz), 1.76–1.86 (m, 4H), 1.30–1.52 (m, 12H), 0.923 (s, 6H) ppm. ^{13}C NMR (100 MHz, $CDCl_3$): δ 194.00, 166.37, 153.85, 153.70, 143.57, 141.27, 133.62, 132.53, 132.37, 130.49, 130.29, 129.88, 128.83, 128.41, 65.31, 31.48, 28.73, 25.73, 22.57, 14.03 ppm. HR-MS (FAB+): calcd. For $C_{52}H_{47}N_4O_6S_2$ $[M+H]^+$ 887.2937; found: 887.2926

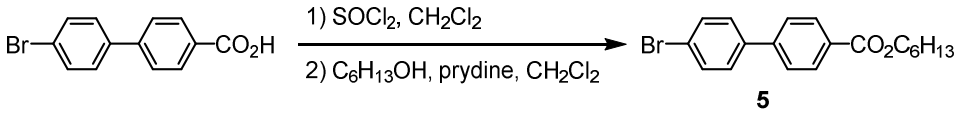

Synthesis of 5. A 200 mL three-necked flask was charged with 4'-bromo-4-biphenylcarboxylic acid (3.00 g, 10.8 mmol) in dehydrated CH_2Cl_2 (80 mL) under nitrogen. Then $SOCl_2$ (1.70 mL, 21.0 mmol) were added dropwise at 0 °C. The mixture was refluxed for 4 h. After cooling to r.t., solvent was removed under vacuum and dissolved dehydrated CH_2Cl_2. Then dehydrated *n*-hexanol (5.0 mL) and triethylamine (6.0 mL) were added and stirred at r.t. for 16 h. The organic phase was diluted with CH_2Cl_2 (40 mL) and washed with 1M HCl_{aq}, water and brine, dried with anhydrous $MgSO_4$, and filtered. The crude product was purified with column chromatography (silica gel, $CHCl_3$/hexane = 1/2 to 1/0) to give **5** (3.40 g, 9.41 mmol, 87%) as a white solid.
M.p. 47.0 °C. ^{1}H NMR (400 MHz, $CDCl_3$): δ 8.11 (d, 2H, J = 8.8 Hz) , 7.58–7.63 (m, 4H) , 4.34 (t, 2H, J = 6.8 Hz) , 1.75–1.82 (m, 2H) , 1.30–1.51 (m, 6H) , 0.92 (t, 3H, J = 7.2 Hz) ppm. ^{13}C NMR (100 MHz, $CDCl_3$): δ 166.4, 144.2, 139.0, 132.1, 130.2, 129.7, 128.8, 126.8, 122.5, 65.2, 31.5, 28.7, 25.7, 22.6, 14.0 ppm. HR-MS (FAB): calcd. For $C_{19}H_{21}O_2Br$ [M+H] 361.0803; found: 361.0805.

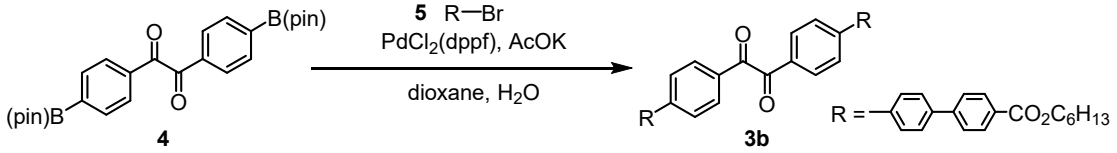

Synthesis of 3b. A 200 mL three-necked flask was charged with **4** (0.948 g, 2.05 mmol), **5** (1.48 mg,4.10 mmol), K_2CO_3 (1.35 g, 10.0 mmol), and $Pd(PPh_3)_4$ (0.474 g, 0.410 mmol) in degassed dioxane (30 mL) and degassed water (5 mL) under nitrogen. Then the reaction mixture was refluxed for 17 h. After cooling to r.t., water (30 mL) was added and the resultant precipitate was collected by filtration, rinsed with water and acetone. The product was purified by washing acetone and AcOEt to give **3a** (1.24 g, 1.58 mmol, 77%) as a gray solid.

M.p. 238.1 °C. ^{1}H NMR (400 MHz, $CDCl_3$): δ 8.13 (m, 8H), 7.81 (d, 4H, J = 8.4 Hz), 7.75 (s, 8H), 4.34 (t, 2H, J = 6.8 Hz), 1.75–1.82 (m, 2H), 1.30–1.51 (m, 6H), 0.92 (t, 3H, J = 7.2 Hz) ppm. ^{13}C NMR (100 MHz, $CDCl_3$): δ 194.0, 166.6, 146.9, 144.6, 140.4, 139.3, 132.0, 130.7, 128.02, 128.00, 127.7, 127.0, 65.3, 31.6, 28.8, 25.8, 22.7, 14.1 ppm. HR-MS (FAB): calcd. For $C_{52}H_{50}O_6$ [M+H] 770.3613; found: 770.3616.

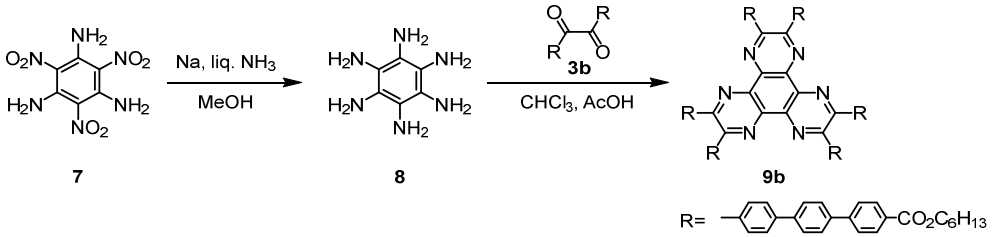

Synthesis of 9b. A 100 mL three-neck flask equipped with magnetic stirrer, gas inlet, and gas condenser was charged with **7** (100 mg, 0.387 mmol) and dehydrated methanol (7 mL) and was steeped in a cool bath. Approximately 10 mL of ammonia was condensed into the flask. To a reaction mixture with stirring was added sodium (160 mg, 6.63 mmol) in small pieces to keep mild reflux of ammonia. After reflux for 30 min, the condenser and bath was removed to allow ammonia evaporating and dehydrated methanol was added to the reaction mixture. The precipitate was collected by filtration, washed with degassed ethanol and degassed diethyl ether to yield **8** (ca. 45.0 mg) as an off-white solid, which was immediately used in the following reaction without further purification.

To a mixture of **3b** (604 mg, 0.783 mmol) in degassed $CHCl_3$ (30 mL) and AcOH (5 mL) heated at 60 °C was added a suspension of the above-synthesized **8** in $CHCl_3$ and stirred for 8 h at 60 °C. After the reaction solvent was removed in vacuo, the product was purified by column chromatography (silica gel, MeOH in $CHCl_3$ = 0% to 1%) to yield **9b** (113 mg, 0.0477 mmol,

11% from **7** in two steps) as brown solid.

M.p. 251.2 °C. ^{1}H NMR (400 MHz, $CDCl_3$): δ 8.13 (d, 12H, J = 8.0 Hz), 8.04 (d, 12H, J = 8.4 Hz), 7.67–7.82 (m, 48H), 4.35 (t, 12H, J = 6.4 Hz), 1.75–1.85 (m, 12H), 1.30–1.54 (m, 36H), 0.92 (t, 18H, J = 7.2 Hz) ppm. ^{13}C NMR (100 MHz, $CDCl_3$): δ 166.5, 153.5, 144.7, 141.4, 140.0, 139.6, 139.4, 137.8, 131.0, 130.1, 129.5, 127.7, 127.6, 127.1, 126.9, 65.2, 31.5, 28.7, 22.6, 14.0 ppm. HR-MS (MALDI): calcd. For $C_{162}H_{151}N_6O_{12}$ $[M+H]^+$ 2372.1285; found: 2372.1364.

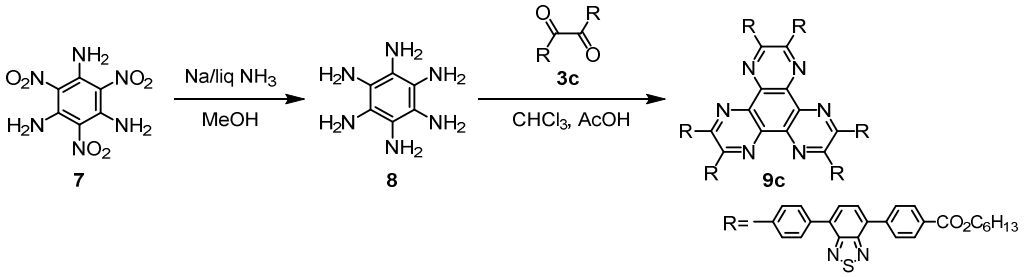

Synthesis of 9c. A 100 mL three-neck flask equipped with magnetic stirrer, gas inlet, and gas condenser was charged with **7** (300 mg, 1.16 mmol) and dehydrated methanol (10 mL), and was steeped in a cool bath. Approximately 10 mL of ammonia was condensed into the flask. To a reaction mixture with stirring was added sodium (480 mg, 20.9 mmol) in small pieces to keep mild reflux of ammonia. After reflux for 30 min, the condenser and bath were removed to allow ammonia evaporating and dehydrated methanol was added to the reaction mixture. The precipitate was collected by filtration, washed with degassed ethanol and degassed diethyl ether to yield **8** (ca. 196 mg) as an off-white solid, which was immediately used in the following reaction without further purification.

To a mixture of **3c** (2.66 g, 3.00 mmol) in degassed $CHCl_3$ (50 mL) and AcOH (10 mL) heated at 70 °C was added a suspension of the above-synthesized **8** in $CHCl_3$ and stirred for 19 h at 70 °C. After the reaction solvent was removed in vacuo, the product was purified by column chromatography (silica gel, AcOEt/$CHCl_3$ = 1/25) and preparative HPLC to give **9c** (113 mg, 0.0477 mmol, 43% from **7** in 2 steps) as green solid.

M.p. 290.0 °C. ^{1}H NMR (400 MHz, $CDCl_3$): δ 8.13–8.29 (m, 36H), 8.05 (d, 12H, J = 8.0 Hz), 7.92 (d, 6H, J = 7.6 Hz), 7.85 (d, 6H, J = 8.0 Hz), 4.37 (t, 12H, J = 6.8 Hz), 1.74–1.86 (m, 12H), 1.30–1.52 (m, 36 H), 0.922 (s, 18H) ppm. ^{13}C NMR (100 MHz, $CDCl_3$): δ 166.4, 154.0, 153.9, 153.6, 133.2, 132.6, 13.8, 129.8, 129.5, 129.2, 128.5, 128.2, 65.3, 34.5, 28.7, 25.7, 22.6, 14.0 ppm. HR-MS (MALDI): calcd. For $C_{162}H_{139}N_{18}O_{12}S_6$ [M+H] 2719.9139; found: 2719.9183.

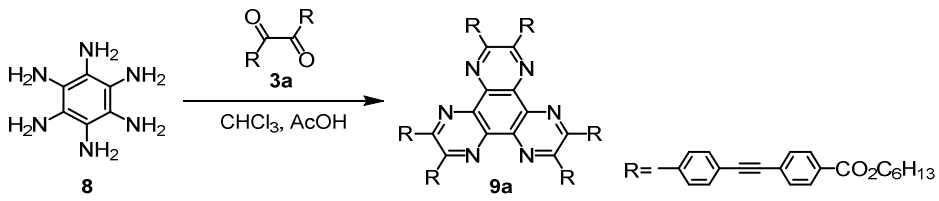

Synthesis of 9a. To a mixture of **3a** (620 mg, 930 μmol) in degassed $CHCl_3$ (13 mL) and AcOH (3 mL) heated at 70 °C was added a suspension of freshly-synthesized **8** (50 mg, 297 μmol) in $CHCl_3$ and stirred for 24 h at 70 °C. After the reaction solvent was removed in vacuo, the residual solid was extracted with $CHCl_3$. The organic phase was combined and washed with *sat.* $NAHCO_{3aq}$, water and brine, dried with anhydrous $MgSO_4$, and filtered. The product was purified by column chromatography (silica gel, $CHCl_3$) and preparative HPLC to yield **9a** (164 mg, 79.7 μmol, 27%) as green solid.

M.p. 240.0 °C. ^{1}H NMR (400 MHz, $CDCl_3$): δ 8.05 (d, 2H, J = 8.8 Hz), 7.99 (d, 2H, J = 8.4 Hz), 7.68 (d, 2H, J = 8.8 Hz), 7.61 (d, 2H, J = 8.4 Hz), 4.33 (t, 2H, J = 6.8 Hz), 1.73–1.83 (m, 2H), 1.27–1.50 (m, 6H), 0.909 (t, 2H, J = 7.2 Hz) ppm. ^{13}C NMR (100 MHz, $CDCl_3$): δ 193.0, 166.0, 132.32, 132.30, 131.7, 130.6, 129.9, 129.60, 129.57, 126.8, 93.2, 90.9, 65.5, 31.4, 28.6, 25.7, 22.5, 14.0 ppm. HR-MS (MALDI): calcd. For $C_{138}H_{126}O_{12}N_6$ $[M]^+$ 2058.9428; found: 2058.9457.

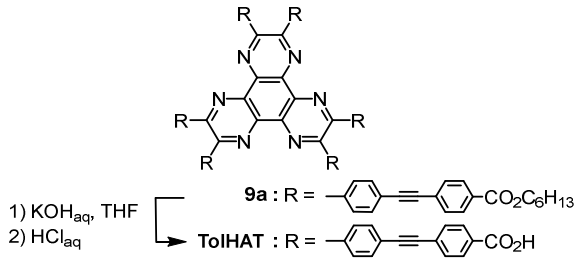

Synthesis of TolHAT. A reaction mixture of **9a** (659 mg, 397 μmol) in THF (20 mL) and 5%-KOH aqueous solution (20 mL) was stirred for 48 h at 60 °C. After cooled to r.t., organic phase was removed in vacuo, following addition of 37%-HCl into the reaction mixture until precipitate was not formed anymore. The precipitate was collected by centrifugation, washed with water, and dried in vacuo to give **TolHAT** (532 mg, 379 μmol, 95%) as brown solid.

M.p. >300 °C. ^{1}H NMR (400 MHz, DMSO-d_6): δ 8.37 (d, 12H, J = 8.4 Hz), 8.16 (d, 12H, J = 8.0 Hz), 8.00–8.15 (m, 24H) ppm. ^{13}C NMR (100 MHz, DMSO-d_6): δ 166.3, 152.4, 139.3, 138.3, 131.3, 131.2, 130.7, 130.1, 129.3, 126.1, 122.7, 91.3, 90.1 ppm. HR-MS (MALDI): calcd. For $C_{126}H_{67}N_{18}O_{12}S_6$ $[M+H]^+$ 2215.3405; found: 2215.3416.

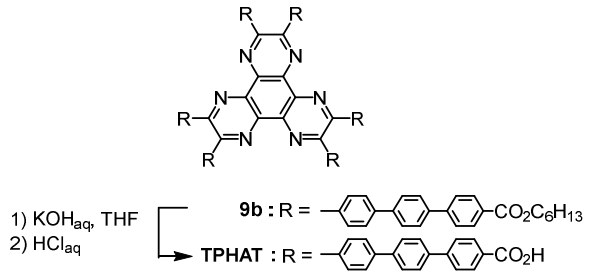

Synthesis of TPHAT. A reaction mixture of **9a** (62.5 mg, 26.7 μmol) in THF (30 mL) and 5%-KOH aqueous solution (20 mL) was stirred for 3 days at 60 °C. After cooled to room temperature, organic phase was removed in vacuo, following addition of 37%-HCl into the reaction mixture until precipitate was not formed anymore. The precipitate was collected by centrifugation, washed with water twice, and dried in vacuo. The obtained solid was washed with $CHCl_3$, to yield **TPHAT** (41.6 mg, 22.3 μmol 85%) as yellow solid.

M.p. >300 °C. ^{1}H NMR (400 MHz, DMSO-d_6): δ 8.30 (s), 7.70–8.10 (m) ppm. ^{13}C NMR spectrum was not obtained due to low solubility of **TPHAT**. HR-MS (MALDI) calc. for $C_{126}H_{77}N_6O_{12}$ [M-H]$^-$ 1865.5594 ; found 1865.5572.

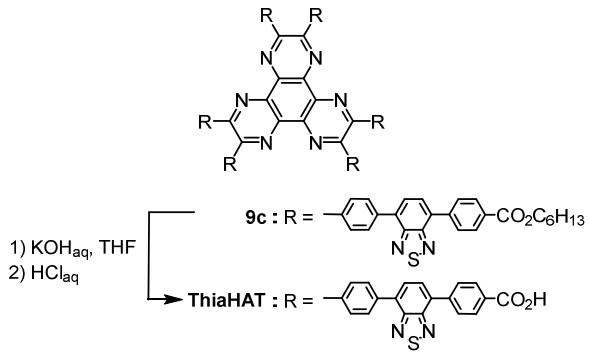

Synthesis of ThiaHAT. A reaction mixture of **9c** (81.8 mg, 30.0 μmol) in THF (30 mL) and 5%-KOH aqueous solution (35 mL) was stirred for 3 days at 60 °C. After cooled to r.t., organic phase was removed in vacuo. Then 6%-HCl was added into the aqueous phase until precipitate was not formed anymore and stirred for 1 h at r.t. The precipitate was collected by centrifugation, washed with water three times, acetone, and THF, and dried in vacuo to give **ThiaHAT** (65.5 mg, 29.6 μmol, 99%) as brown solid.

M.p. >300 °C. ^{1}H NMR (400 MHz, NMP-d_9): δ 8.30 (s), 7.70–8.10 (m) ppm. ^{13}C NMR spectrum was not obtained due to low solubility of **ThiaHAT**. HR-MS (MALDI): calcd. For $C_{126}H_{67}N_{18}O_{12}S_6$ $[M+H]^+$ 2215.3505; found: 2215.3461. Elemental analisys: calculated for $[M+3H_2O]$ C:66.60, H:3.20, N:11.10; found C:66.45, H:3.22, N: 10.72.

2-2. BPTp

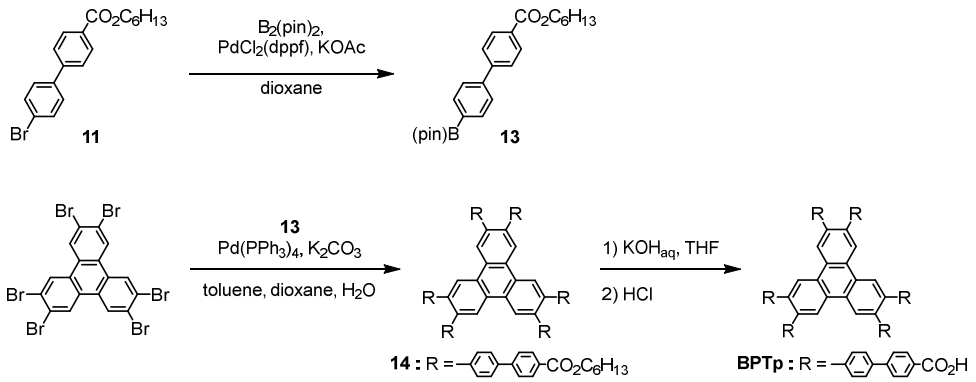

Scheme S2. Synthesis of triphenylene derivative **BPTp** with carboxybiphenyl groups.

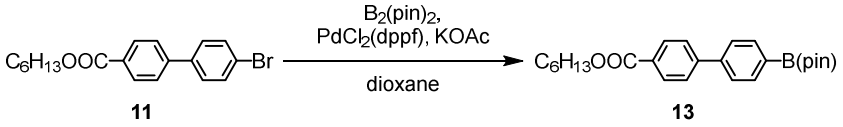

Synthesis of 13. A 100 mL three-necked flask was charged with **11** (2.02 g, 5.60 mmol), bis(pinacolato)diboron (1.56 g, 6.10 mmol), AcOK (1.90 g, 19.3 mmol), and $PdCl_2$(dppf) (0.130 g, 0.173 mmol) under nitrogen. Then degassed dioxane (15 mL) were added and the reaction mixture was stirred at 90 °C for overnight. After cooling to r.t., the product was extracted with AcOEt. The organic phase was combined and washed with water, dried with anhydrous $MgSO_4$, and filtered. The product was purified with column chromatography (silica gel, AcOEt/hexane = 1/6) to give crude **13** as a white solid (3.14 g) which was used in the following reaction without further purification.

^{1}H NMR (400 MHz, $CDCl_3$) : δ 8.13 (d, 2H, J = 8.4 Hz), 7.63–7.75 (m, 6H), 7.59 (d, 2H, J = 8.8 Hz), 7.51 (d, 2H, J = 8.4 Hz), 4.35 (t, 2H, J = 6.6 Hz), 1.74–1.84 (m, 2H), 1.30–1.52 (m, 6H), 0.915 (t, 2H, J = 7.6 Hz) ppm.

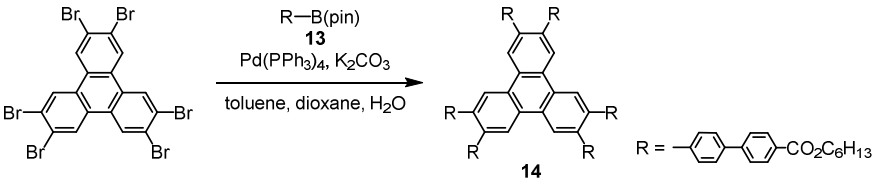

Synthesis of 14. A 100 mL three-necked flask was charged with 2,3,6,7,10,11-hexabromotriphenylene (236 mg, 0.336 mmol), the above-synthesized **13** (892 mg, ca. 2.2 mmol), K_2CO_3 (700 mg, 5.19 mmol), and $Pd(PPh_3)_4$ (130 mg, 1.11 mmol) in degassed toluene (10 mL), dioxane (15 mL) and water (5 mL)

under nitrogen. Then the reaction mixture was stirred at 100 °C for 36 h. After removing solvent in vacuo, the product was extracted with $CHCl_3$. The organic phase was combined and washed with water and brine, dried with anhydrous $MgSO_4$, and filtered. The product was purified with column chromatography (silica gel, CH_2Cl_2 in MeOH 0% to 1%) to give **14** (388 mg, 0.203 mmol, 60%) as a pale yellow solid.

M.p. >300 °C. ^{1}H NMR (400 MHz, $CDCl_3$): δ 8.11 (d, 2H, J = 8.8 Hz), 7.70 (d, 2H, J = 8.0 Hz), 7.63 (d, 2H, J = 7.2 Hz), 7.50 (d, 2H, J = 7.2 Hz), 4.34 (t, 2H, J = 6.8 Hz), 1.74–1.84 (m, 2H), 1.30–1.52 (m, 6H), 0.941 (t, 2H, J = 7.6 Hz) ppm. ^{13}C NMR (100 MHz, $CDCl_3$): δ 166.5, 144.8, 141.2, 139.5, 138.6, 130.1, 129.4, 127.1, 126.8, 125.8, 65.2, 31.5, 28.7, 22.6, 14.0 ppm. HR-MS (MALDI): calcd. For $C_{132}H_{132}O_{12}$ [M] 1908.9713; found: 1908.9688.

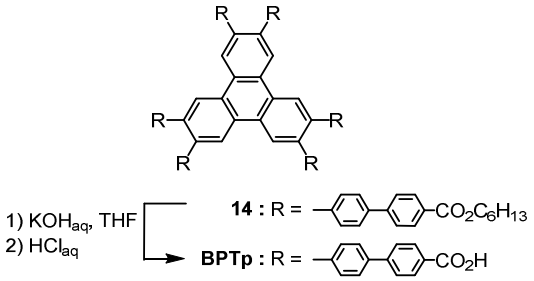

Synthesis of BPTp A reaction mixture of **14** (196 mg, 1.02 mmol) in THF (15 mL) and 5%-KOH aqueous solution (10 mL) was stirred for 3 days at 60 °C. After cooled to room temperature, organic phase was removed in vacuo, following addition of 37%-HCl into the reaction mixture until precipitate was not formed anymore. The precipitate was collected by centrifugation, washed with water, and dried in vacuo to give **BPTp** (131 mg, 0.932 μmol, 91%) as pale brown solid.

M.p. >300 °C. ^{1}H NMR (400 MHz, DMSO-d_6): δ 9.00 (br, 6H), 7.99 (d, 12H, J = 8.0 Hz), 7.82 (d, 12H, J = 8.0 Hz), 7.74 (d, 12H, J = 8.4 Hz), 7.55 (d, 12H, J = 8.4 Hz) ppm. ^{13}C NMR (100 MHz, DMSO-d_6): δ 167.11, 160.46, 152.93, 143.52, 140.75, 139.19, 137.12, 130.77, 129.96, 128.61, 126.62, 126.59 ppm. HR-MS (MALDI): calcd. For $C_{96}H_{59}O_{12}$ [M^+] 1403.4001; found: 1403.4025.

3. Crystallography

3-1 Crystal data

Table S1. Crystal data of **TolHAT-1**, **ThiaHAT-1**, and **BPTp-1**

	TolHAT-1	**ThiaHAT-1**	**BPTp-1**
System	*trigonal*	*trigonal*	*Monoclinic*
Space group	*R-3c*	*R-3c*	*I2/a*
Formula	$C_{102}H_{60}N_6O_{12}$	$C_{126}H_{66}N_{18}O_{12}S_6$	$C_{96}H_{66}O_{12}$•2($C_6H_3Cl_3$)
Fw	1555.584	1802.094	1774.35
a / Å	59.5294(11)	65.827(5)	9.3082(3)
b / Å	59.5294(11)	65.827(5)	53.6910(12)
c / Å	6.96369(19)	6.9879(7)	30.7096(6)
α / °	90	90	90
β / °	90	90	97.504(2)
γ / °	120	120	90
V / Å^3	21371.4(8)	26223(4)	15216.2(7)
Z	6	6	4
D / g cm^3	0.728	0.843	1.337
Crystal size / mm	0.05 × 0.008 × 0.008	0.1 × 0.02 × 0.02	0.1 × 0.1 × 0.1
Crystal color	yellow green	yellow	colorless
R1 (I > 2.0σ(I))	0.1267	0.1688	0.1349
*wR*2 (all)	0.3874	0.4127	0.3858
Completeness	1.00	0.999	0.997
GOF	1.265	1.386	1.377
λ / Å	0.42112 (synchrotron)	0.81106 (synchrotron)	1.54184
T / K	90	95	93
CCDC no.	2081132	2081131	2081133

3-2 Crystallography of TPHAT-P

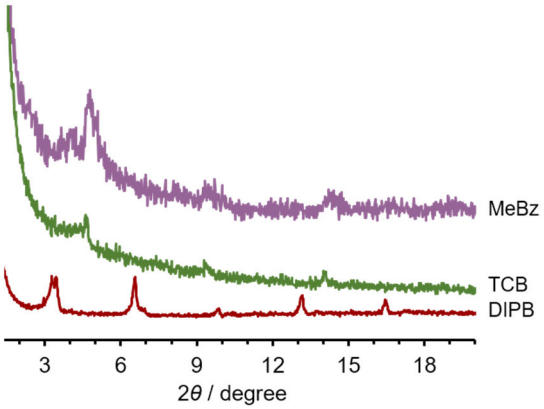

Fig. S1 PXRD patterns of **TPHAT-P** crystalized in a mixture of solvents, where DMA is the main solvent and MeBz (methyl benzoate) TCB (1,2,4-trichlorobenzene) and DIPB (1,3-diisopropylbenzene) act as a co-solvent, respectively.

3-3 Crystallography of BPTp

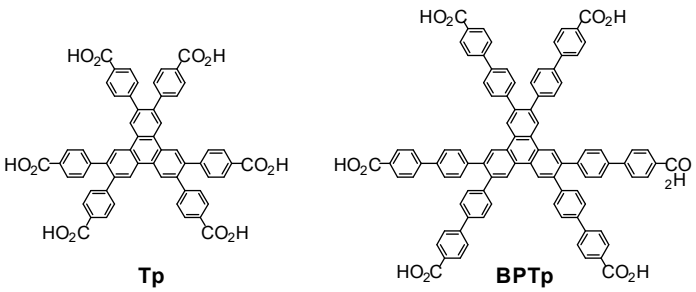

Chart S1. Chemical structures of triphenylene derivatives **Tp** and **BPTp**.

To construct HOFs, the synthesized **BPTp** was then crystallized by slow evaporation from a mixed solution of DMF and 1,2,4-trichlorobenzene (TCB) at 100 °C. A crystal structure of the obtained crytal **BPTp-1** is shown in Fig. S2. **BPTp** forms 2D assembling structure of hexagonal networks (HexNet) motifs through H-bonding. These adjacent HexNet stacked by two edge-to-face stackings (CH-π interactions). One is between hydrogen of the phenylene ring I and π-conjugated plane of the triphenylene ring, and another is between hydrogen of the phenylene ring I and π-conjugated plane of the phenylene ring II. (Fig. S3a,b) Two of three carboxyphenyl groups in an asymmetric unit are disordered in two position described in Fig. S2c,d. In each position, **BPTp** molecules form phenylene triangle motifs through complementary H-bonding. The

molecule of TCB in a gap between the biphenyl arms was crystallographically solved. (Fig. S2a) Other guests are not solved due to sever disorder.

Compared with the crystal structure of **Tp-1**[S7] (Fig. S3), **BPTp** constructs a similar HexNet through complimentary H-bonding and, considering only adjacent two layers, an isostructural stacking structure with simply extended arm moieties, whose inter-layer distances are similar as **Tp** structures of 4.48 Å. On the other hand, these whole structures are different. In **Tp-1**, an orientation of stacking changes every HexNets. While in **BPTp-1**, HexNets stacks in the same orientation. This is caused from a lack of preferable unique stacking geometry between flat **Tp** cores.

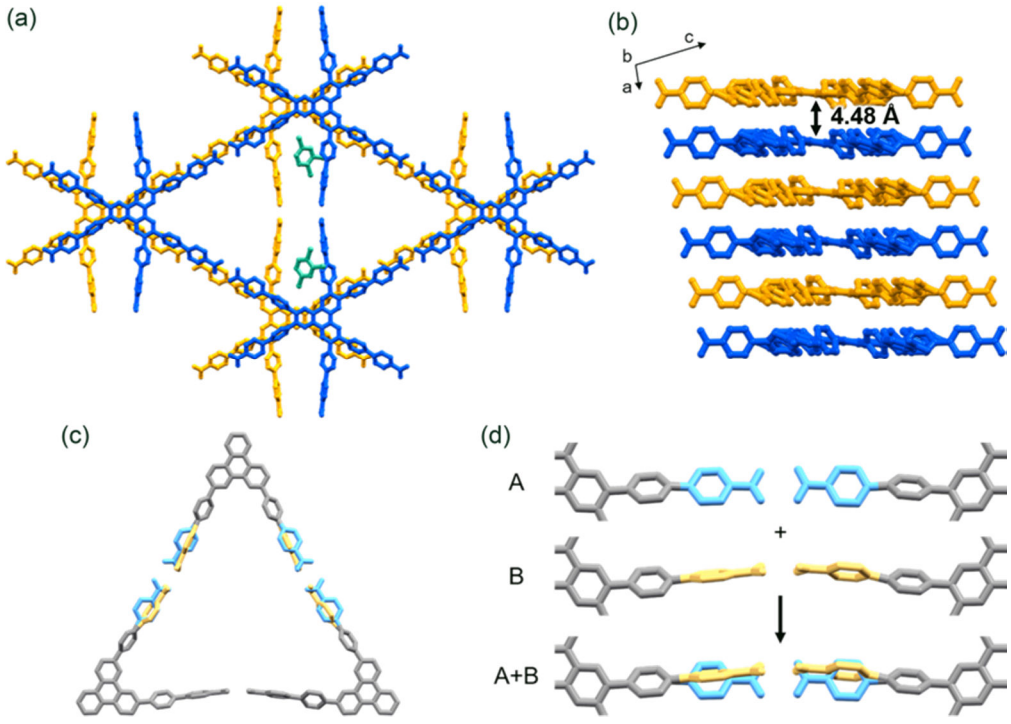

Fig. S2 Crystal structure of **BPTp-1**. (a) Packing diagram. Guest molecules (TCB) shows green. (b) Stacking diagram, (c) H-bonding network motif, and (d) disordered conformation of arm in two position.

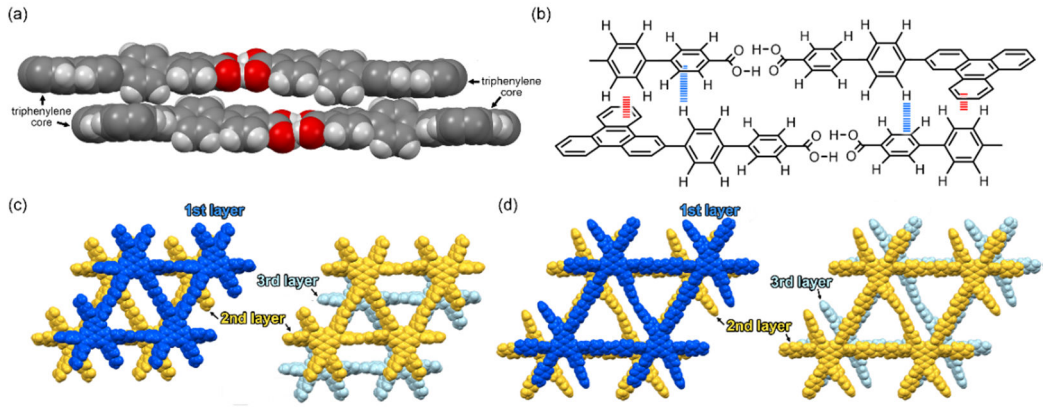

Fig. S3 Leading intermolecular interactions observed between the adjacent HexNet sheets of **BPTp** molecules drawn as (a) space filling models and (b) chemical structures. The phenylene rings in the order adjacent to the Tp core were named as I and II. Comparison between stacking structures of (c) **Tp-1** and (d) **BPTp-1**.

3-4 Crystallography of ThiaHAT-1

Disordered structure of ThiaHAT-1. The arm moiety is disordered in two positions: sites A and B. A crystal structure composed of the molecule in the B-site is shown in Fig. S4. The height and base of the aperture for the B-site structure are 19.7 Å and 19.0 Å, respectively, which are longer than those of the A-site one. Similarly, the void ratio of the B-site one is larger than that of the A-site one, which are 49% and 48%, respectively.

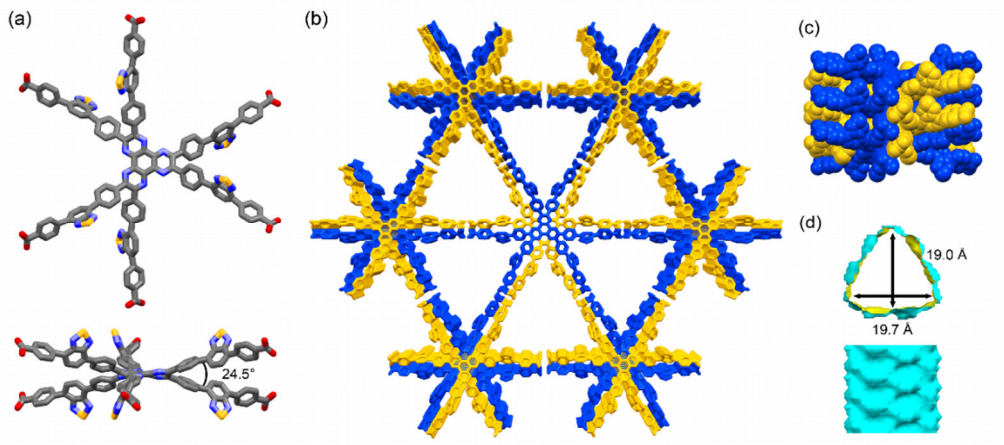

Fig. S4 Crystal structure of **ThiaHAT-1** in the B-site. (a) Twisted nonplanar conformations viewed down the *c* axis (top) and the (100) planes (bottom). (b) Packing diagrams. (c) 1D π-stacked columnar structure. (d) Visualized void surfaces viewed down along the *c* axis (top) and the *ab* planes (bottom). (yellow: inside, cyan: outside). The structure in site A is not shown for clarity.

Interlayer and interlayer H-bonding interaction. In both of conformations, there is an intermolecular H-bonding interaction between nitrogen of Ar-II and hydrogen of Ar-III of two molecules away. The interaction length of site A is 2.55 Å, which is shorter than site B of 2.75 Å. Only in site A, there is an intramolecular H-bonding interaction between Ar-II nitrogen and Ar-III hydrogen, whose length is 2.01 Å due to the approximately planner conformation of Ar-II and III.

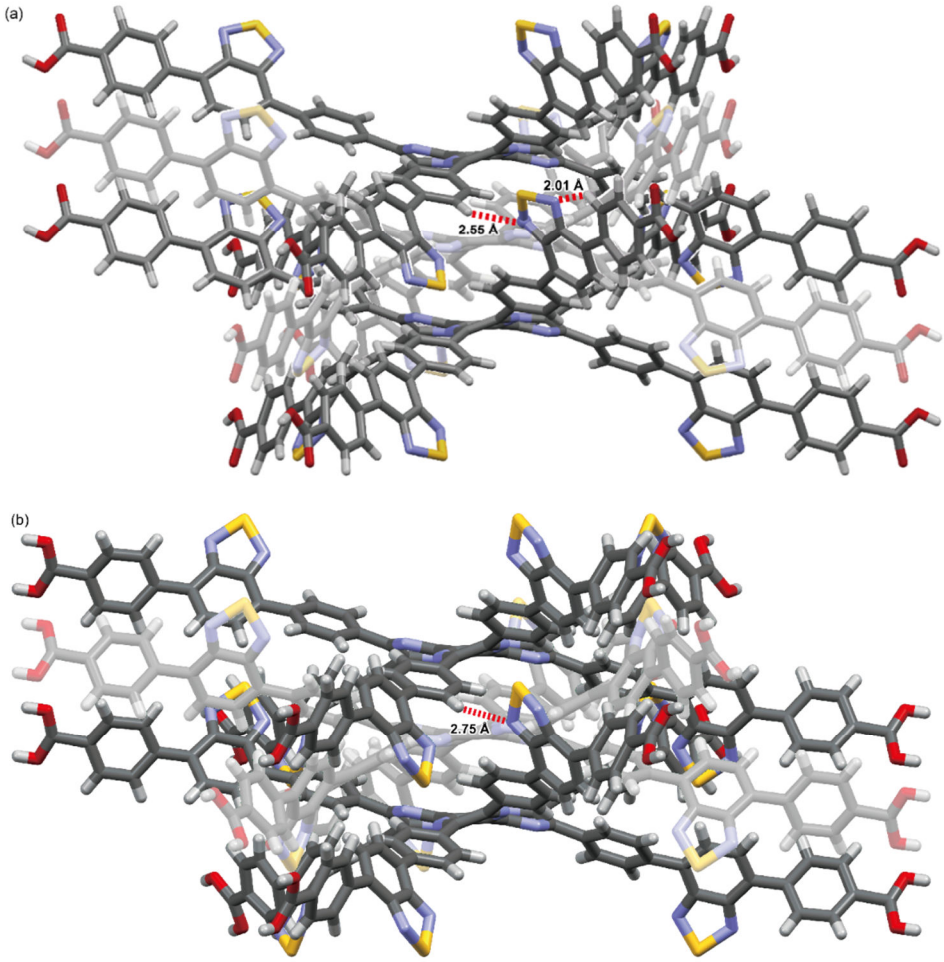

Fig. S5 Interlayer and Intralayer H-bonding interaction between N atom and H atom of (a) A-site and (b) B-site structures.

Assembling manner of the arm in the B site. Compared with the A-site structure, Ar-II and Ar-III in the B-site structure have different conformations. Ar-II (Tz group) rotate though an angle from HAT core of 62.6°, which is different from other HAT derivatives and smaller than A-site structure. Thus, Ar-II aligned along the *c* axis and stacked via edge-to-face pi interaction at a large interlayer angle of 54.4° Ar-III also rotate though a large distortion angle from HAT core of 41.7°. Thus, Ar-III stacked via edge-to-face CH/π interaction at an interlayer angle of 83.0°. Therefore, Ar-II and III were assembled via vertical edge-to-face CH/π stacking. Ar-II of site B is similar than that of site A, but in Ar-III, rotation direction of the B-site structure is opposite to that of the A-site one. Frameworks at the both sites have the same network topology, although the details of hydrogen bonding and arm assembling were different.

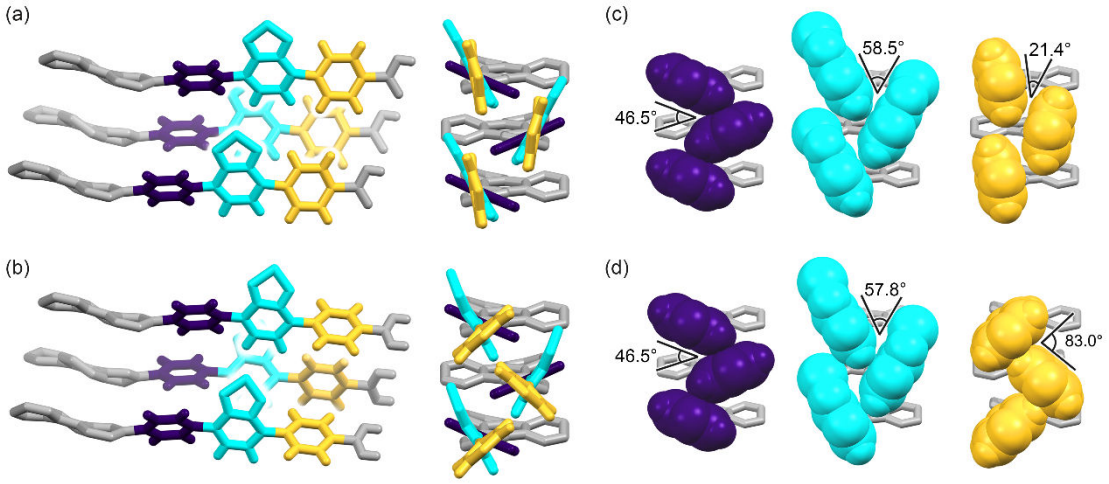

Fig. S6 Arm assembling manners at (a) the A- and (b) the B-sites in **ThiaHAT-1**. (Left) Views form the side of arms. (Right) Views form the carboxylic acid moiety to the HAT core. (c,d) Assembling manners of Ar-I (left), Ar-II (center), and Ar-III (right) in the A and B sites, respectively, in **ThiaHAT-1**. The HAT core is colored gray and the aromatic rings in the order adjacent to the HAT core were defined a name and a color as Ar-I: purple, Ar-II: cyan, and Ar-III: yellow, respectively.

4. Activation of the frameworks

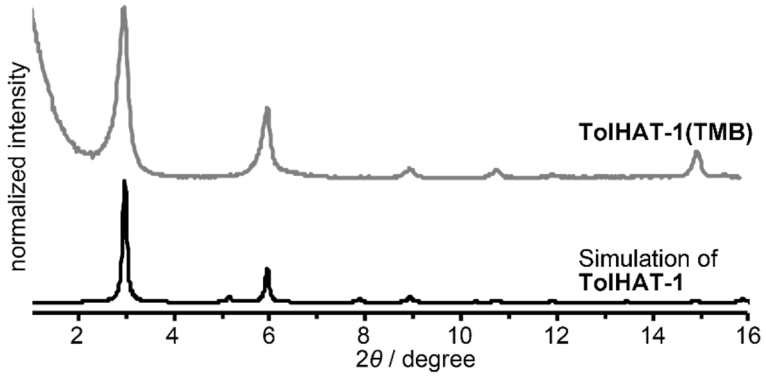

Fig. S7 A PXRD pattern of **TolHAT-1** obtained from 1,3,5-trimethylbenzene (TMB) (top) and that simulated from X-ray diffraction analysis on a single crystal obtained from 1,2,4-trichlorobenzene (TCB), indicating that both have the same crystal structure.

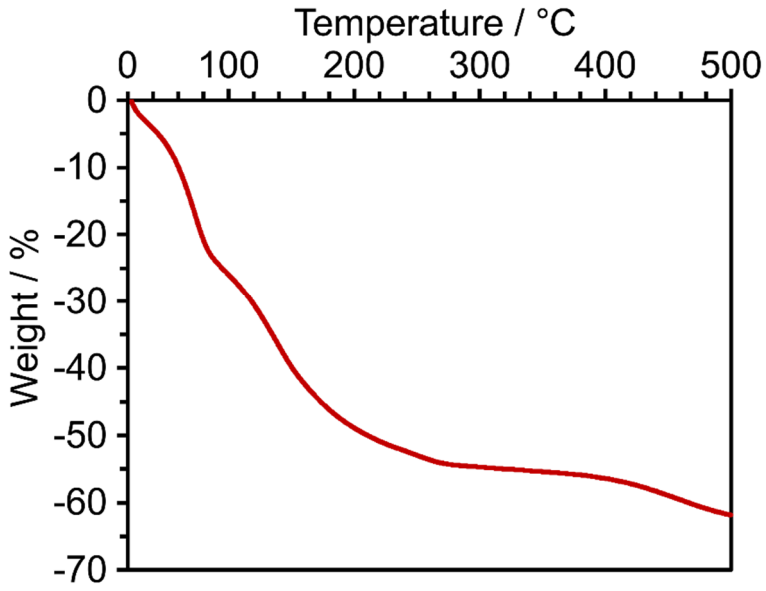

Fig. S8 TG analysis of **TolHAT-1**.

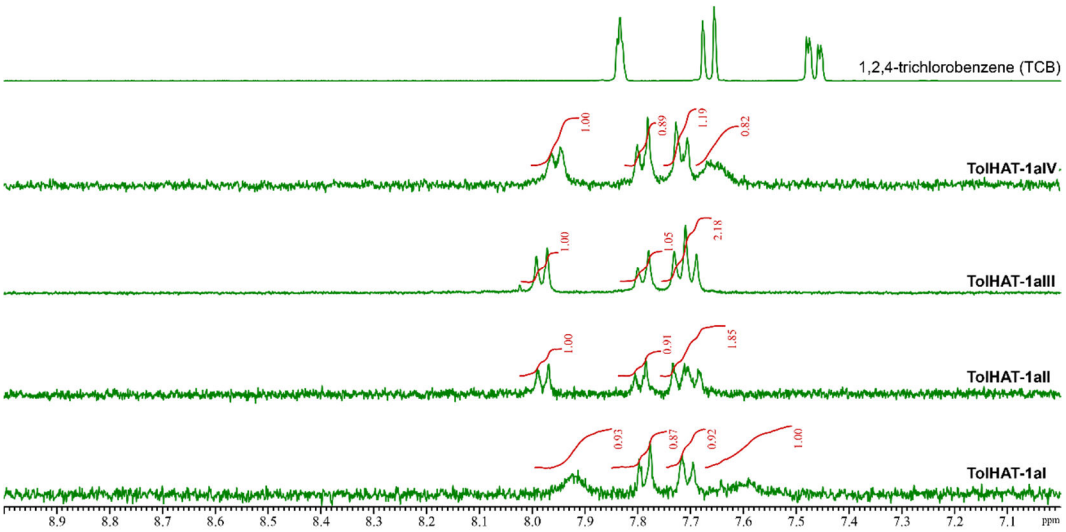

Fig. S9 ^{1}H NMR (400 MHz) spectra of the activated HOF **TolHAT-1a*N*** (*N*=I–IV) dissolved in DMSO-d_6. Chemical shift of **TolHAT** changes with concentration due to an aggregation in DMSO solution.

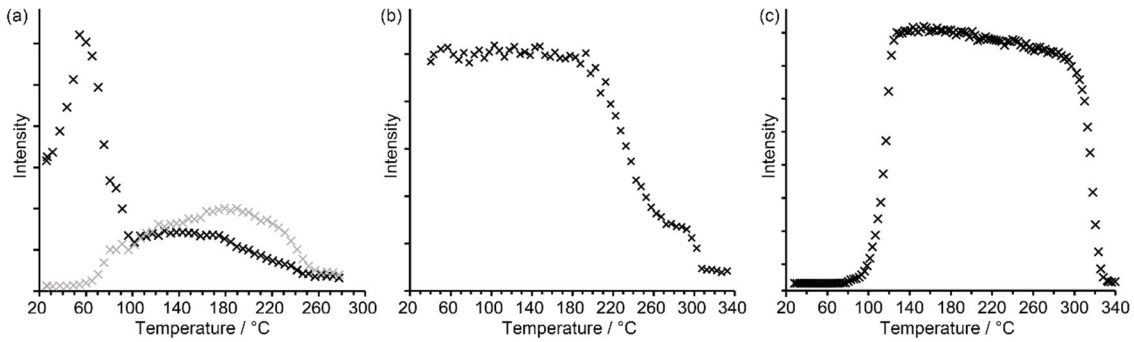

Fig. S10 Representation of the intensity of selected PXRD peaks vs the temperature. (a) Plot of the (100) peak (black) and new detected peak at around $2\theta = 3.60°$ (gray) in **TolHAT-1(TMB)**. A decay of (100) peak intensity and an increase of the new one began at 70 °C. (b) The plot of (100) peak in **TolHAT-1aIV**. The intensity began to decay at 190 °C and completely vanishes at 298 °C. (c) The plot of (100) peak in **ThiaHAT-1**. The intensity rapidly decreased at 300–330 °C, which indicates a collapse of the framework.

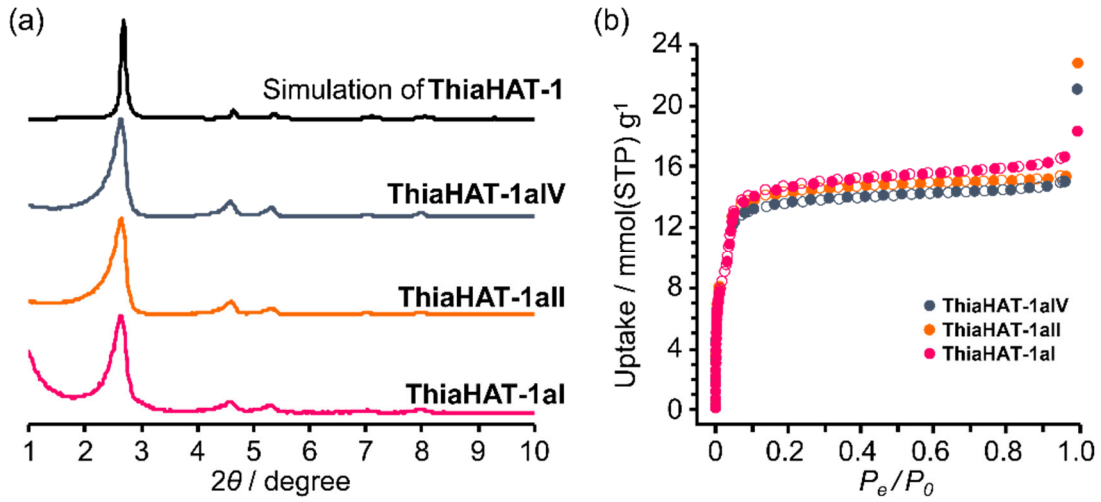

Fig. S11 Evaluation of **ThiaHAT-1a*N*** (***N*** = **I**, **II**, and **IV**) (a) PXRD patterns and (b) N_2 gas sorption isotherms at 77K. open symbol: adsorption, solid symbol: desorption.

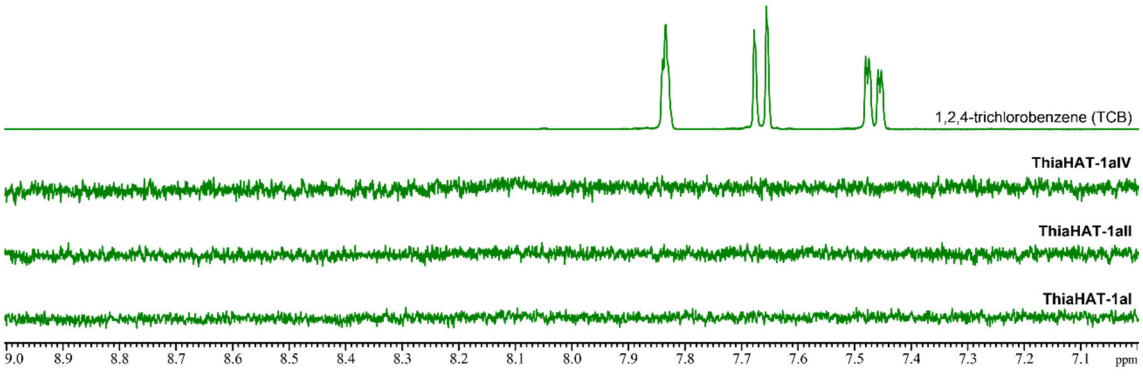

Fig. S12 ^{1}H NMR (400 MHz) spectra of the activated HOF **ThiaHAT-1a*N*** **(*N* = I, II,** and **IV)** dissolved in DMSO-d_6. **ThiaHAT** is almost insoluble to DMSO.

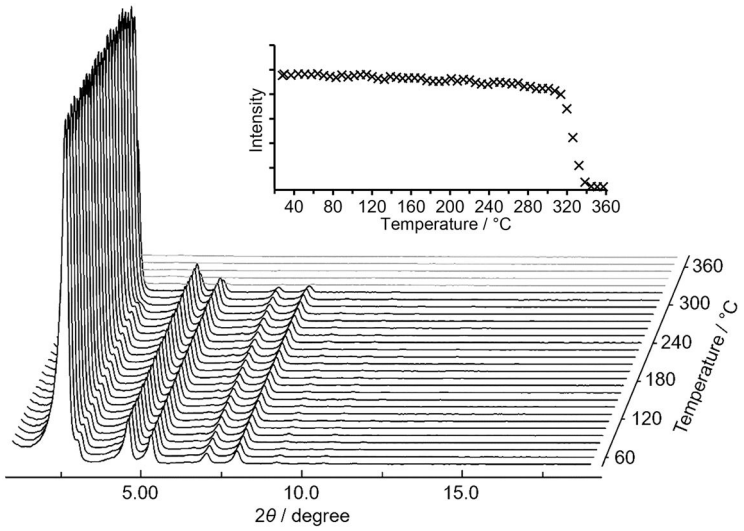

Fig. S13 VT-PXRD patterns of **ThiaHAT-1a** heated from rt to 360 °C. Inset: Changes of the (100) peak intensity with temperature. The intensity rapidly decreased at 306–330 °C, which indicates a collapse of the framework.

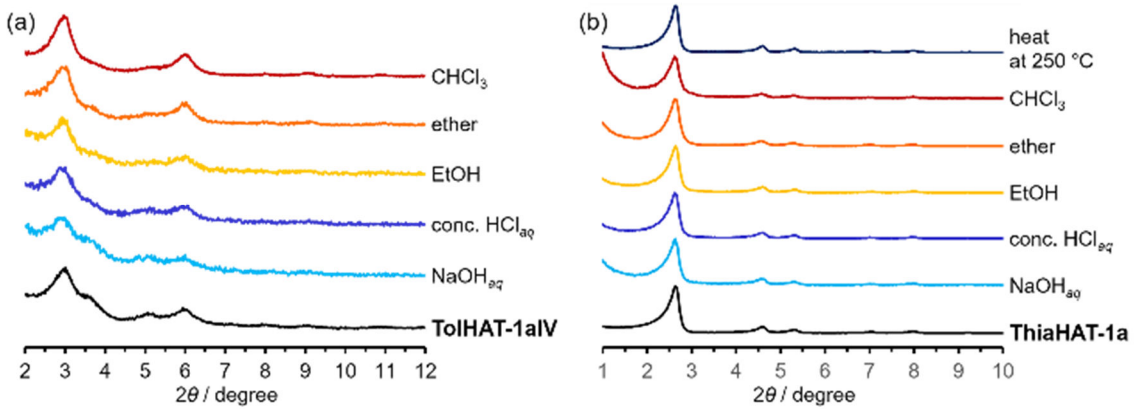

Fig. S14 PXRD patterns of (a) **TolHAT-1aIV,** and (b) **ThiaHAT-1a** after soaked in various solvents for 24 h.

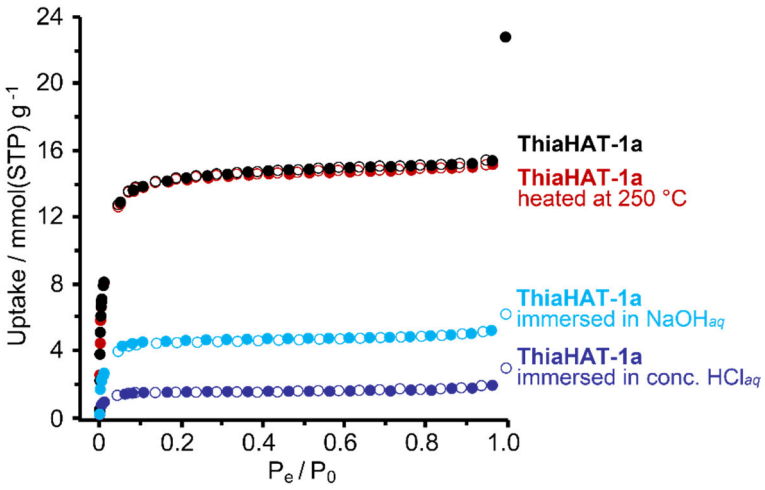

Fig. S15 N_2 gas sorption isotherms of different **ThiaHAT-1a** samples at 77K. open symbol: adsorption, solid symbol: desorption.

Table S2. BET surface areas and NLDFT pore diameters of different samples of **ThiaHAT-1a** estimated from N_2 adsorption.

	SA_{BET} / m^2g^{-1}	D_{NLDFT} / Å
1a	1394	1.55
after heated at 250 °C	1327	1.02
after immersed in conc. HCl_{aq}	138.5	1.09
after immersed in $NaOH_{aq}$ (pH = 10)	425.7	1.09

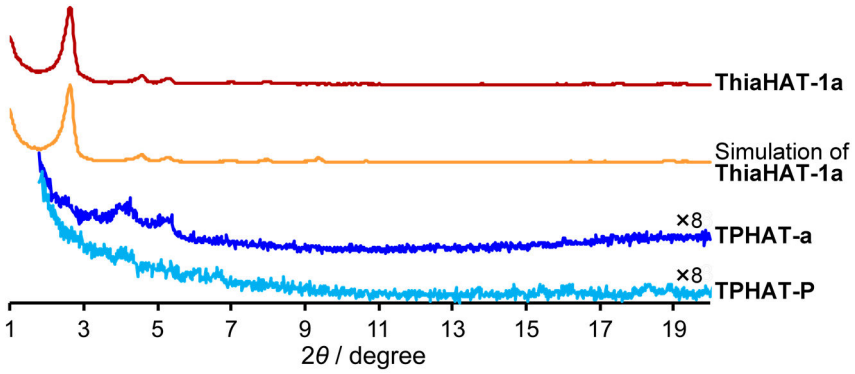

Fig. S16 Comparison of PXRD patterns between **TPHAT** and **ThiaHAT**. Clearly, the lack of a diffraction peak at 2θ = 2.68° for **TPHAT** evidences that this material is not isostructural to the other HAT derivatives. **TPHAT-a** was obtained by **TPHAT-P** heating at 120 °C under vacuum for 24 h. A removal of guest molecule (TCB) was confirmed by ^{1}H-NMR (Fig. S17).

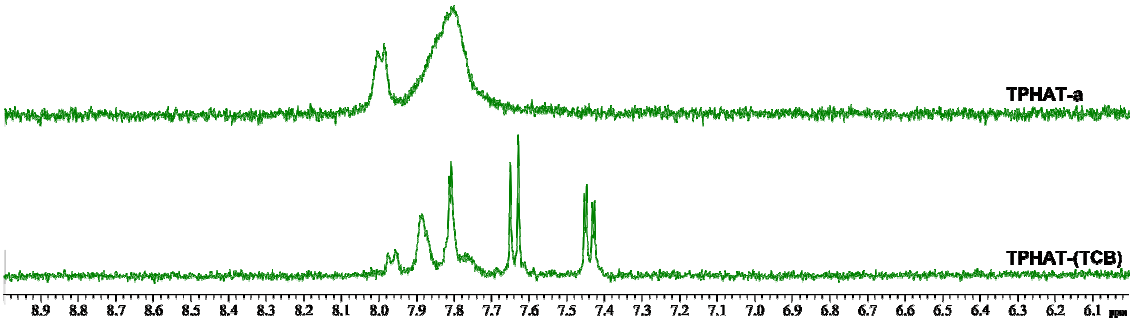

Fig. S17 ^{1}H-NMR spectra of **TPHAT-(TCB)** (bottom) and **TPHAT-a** (top). Chemical shift of **TPHAT** changes with concentration due to an aggregation in DMSO solution.

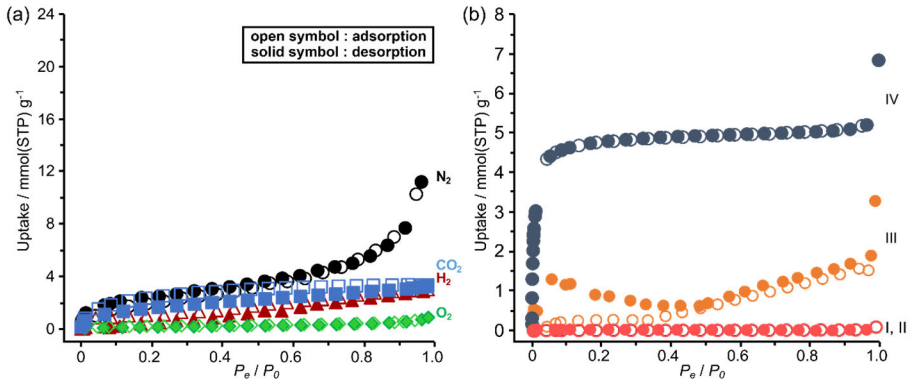

Fig. S18 (a) Gas sorption isotherms of **TPHAT-a**, and (b) N_2 gas sorption isotherms of **TolHAT-a*N*** (*N* = I–IV) at 77K. open symbol: adsorption, solid symbol: desorption. **TPHAT-a** (dried sample of **TPHAT-P** at 120 °C for 24 h under vacuum) has low gas uptakes [N_2: 11.2, O_2: 0.886, H_2: 0.132, CO_2: 3.32 / mmol(STP)g^{-1}] and the BET surface area was calculated to be 8.8 m^2g^{-1} based on a N_2 adsorption isotherm, indicating an almost non-porous structure.

Table S3. N_2 gas uptakes of **TolHAT-1a*N*** (*N* = I–IV)

TolHAT-1a	N_2 uptake / mmol(STP)g^{-1}
I	0.0241
II	0.188
III	3.27
IV	6.84

Table S4. Gas uptakes, BET surface areas, and NLDFT pore diameters of **TPHAT-a**, **TolHAT-1aIV**, and **ThiaHAT-1a**. BET surface area and NLDFT pore diameter were based on N_2 adsorption.

	TPHAT-a	**TolHAT-1aIV**	**ThiaHAT-1a**	cf. **CBPHAT-1a**[b]
N_2 uptake / mmol(STP)g^{-1}	11.2[a]	6.84	18.3	16.1
CO_2 uptake / mmol(STP)g^{-1}	3.32	7.43	13.8	13.4
O_2 uptakes / mmol(STP)g^{-1}	0.866	6.96	21.9	18.8
H_2 uptakes / mmol(STP)g^{-1}	0.132	1.94	3.28	4.90
$S_{A(BET)}$ / m^2g^{-1}	8.8	330	1394	1288
$d_{(NLDFT)}$ / nm	———	1.49	1.55	1.24

[a] Due to the large amount of surface sorption in the N_2 isotherm of **TPHAT-a**, the N_2 uptake at P_e/P_0 = 1.0 was larger than **TolHAT-1aIV**.

[b] Ref. S8

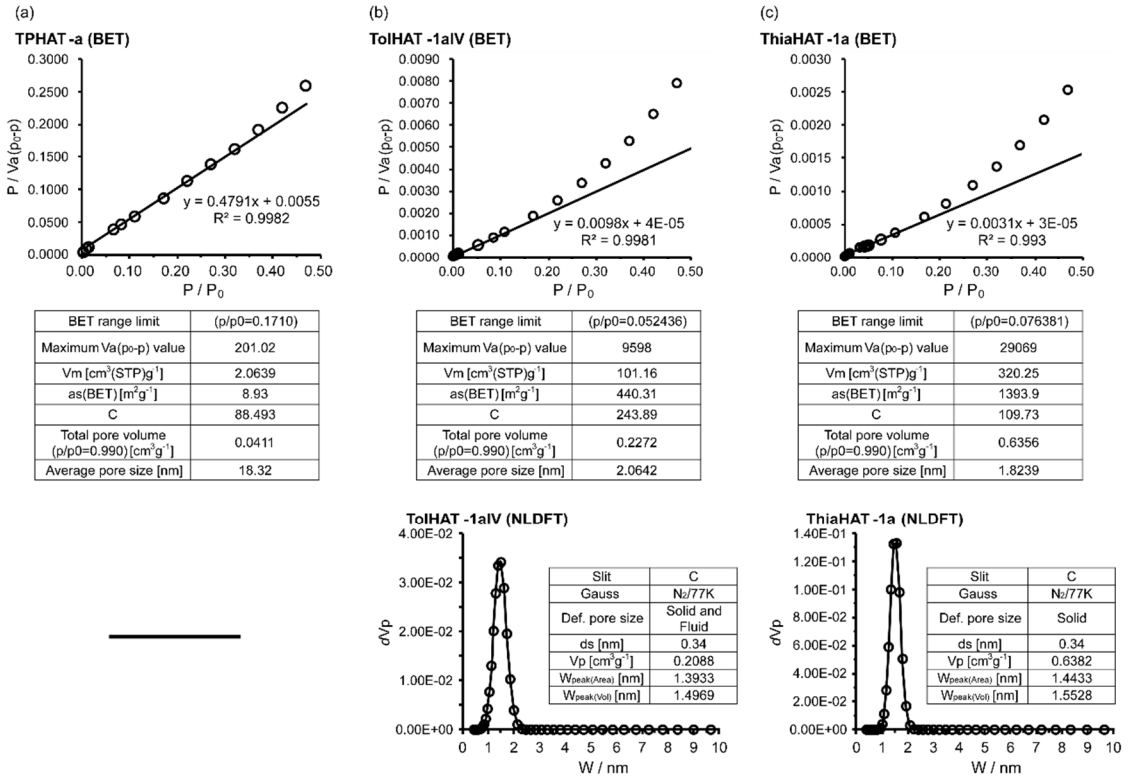

Fig. S19 BET (upper) and NLDFT (bottom) plots of (a) **TPHAT-a**, (b) **TolHAT-1aIV**, and (c) **ThiaHAT-1a**.

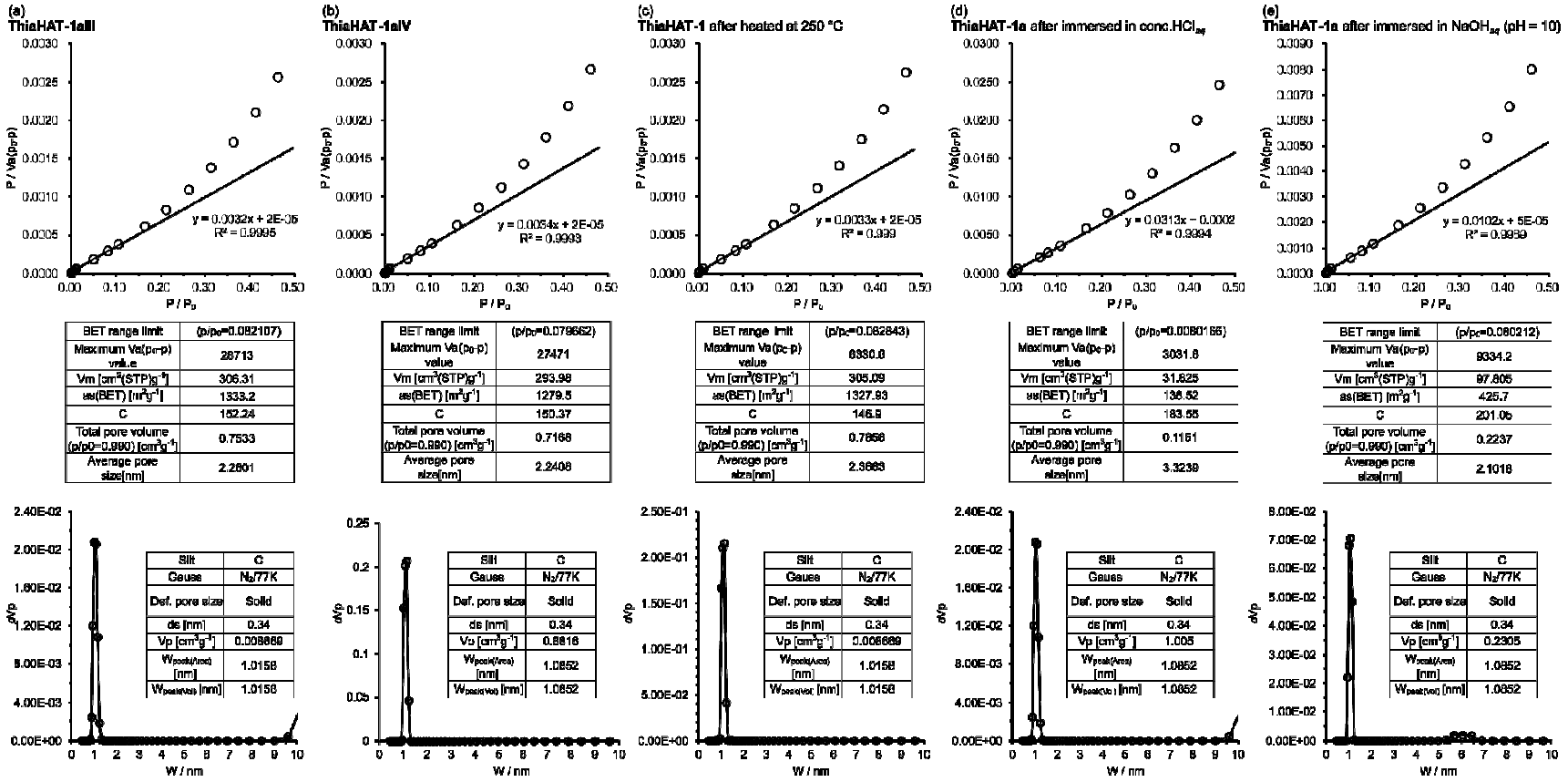

Fig. S20 BET (upper) and NLDFT (bottom) plots of (a) **ThiaHAT-1aII**, (b) **ThiaHAT-1aIV**, (c) **ThiaHAT-1a heat**, (d) **ThiaHAT-1a HCl$_{aq}$ soaked**, and (e) **ThiaHAT-1a NaOH$_{aq}$**

5. Theoretical calculation

5-1. Geometry optimization of single molecule

Optimized structures of **TolHAT** and **ThiaHAT** were calculated by the DFT method at the B3LYP/6-31G level. These calculations were carried out using Gaussian09W.[S9]

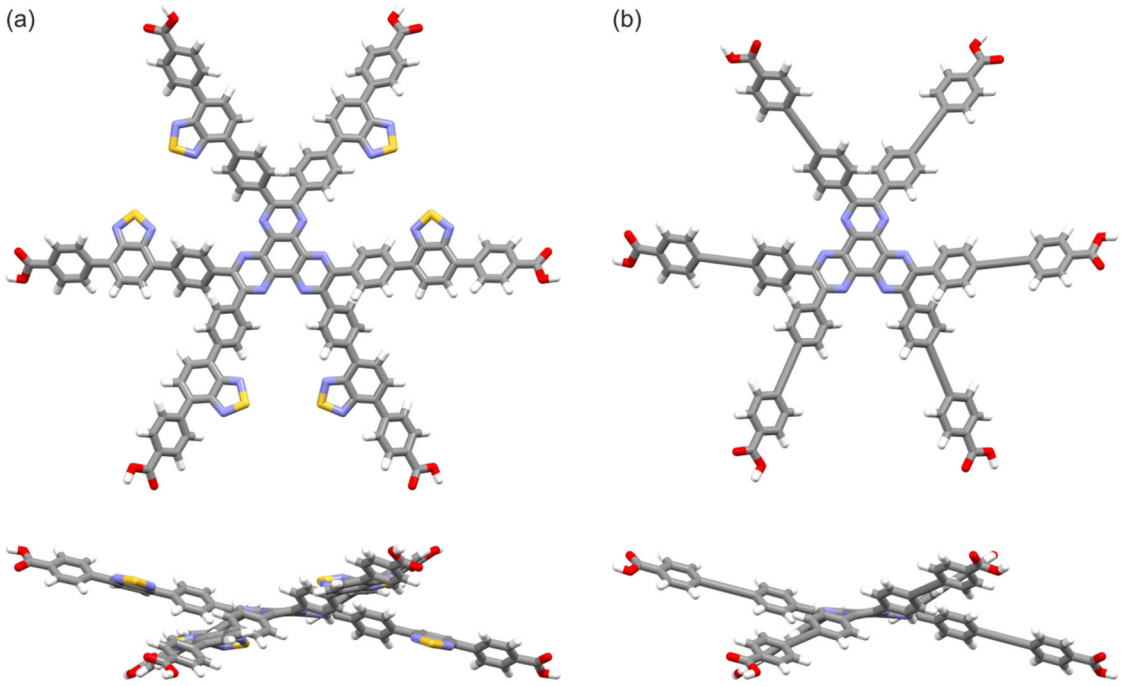

Fig. S21 Optimized structure of (a) **TolHAT** and (b) **ThiaHAT** viewed from top (up) and side (bottom)

Table S5. Atomic coordinates of **TolHAT** obtained from the DFT calculation

O	14.66778	7.09312	-2.89693	C	6.18636	4.49868	-1.21846	H	13.14480	5.51993	-1.88931
H	15.48736	7.54626	-3.18820	C	6.10873	3.30518	-0.46419	C	12.28430	7.18628	-2.95033
O	13.69427	8.83825	-4.00687	H	7.02491	2.81069	-0.16101	C	11.09320	7.81792	-3.35061
N	2.39001	1.42220	-0.14764	C	4.87478	2.76537	-0.11689	H	11.15727	8.73002	-3.93286
C	1.23201	0.73734	-0.03159	H	4.81662	1.83684	0.43839	C	9.86053	7.27767	-3.00300
C	2.38182	2.76841	-0.14459	C	7.44696	5.05385	-1.57741	H	8.94236	7.76430	-3.31159
C	3.67506	3.40561	-0.48792	C	8.52885	5.52993	-1.88426	C	13.56556	7.79885	-3.34405
C	3.75031	4.58788	-1.25138	C	9.78904	6.08615	-2.24251	O	-1.35903	16.31727	2.96516
H	2.84203	5.08123	-1.57642	C	10.99262	5.45801	-1.84462	O	0.64904	16.18325	4.04904
C	4.98205	5.12483	-1.61352	H	10.94440	4.54503	-1.26203	H	0.44640	17.12184	4.24874
H	5.02626	6.02912	-2.21004	C	12.22468	6.00200	-2.19463	N	-0.00699	2.78111	0.12562

C	0.00000	1.43579	0.00892
C	1.15242	3.46524	0.12336
C	1.03493	4.90184	0.46807
C	2.00896	5.57172	1.23539
H	2.89760	5.04461	1.56180
C	1.83677	6.90382	1.59940
H	2.58861	7.40476	2.19886
C	0.68254	7.61690	1.20223
C	-0.29974	6.93930	0.44371
H	-1.19327	7.47258	0.13866
C	-0.12900	5.60374	0.09471
H	-0.89455	5.07842	-0.46374
C	0.51084	8.98303	1.56333
C	0.36296	10.15523	1.87217
C	0.18993	11.52144	2.23177
C	-0.96220	12.23390	1.82166
H	-1.71453	11.72677	1.22843
C	-1.12761	13.56807	2.17482
H	-2.00674	14.12140	1.86497
C	-0.15134	14.22580	2.94435
C	0.99716	13.52737	3.35704
H	1.74557	14.03868	3.94924
C	1.16650	12.19164	3.00548
H	2.05120	11.65135	3.32266
C	-0.37364	15.64042	3.29258
O	13.69058	-8.65371	4.04904
H	14.60475	-8.94751	4.24874
O	14.81068	-6.98168	2.96516
N	2.41201	-1.38450	0.12562
C	1.24343	-0.71789	0.00892
C	2.42478	-2.73065	0.12336
C	3.72766	-3.34719	0.46807
C	3.82077	-4.52567	1.23539
H	2.91996	-5.03170	1.56180
C	5.06050	-5.04260	1.59940
H	5.11841	-5.94418	2.19886

C	6.25516	-4.39954	1.20223
C	6.15948	-3.21007	0.44371
H	7.06808	-2.70289	0.13866
C	4.91748	-2.69015	0.09471
H	4.84532	-1.76451	-0.46374
C	7.52411	-4.93392	1.56333
C	8.61321	-5.39195	1.87217
C	9.88289	-5.92521	2.23177
C	9.97503	-7.10604	3.00548
H	9.06476	-7.60207	3.32266
C	11.21647	-7.62725	3.35704
H	11.28507	-8.53105	3.94924
C	12.39557	-6.98184	2.94435
C	12.31410	-5.80750	2.17482
H	13.23286	-5.32281	1.86497
C	11.07596	-5.28366	1.82166
H	11.01294	-4.37856	1.22843
C	13.73181	-7.49663	3.29258
O	-13.47671	9.15611	-2.89693
H	-14.27894	9.63932	-3.18820
O	-14.50128	7.44046	-4.00687
N	-2.42667	1.35871	-0.14764
C	-1.25456	0.69828	-0.03159
C	-3.58842	0.67851	-0.14459
C	-4.78687	1.47989	-0.48792
C	-5.84838	0.95393	-1.25138
H	-5.82149	-0.07935	-1.57642
C	-6.92926	1.75217	-1.61352
H	-7.73451	1.33831	-2.21004
C	-6.98915	3.10820	-1.21846
C	-5.91674	3.63773	-0.46419
H	-5.94658	4.67841	-0.16101
C	-4.83227	2.83900	-0.11689
H	-3.99906	3.25290	0.43839
C	-8.10024	3.92233	-1.57741
C	-9.05348	4.62124	-1.88426

C	-10.16528	5.43449	-2.24251
C	-10.22308	6.79089	-1.84462
H	-9.40831	7.20561	-1.26203
C	-11.31022	7.58588	-2.19463
H	-11.35280	8.62377	-1.88931
C	-12.36565	7.04538	-2.95033
C	-12.31712	5.69804	-3.35061
H	-13.13905	5.29747	-3.93286
C	-11.23291	4.90063	-3.00300
H	-11.19526	3.86216	-3.31159
C	-13.53678	7.84870	-3.34405
O	-1.19107	-16.24922	-2.89693
H	-1.20843	-17.18558	-3.18820
O	0.80702	-16.27871	-4.00687
N	0.03665	-2.78091	-0.14764
C	0.02255	-1.43562	-0.03159
C	1.20660	-3.44692	-0.14459
C	1.11181	-4.88550	-0.48792
C	2.09807	-5.54181	-1.25138
H	2.97946	-5.00188	-1.57642
C	1.94721	-6.87700	-1.61352
H	2.70824	-7.36743	-2.21004
C	0.80279	-7.60688	-1.21846
C	-0.19199	-6.94291	-0.46419
H	-1.07833	-7.48910	-0.16101
C	-0.04251	-5.60437	-0.11689
H	-0.81756	-5.08974	0.43839
C	0.65329	-8.97618	-1.57741
C	0.52463	-10.15117	-1.88426
C	0.37624	-11.52064	-2.24251
C	-0.76954	-12.24889	-1.84462
H	-1.53609	-11.75065	-1.26203
C	-0.91445	-13.58788	-2.19463
H	-1.79200	-14.14370	-1.88931
C	0.08135	-14.23166	-2.95033
C	1.22391	-13.51595	-3.35061

H	1.98178	-14.02749	-3.93286	C	-5.82973	-1.04605	1.23539	C	-10.07282	-5.59623	2.23177
C	1.37238	-12.17830	-3.00300	H	-5.81756	-0.01291	1.56180	C	-10.11376	-6.95024	1.82166
H	2.25291	-11.62646	-3.31159	C	-6.89727	-1.86122	1.59940	H	-9.29842	-7.34821	1.22843
C	-0.02878	-15.64755	-3.34405	H	-7.70702	-1.46058	2.19886	C	-11.18649	-7.76057	2.17482
O	-13.45165	-9.33559	2.96516	C	-6.93770	-3.21735	1.20223	H	-11.22612	-8.79859	1.86497
O	-14.33962	-7.52954	4.04904	C	-5.85974	-3.72924	0.44371	C	-12.24424	-7.24396	2.94435
H	-15.05115	-8.17433	4.24874	H	-5.87481	-4.76969	0.13866	C	-12.21363	-5.90012	3.35704
N	-2.40501	-1.39661	0.12562	C	-4.78848	-2.91359	0.09471	H	-13.03064	-5.50763	3.94924
C	-1.24343	-0.71789	0.00892	H	-3.95077	-3.31391	-0.46374	C	-11.14152	-5.08561	3.00548
C	-3.57720	-0.73460	0.12336	C	-8.03495	-4.04912	1.56333	H	-11.11596	-4.04928	3.32266
C	-4.76258	-1.55465	0.46807	C	-8.97617	-4.76328	1.87217	C	-13.35818	-8.14379	3.29258

Table S6. Atomic coordinates of **ThiaHAT** obtained from the DFT calculation

C	0.01356	-1.43741	-0.01894	C	1.87257	-6.86254	-1.60158	H	2.86702	4.98792	-1.62702
C	0.01350	1.43740	0.02000	C	-0.20169	-6.94992	-0.37772	H	4.83105	1.85111	0.55139
C	1.23808	-0.73039	0.02000	H	-0.81241	-5.10937	0.55139	H	7.02527	2.81564	-0.03393
C	-1.25158	-0.70701	0.02000	H	2.88616	-4.97687	-1.62702	H	5.04203	5.91953	-2.25524
C	-1.25161	0.70696	-0.01894	H	2.60545	-7.32630	-2.25524	C	1.07113	4.87823	0.45671
C	1.23805	0.73044	-0.01894	H	-1.07422	-7.49188	-0.03393	C	0.76353	7.60921	1.16147
N	2.39837	-1.39263	0.13480	C	3.68911	-3.36674	0.45671	C	-0.05325	5.60978	0.04098
C	2.38984	-2.72450	0.12998	C	6.20800	-4.46584	1.16147	C	2.02855	5.52668	1.25355
C	1.16472	-3.43184	-0.12915	C	4.88484	-2.75878	0.04098	C	1.87304	6.86301	1.60121
N	0.00699	-2.77337	-0.13381	C	3.77198	-4.52011	1.25355	C	-0.20230	6.94979	0.37911
N	-2.40531	1.38063	-0.13381	C	5.00702	-5.05361	1.60121	H	-0.81340	5.10898	-0.54925
C	-3.55442	0.70724	-0.12915	C	6.11984	-3.29970	0.37911	H	2.88692	4.97751	1.62626
C	-3.55441	-0.70741	0.12998	H	4.83121	-1.85006	-0.54925	H	2.60639	7.32707	2.25412
N	-2.40524	-1.38073	0.13480	H	2.86719	-4.98890	1.62626	H	-1.07522	7.49154	0.03598
N	2.39832	1.39274	-0.13381	H	5.04223	-5.92074	2.25412	C	-4.76022	1.51130	-0.45602
C	2.38970	2.72460	-0.12915	H	7.02548	-2.81460	0.03598	C	-6.97141	3.14325	-1.16103
C	1.16457	3.43191	0.12998	C	3.68893	3.36682	-0.45602	C	-5.79997	1.00669	-1.25374
N	0.00687	2.77336	0.13480	C	6.20784	4.46579	-1.16103	C	-4.83204	2.85054	-0.03952
C	1.07129	-4.87812	-0.45602	C	3.77180	4.51958	-1.25374	C	-5.91797	3.64963	-0.37772
C	0.76357	-7.60904	-1.16103	C	4.88466	2.75940	-0.03952	C	-6.87942	1.80957	-1.60158
C	-0.05262	-5.60994	-0.03952	C	6.11966	3.30029	-0.37772	H	-5.75318	-0.01105	-1.62702
C	2.02817	-5.52627	-1.25374	C	5.00685	5.05296	-1.60158	H	-4.01863	3.25825	0.55139

H	-5.95105	4.67625	-0.03393
H	-7.64748	1.40676	-2.25524
C	-4.76023	-1.51149	0.45671
C	-6.97153	-3.14337	1.16147
C	-4.83159	-2.85100	0.04098
C	-5.80052	-1.00657	1.25355
C	-6.88006	-1.80941	1.60121
C	-5.91754	-3.65009	0.37911
H	-4.01781	-3.25892	-0.54925
H	-5.75411	0.01139	1.62626
H	-7.64863	-1.40633	2.25412
H	-5.95026	-4.67694	0.03598
C	7.50525	-5.08891	1.50418
C	9.95384	-4.98696	2.11220
C	8.87093	-7.10206	1.93195
C	10.04314	-6.42071	2.19659
C	7.64849	-6.46028	1.59697
C	8.69831	-4.32801	1.77078
H	6.79439	-7.09162	1.37169
H	8.88250	-8.18779	1.94424
C	0.65450	-9.04398	-1.50393
C	1.71526	-11.23275	-1.93404
C	-0.65826	-11.11395	-2.11029
C	0.53893	-11.90761	-2.19695
C	-0.60117	-9.69719	-1.76869
C	1.77067	-9.85330	-1.59868
H	2.64995	-11.78527	-1.94812
H	2.74466	-9.42902	-1.37477
C	-8.15975	-3.95529	1.50418
C	-9.29575	-6.12680	2.11220
C	-10.58603	-4.13142	1.93195
C	-10.58206	-5.48726	2.19659
C	-9.41901	-3.39365	1.59697
C	-8.09732	-5.36895	1.77078
H	-11.53209	-3.59857	1.94424
H	-9.53872	-2.33831	1.37169

C	-8.15957	3.95518	-1.50393
C	-10.58548	4.13091	-1.93404
C	-9.29583	6.12704	-2.11029
C	-10.58176	5.48708	-2.19695
C	-8.09743	5.36922	-1.76869
C	-9.41855	3.39320	-1.59868
H	-9.53810	2.33756	-1.37477
H	-11.53132	3.59771	-1.94812
C	0.65450	9.04419	1.50418
C	-0.65809	11.11375	2.11220
C	1.71510	11.23348	1.93195
C	0.53893	11.90797	2.19659
C	1.77052	9.85393	1.59697
C	-0.60099	9.69696	1.77078
H	2.64959	11.78637	1.94424
H	2.74432	9.42993	1.37169
C	7.50507	5.08880	-1.50393
C	8.87022	7.10184	-1.93404
C	9.95409	4.98690	-2.11029
C	10.04283	6.42053	-2.19695
C	8.69860	4.32797	-1.76869
C	7.64787	6.46010	-1.59868
H	6.79344	7.09146	-1.37477
H	8.88137	8.18756	-1.94812
N	-1.80271	-9.10819	-1.76315
S	-2.90078	-10.26307	-2.15458
N	-1.90053	-11.54934	-2.35085
N	-6.98612	-6.11452	1.76741
S	-7.43701	-7.64262	2.16027
N	-9.05133	-7.41986	2.35489
N	-6.98656	6.11529	-1.76315
S	-7.43769	7.64369	-2.15458
N	-9.05175	7.42057	-2.35085
N	8.78928	2.99290	-1.76315
S	10.33847	2.61938	-2.15458
N	10.95228	4.12876	-2.35085

N	8.78839	-2.99289	1.76741
N	10.95145	-4.12875	2.35489
N	-1.80227	9.10741	1.76741
N	-1.90013	11.54861	2.35489
S	-2.90020	10.26195	2.16027
S	10.33721	-2.61933	2.16027
C	-11.82320	6.21336	-2.54705
C	-14.24060	7.52329	-3.17395
C	-12.06680	7.52679	-2.10262
C	-12.81268	5.57821	-3.32144
C	-14.00597	6.21988	-3.63213
C	-13.26006	8.16877	-2.40922
H	-11.31736	8.04067	-1.51335
H	-12.63028	4.57989	-3.70776
H	-14.75336	5.71871	-4.23710
H	-13.45312	9.17774	-2.06003
C	0.53064	13.34641	2.54594
C	0.60459	16.09536	3.17099
C	-0.48660	14.21319	2.10335
C	1.57691	13.88692	3.31752
C	1.61772	15.24140	3.62726
C	-0.44614	15.56778	2.40908
H	-1.30744	13.82023	1.51618
H	2.35166	13.23056	3.70240
H	2.42665	15.63897	4.23001
H	-1.22469	16.23873	2.06135
C	11.29252	7.13251	-2.54705
C	13.63566	8.57108	-3.17395
C	12.55179	6.68676	-2.10262
C	11.23721	8.30700	-3.32144
C	12.38956	9.01959	-3.63213
C	13.70440	7.39917	-2.40922
H	12.62210	5.78079	-1.51335
H	10.28144	8.64820	-3.70776
H	12.32923	9.91742	-4.23710
H	14.67472	7.06187	-2.06003

C	11.29301	-7.13275	2.54594
C	13.63669	-8.57127	3.17099
C	12.55229	-6.68519	2.10335
C	11.23797	-8.30910	3.31752
C	12.39058	-9.02169	3.62726
C	13.70516	-7.39752	2.40908
H	12.62239	-5.77784	1.51618
H	10.28217	-8.65188	3.70240
H	12.33042	-9.92103	4.23001
H	14.67550	-7.05875	2.06135
C	0.53067	-13.34587	-2.54705
C	0.60495	-16.09437	-3.17395
C	-0.48499	-14.21355	-2.10262
C	1.57546	-13.88521	-3.32144
C	1.61641	-15.23947	-3.63213
C	-0.44433	-15.56794	-2.40922
H	-1.30474	-13.82146	-1.51335
H	2.34884	-13.22808	-3.70776

H	2.42413	-15.63614	-4.23710
H	-1.22160	-16.23961	-2.06003
C	-11.82365	-6.21366	2.54594
C	-14.24129	-7.52409	3.17099
C	-12.06569	-7.52801	2.10335
C	-12.81488	-5.57782	3.31752
C	-14.00830	-6.21971	3.62726
C	-13.25902	-8.17026	2.40908
H	-11.31495	-8.04239	1.51618
H	-12.63383	-4.57868	3.70240
H	-14.75707	-5.71795	4.23001
H	-13.45081	-9.17998	2.06135
C	14.90033	9.28975	-3.47262
C	-15.49604	-8.26027	3.46882
C	14.90163	-9.28983	3.46882
C	0.59499	-17.54894	-3.47262
O	16.00383	8.94415	-3.09922
O	16.00516	-8.94259	3.09707

O	-0.25605	-18.33180	-3.09922
O	-15.74709	-9.38958	3.09707
C	-15.49532	8.25919	-3.47262
C	0.59441	17.55010	3.46882
O	-15.74778	9.38765	-3.09922
O	-0.25807	18.33217	3.09707
O	-16.37171	-7.53862	4.21720
H	-17.14464	-8.11873	4.34630
O	-16.36911	7.53844	-4.22406
H	-17.14217	8.11830	-4.35347
O	1.65722	17.94763	4.21720
H	1.54129	18.90706	4.34630
O	14.71304	10.40685	-4.22406
H	15.60174	10.78641	-4.35347
O	14.71449	-10.40901	4.21720
H	15.60335	-10.78832	4.34630
O	1.65608	-17.94529	-4.22406
H	1.54043	-18.90471	-4.35347

5-2. Energy evaluation for stacking dimers.

Atomic coordinates in the crystal structures were adopted except for hydrogen atoms which were optimized at B3LYP-D3/6-311G(d,p) level of theory. The complexation energy was evaluated by the following three methods: B3LYP-D3/6-311G(d,p), M062X/6-311G(d,p), and ωB97XD/6-311G(d,p). The corrections of basis set superposition error (BSSE) are evaluated by means of counterpoise method. These calculations were carried out using Gaussian09W. In Fig. 8, the complexation energies for **TolHAT-1**, **ThiaHAT-1**, **CBPHAT-1**, and **CPHAT-1** are plotted against a linker length. The linker length means a distance between a C atom of HAT adjacent to arm moiety and that of carboxylic acid.

Table S7. Complexation energy and linker lengths.

	Linker length / Å	Energy of B3LYP-D3 / kcal mole^{-1}	Energy of M062X / kcal mole^{-1}	Energy of ωB97XD / kcal mole^{-1}
CPHAT	5.757	-54.66	-38.47	-58.39
BPHAT	10.06	-81.16	-63.89	-90.92
TolHAT	12.57	-97.54	-82.12	-108.56
ThiaHAT	14.42	-103.5	-73.97	-112.69

5-3 Molecular Dynamics simulations

MD (molecular dynamics) simulations were performed at 300 K and 1 bar using GROMACS 2016-4.[S10] The initial configuration of each HOF system was constructed by retrieving the unit-cell structure of the crystal in CIF format and replicating it periodically 9, 9, and 12 times along the *a, b*, and *c* directions, respectively. The unit cell of MD was then a parallelepiped, and the periodic boundary condition was employed with minimum image convention. The force field was GAFF (general AMBER force field), and the atomic partial charges were determined with RESP (restrained electrostatic potential).[S11,S12] The RESP procedure was carried out after DFT calculations for the monomeric forms at the B3LYP/6-31G(d,p) level with Gaussian09.[S9] In DFT, the geometrical optimization was done only for the hydrogen atoms and the non-hydrogen atoms were kept fixed at the coordinates in the CIF file. After the energy minimization with the steepest descent method for 50000 steps, MD was carried in the *NPT* ensemble at 1 bar over 2 ns for equilibration and over 10 ns for production; see the next paragraph for the procedure of equilibration. The RMSD was computed by referencing the average structure of the crystal

obtained from the production run.

In MD, the electrostatic interaction was handled by the smooth particle-mesh Ewald (PME) method with a real-space cutoff of 12 Å, a spline order of 6, a relative tolerance 10^{-5}, and a reciprocal-space mesh size of 90 along the *c* direction. The numbers of meshes along (*a*, *b*) are (200, 180), (270, 240), (300, 270), and (360, 300) for **CPHAT-1**, **CBPHAT-1**, **TolHAT-1**, and **ThiaHAT-1**, respectively.[S13] The Lennard-Jones (LJ) interaction was truncated at 12 Å with a switching range of 10-12 Å,[S14] and the long-range correction was not incorporated. The Lorentz-Berthelot rule was employed to combine the LJ interaction between unlike pairs of atoms, and the truncation was applied on atom-atom basis both for the real-space part of PME and for LJ. The leap-frog method was adopted to integrate the equation of motion at a time step of 1 fs.[S15] The equilibration consisted of 7 steps. In the 1st, 3rd, and 5th steps, the temperature was elevated linearly against time with a duration of 200 ps from 0 to 100 K, from 100 to 200 K, and from 200 to 300 K, respectively, and in the 2nd, 4th, and 6th, the temperature was fixed at 100, 200, and 300 K respectively, over 300 ps. The 7th step was performed at constant temperature at 300 K over 500 ps. In the 1st to 6th steps, the temperature and pressure were regulated by the velocity rescaling with a time constant of 0.1 ps and the Berendsen barostat with a coupling time of 2 ps, respectively, and in the 7th step of equilibration and the production run, the velocity rescaling with 1 ps and the Parrinello-Rahman barostat at a coupling time of 2 ps were employed.[S16–S18] In both of the Berendsen and Parrinello-Rahman barostats, the isothermal compressibility was set to 4.5×10^{-6} bar^{-1} and the semi-isotropic coupling was employed for the lateral (*a* and *b*) and normal (*c*) directions. The LINCS algorithm was used to fix the lengths of all the bonds involving a hydrogen atom.[S19]

6. **Photo-physical properties**

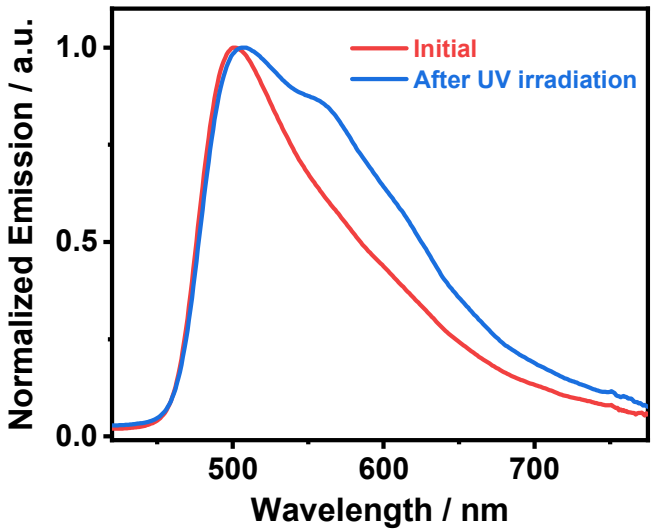

Fig. S22 Emission spectra of **TolHAT-1** before and after irradiation with a wavelength of 400 nm. Clearly, after the irradiation, the material is photodegrading and creating new species with different photoproperties.

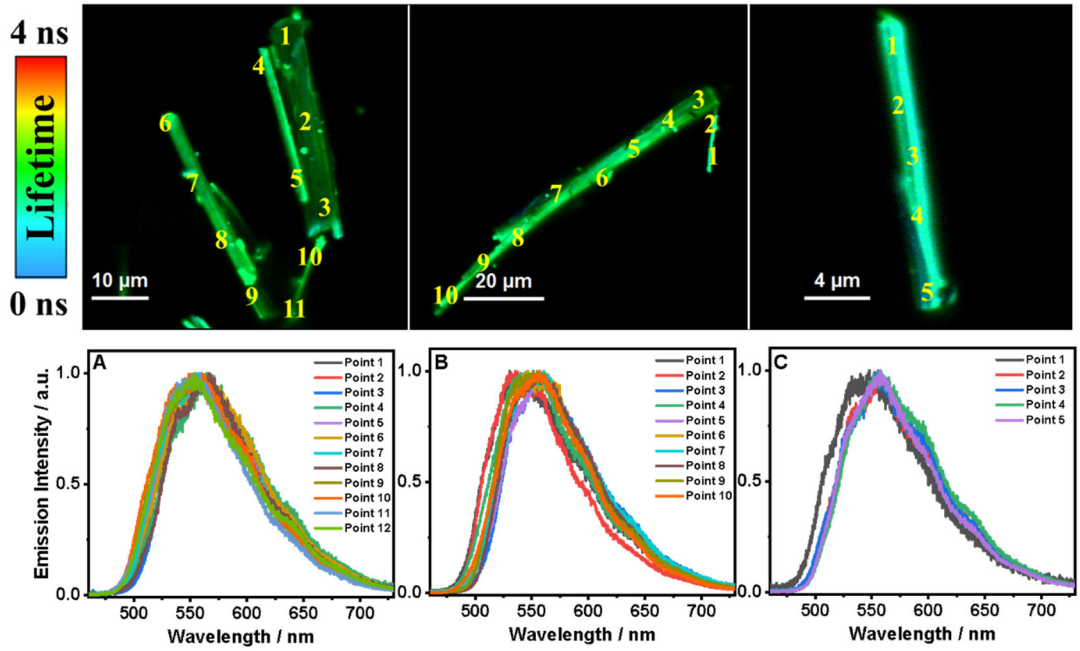

Fig. S23 The top figures are FLIM images of different **ThiaHAT-1** isolated crystals. **A–C)** Emission spectra collected at different points (indicated in the top images) of the **ThiaHAT-1** crystals. The excitation wavelength was 390 nm.

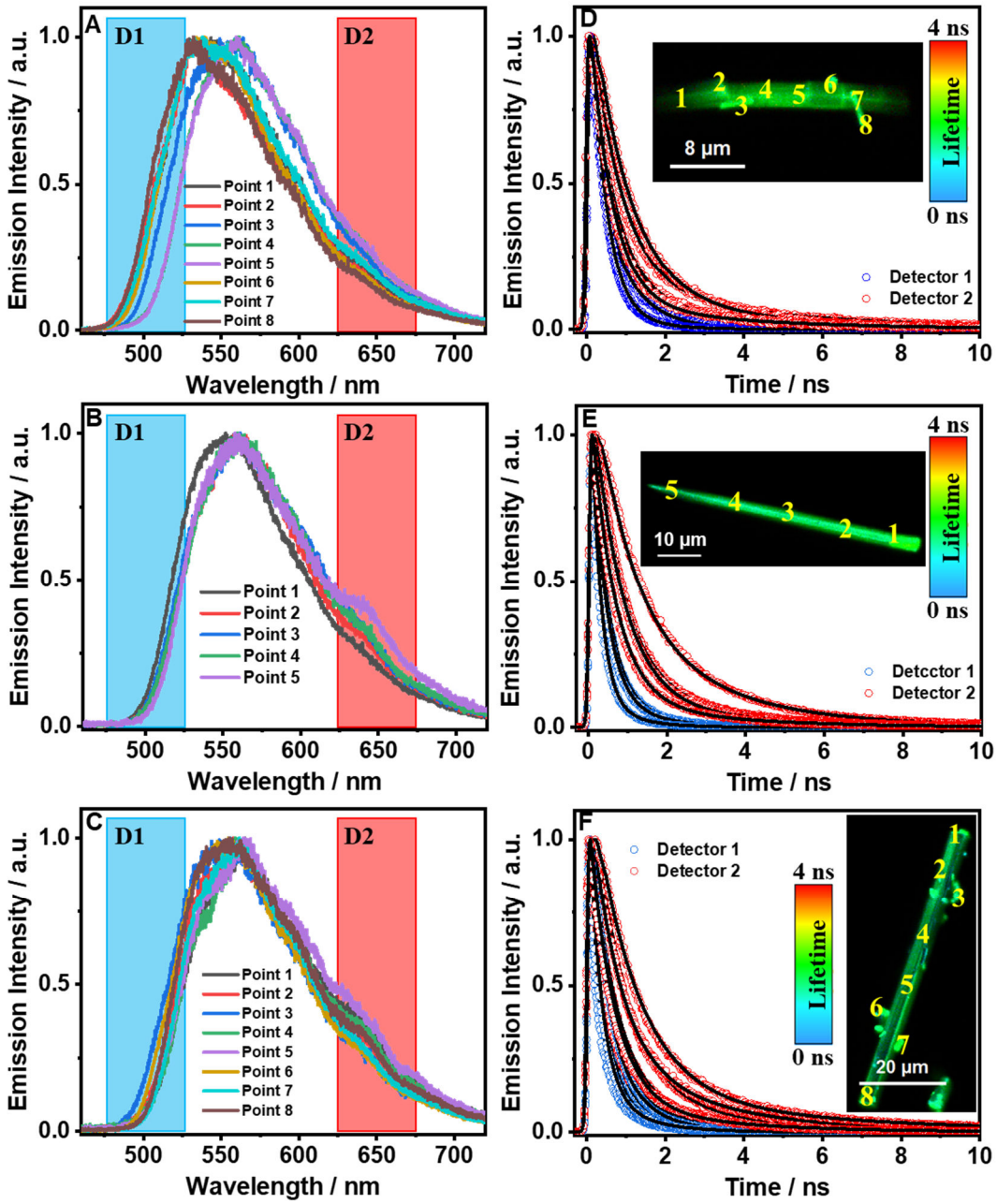

Fig. S24 A-C) Emission spectra and **D-F)** emission decays at selected spectral range using two different filters of transmission to gate at blue and red regions (shown in figures A-C as D1 and D2 regions, respectively) at designated points in the **ThiaHAT-1** crystals. The solid lines are from the best-fit using a multiexponential function. The excitation wavelength was 390 nm.

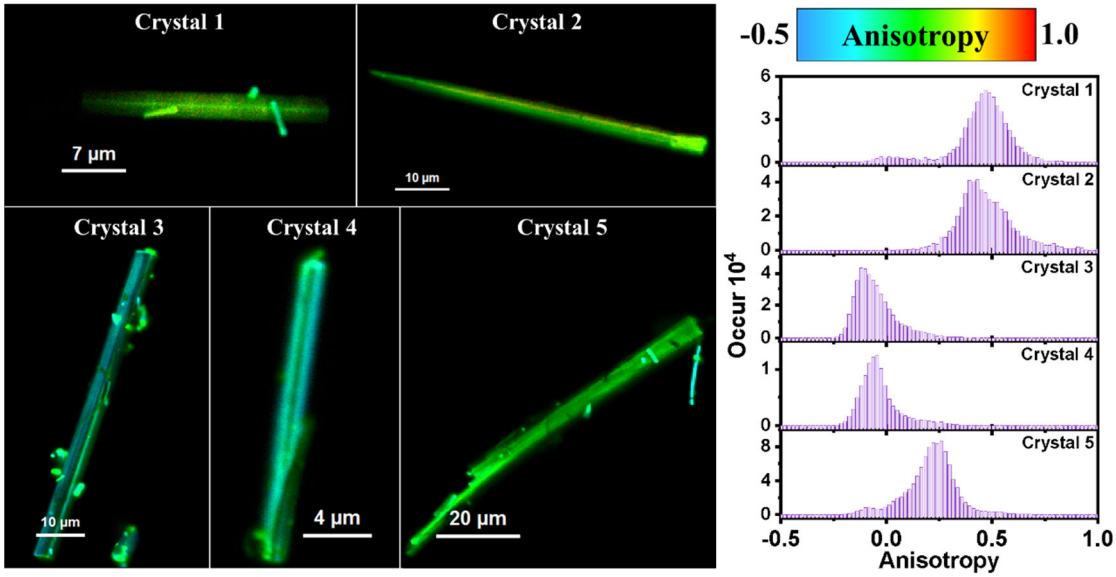

Fig. S25 Figures in the left correspond to the FLIM images of **ThiaHAT-1** crystals having different orientation. The figure in the right is a histogram of the emission anisotropy of those crystals.

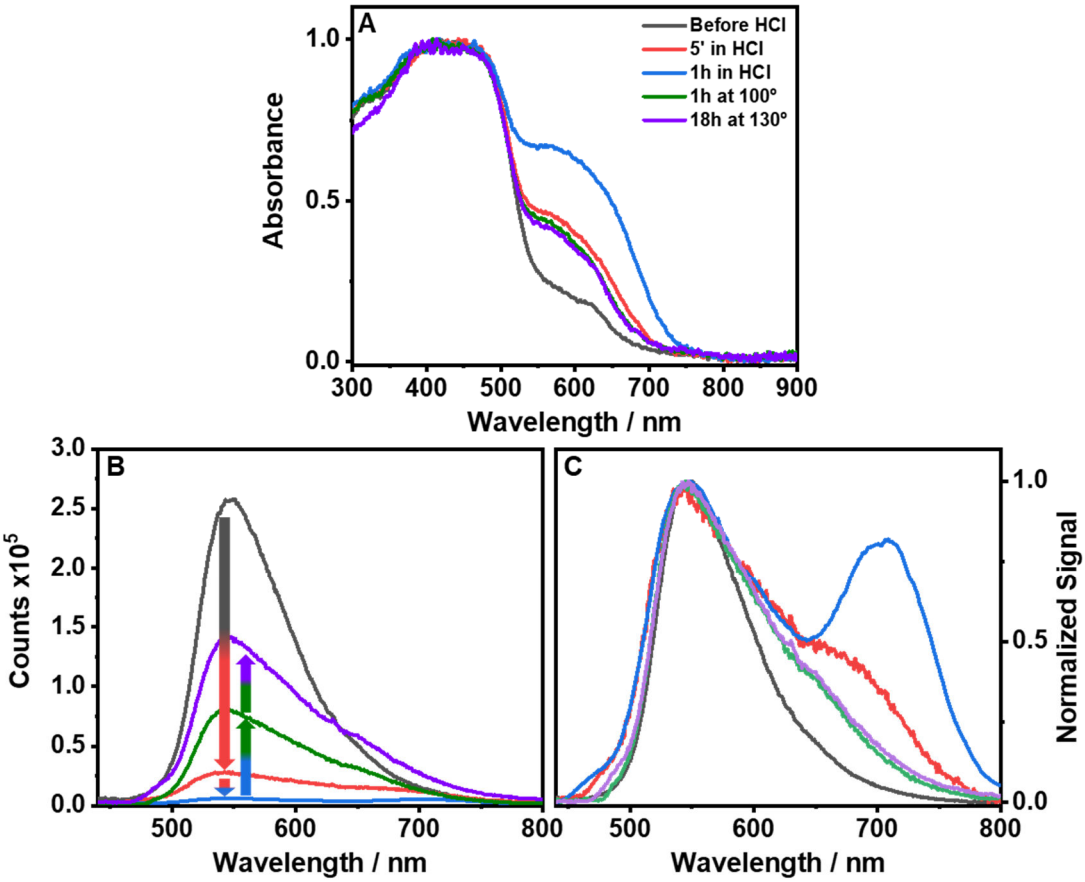

Fig. S26 A) Absorption, **B)** emission and **C)** normalized emission spectra of **ThiaHAT-1** before and after being exposed to vapors of HCl, and the subsequent recover of its photoproperties after heating the sample at 100 ºC for 1 h (green line) and 130 ºC for 18h (purple line), respectively.

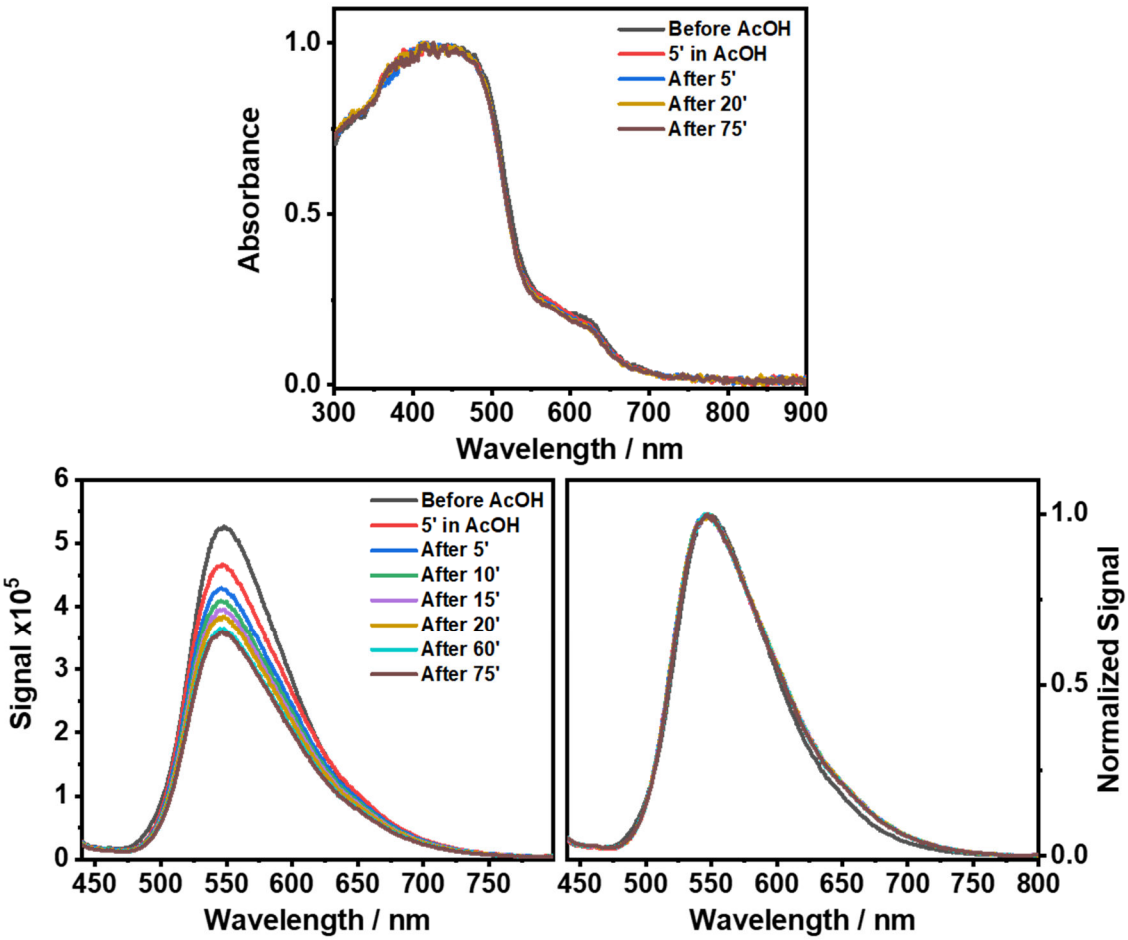

Fig. S27 A) Absorption, **B)** emission and **C)** normalized emission spectra of **ThiaHAT-1** before and after being dosed with AcOH for increasing periods of time.

Table S8. Values of time Constants (τ_i), normalized (to 100) pre-exponential factors (A_i), and contributions ($c_i = \tau_i \times A_i$) obtained from a global multiexponential fit of the emission decays of **ThiaHAT-1** in solid state upon excitation with wavelengths of 371 and 515 nm, and observation as indicated.

Sample	λ_{obs} (nm)	τ_1 (ps) ±20 ps	A_1	c_1	τ_2 (ps) ±50 ps	A_2	c_2	τ_3 (ns) ±0.2 ns	A_3	c_3
ThiaHAT-1 λ_{exc}=371 nm	500	180	77	45	710	22	49	2.5	1	6
	525		69	37		29	52		2	11
	550		61	29		36	53		3	18
	575		53	20		42	54		5	26
	600		47	15		46	55		7	30
	625		42	12		48	52		10	36
	650		38	10		50	50		12	40
	675		36	9		51	48		13	43
	700		34	8		51	46		15	46
ThiaHAT-1 λ_{exc}=515 nm	560	160	48	15	720	45	55	2.3	7	30
	575		48	14		44	55		8	31
	600		46	12		45	52		9	34
	625		45	11		44	50		11	39
	650		45	11		43	47		12	42
	675		45	10		41	44		14	46
	700		46	11		40	40		14	49

Table S9. Values of time constants (τ_i) and normalized (to 100) pre-exponential factors (A_i) and contributions ($c_i = \tau_i \times A_i$) obtained from the best fit of the femtosecond emission decays of **ThiaHAT-1** upon excitation at 410 nm and observation as indicated.

Sample	λ_{obs} (nm)	τ_1 (fs)	A_1	c_1	τ_2 (ps)	A_2	c_2	Offset (ps)
ThiaHAT-1/DMF λ_{exc}=410 nm	450	450	70	19	4.4	30	81	310
	475	450	51	9	4.4	49	91	330
	500	450	31	4	5.0	69	96	320
	550	450	-100	-100	6.5	100	100	290
	600	450	-100	-100	-	100	100	330
	650	450	-77	-25	4.4	-23	-75	320

Table S10. Values of time constants (τ_i) and normalized (to 100) pre-exponential factors (a_i) obtained from the fit of the emission decays collected at different points of the three **TiaHAT-1** isolated crystals showed in **Fig. S24**. Detector 1 and 2 recorded the signal in the blue and red regions (D1 and D2) represented in **Fig. S24**.

		Crystal 1 (FLIM in D)				Crystal 2 (FLIM in E)				Crystal 3 (FLIM in F)			
Point	**Detector**	**τ_1 (ns)**	**a_1**	**τ_2 (ns)**	**a_2**	**τ_1 (ns)**	**a_1**	**τ_2 (ns)**	**a_2**	**τ_1 (ns)**	**a_1**	**τ_2 (ns)**	**a_2**
1	1	0.3	75	0.7	25	0.3	80	0.8	20	0.3	86	0.8	14
	2	0.6	67	2.5	33	0.8	69	2.7	31	0.7	71	2.7	9
2	1	0.3	85	0.7	15	0.3	66	0.8	34	0.3	82	0.9	18
	2	0.6	73	2.5	27	0.7	87	2.7	13	0.7	89	2.7	11
3	1	0.3	33	0.8	67	0.3	66	0.8	34	0.3	73	0.9	27
	2	0.7	75	2.5	25	0.7	86	2.7	14	0.7	83	2.7	13
4	1	0.2	48	0.8	52	0.3	74	0.8	26	0.3	87	0.9	13
	2	0.9	79	2.5	21	0.7	88	2.7	12	0.7	92	2.7	8
5	1	0.2	40	0.5	60	0.3	90	0.8	10	0.3	86	0.9	14
	2	0.8	77	2.5	23	0.7	90	2.7	10	0.7	92	2.7	8
6	1	0.3	83	0.8	17					0.3	66	0.9	34
	2	0.8	85	2.5	15					0.7	76	2.7	24
7	1	0.3	82	0.8	18					0.3	65	0.9	35
	2	0.6	85	2.5	15					0.7	65	2.7	35
8	1	0.3	87	0.8	13					0.3	80	0.9	20
	2	0.6	88	2.5	12					0.7	90	2.7	10

7. NMR spectra of the newly synthesized compound

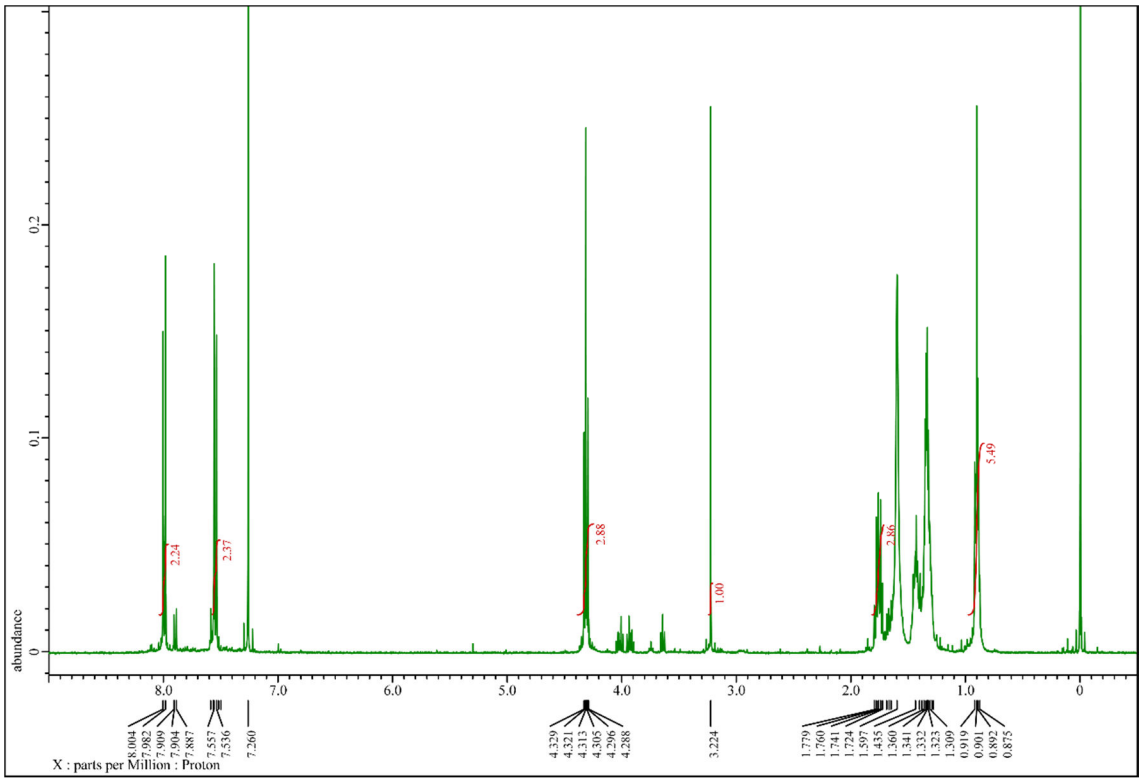

Fig. S28 ^{1}H NMR (400 MHz, $CDCl_3$) spectrum of **2**.

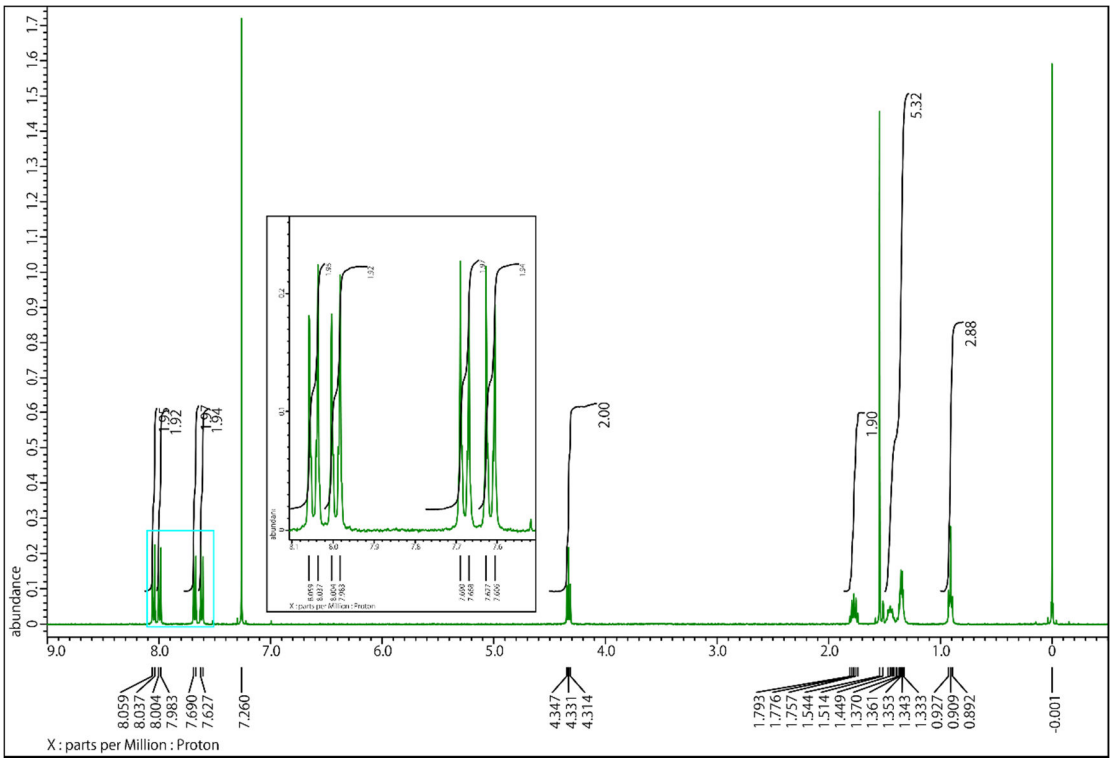

Fig. S29 ^{1}H NMR (400 MHz, $CDCl_3$) spectrum of **3a**.

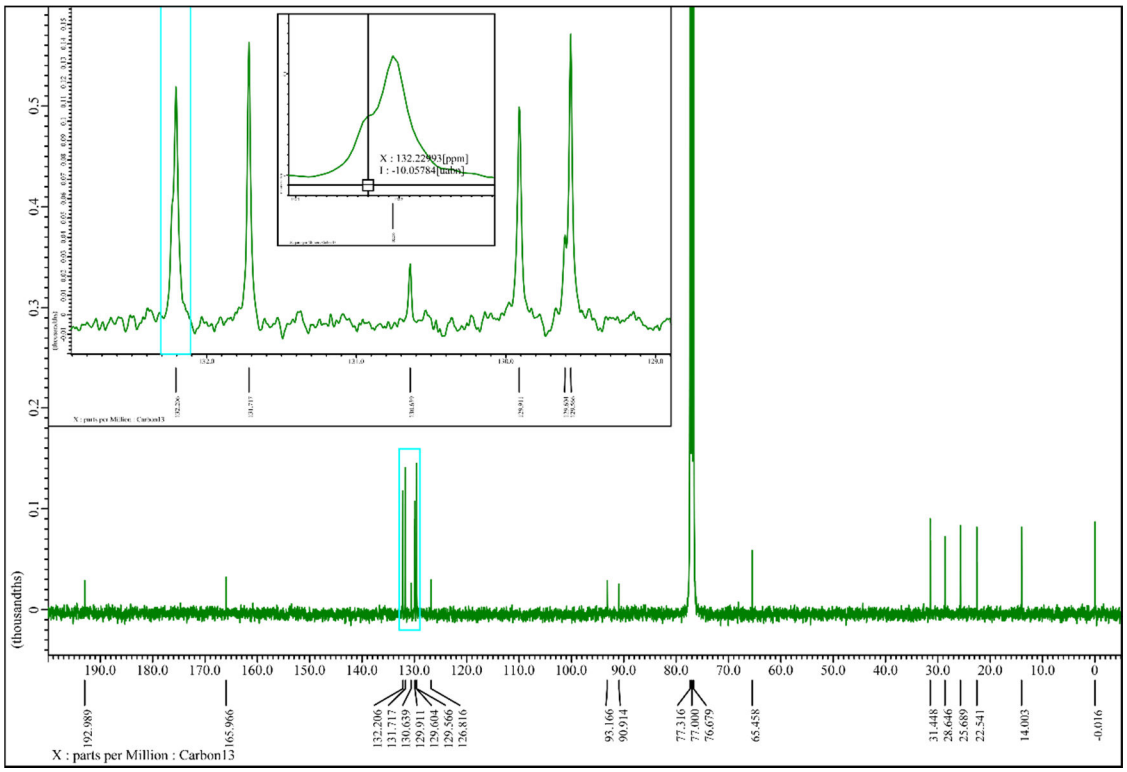

Fig. S30 ^{13}C NMR (100 MHz, $CDCl_3$) spectrum of **3a**.

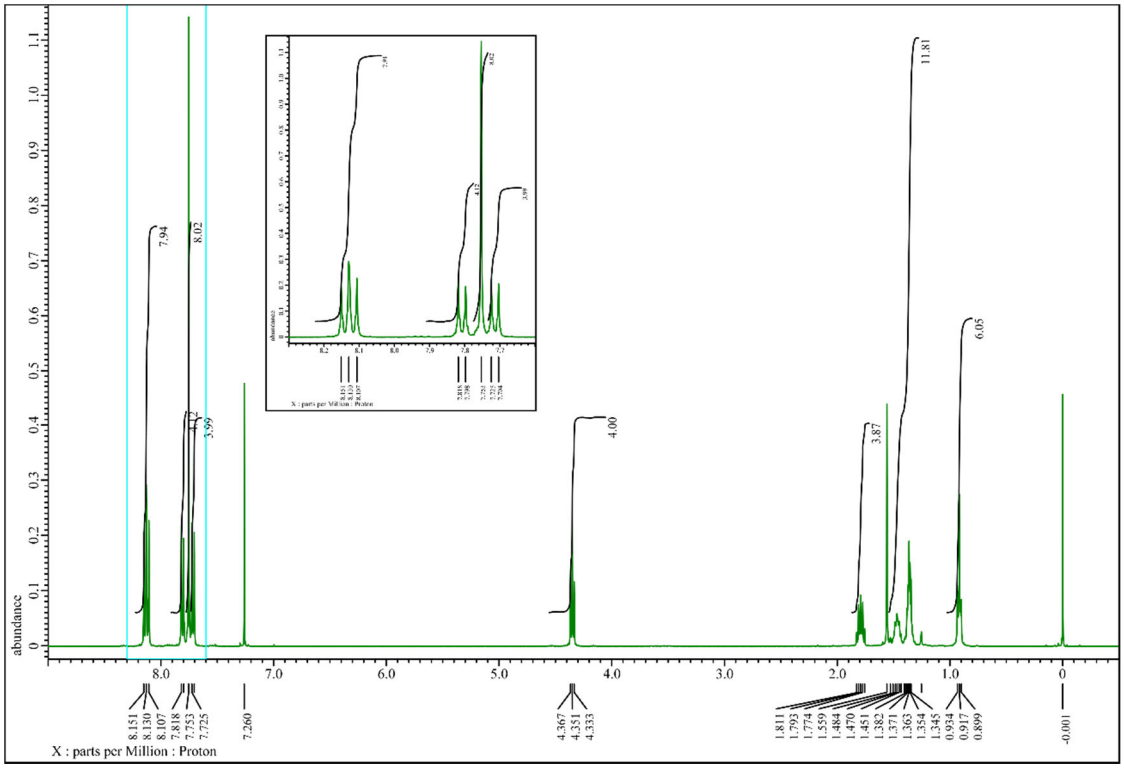

Fig. S31 ^{1}H NMR (400 MHz, $CDCl_3$) spectrum of **3b**.

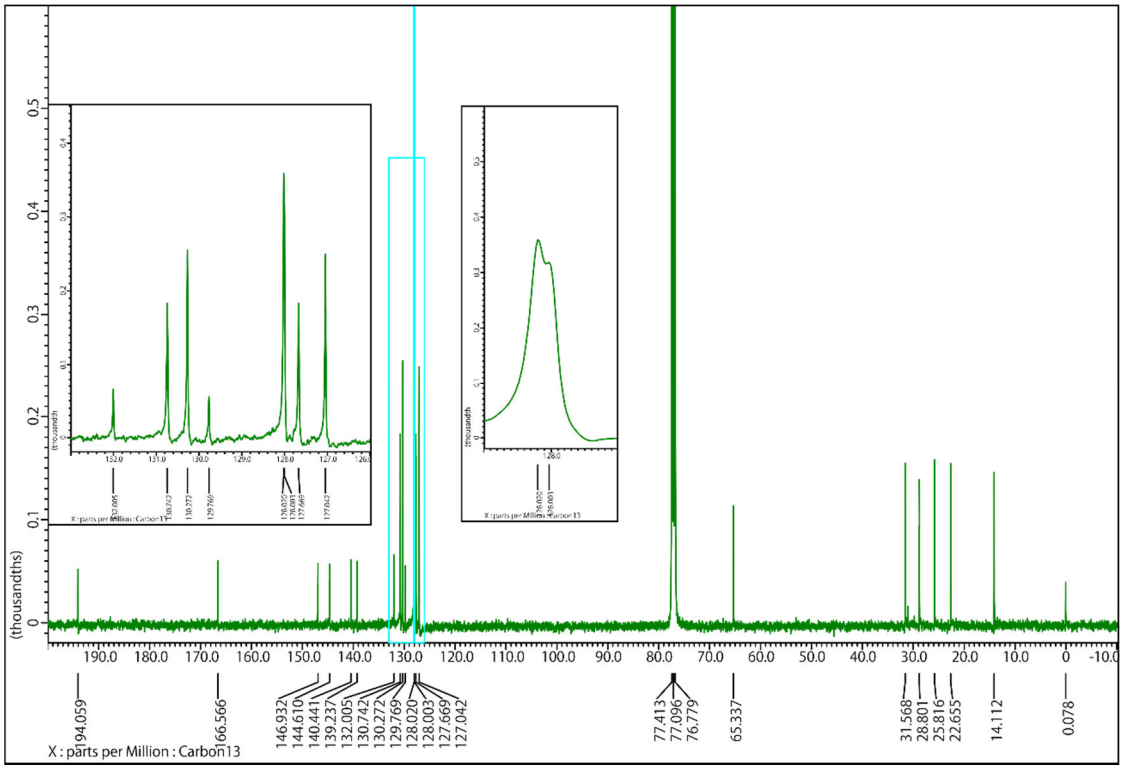

Fig. S32 ^{13}C NMR (100 MHz, $CDCl_3$) spectrum of **3b**.

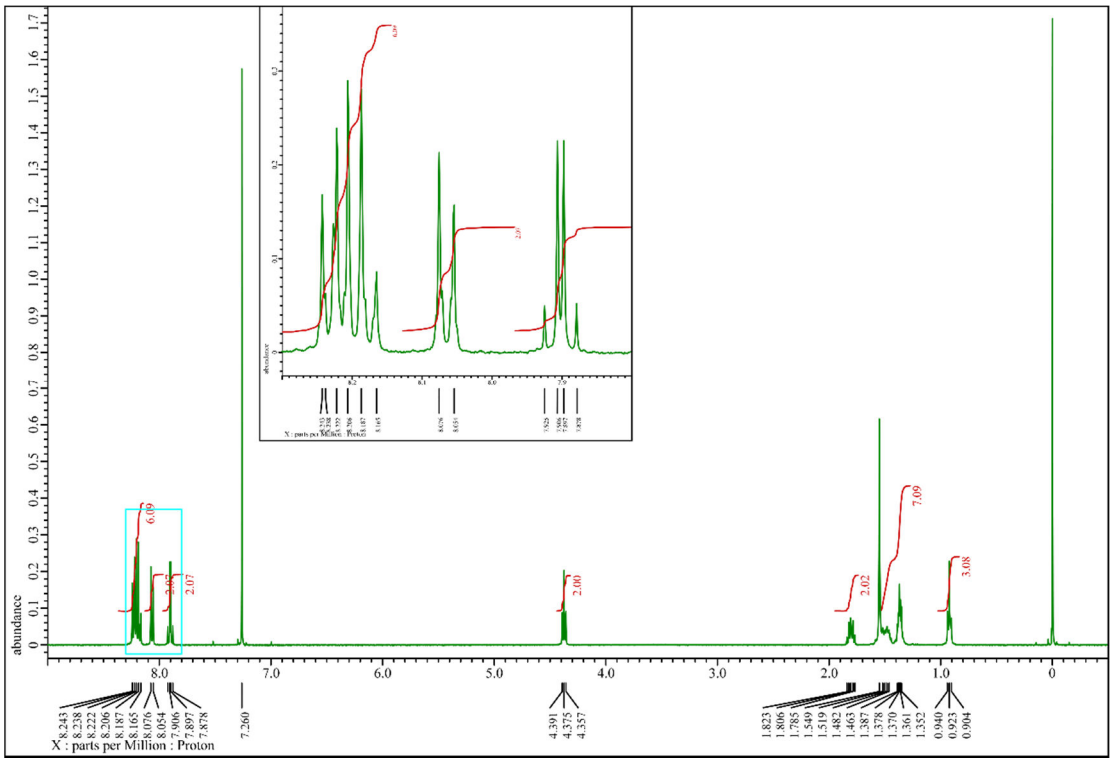

Fig. S33 ^{1}H NMR (400 MHz, $CDCl_3$) spectrum of **3c**.

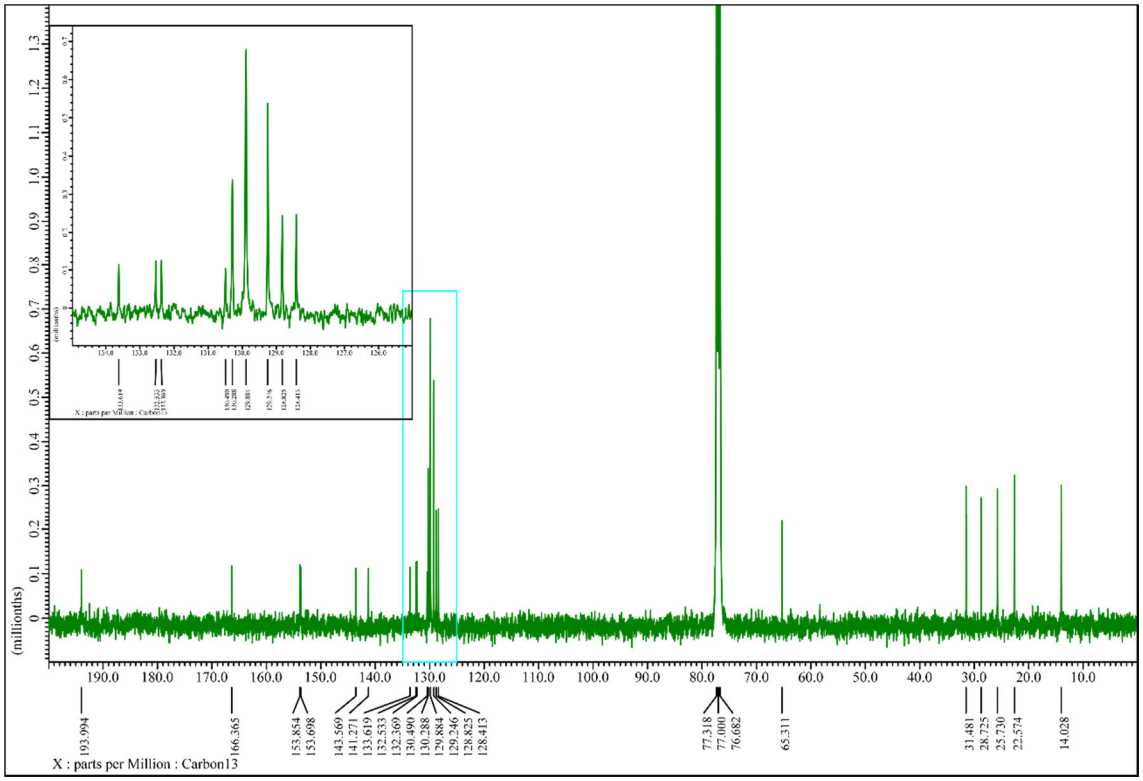

Fig. S34 ^{13}C NMR (100 MHz, $CDCl_3$) of **3c**.

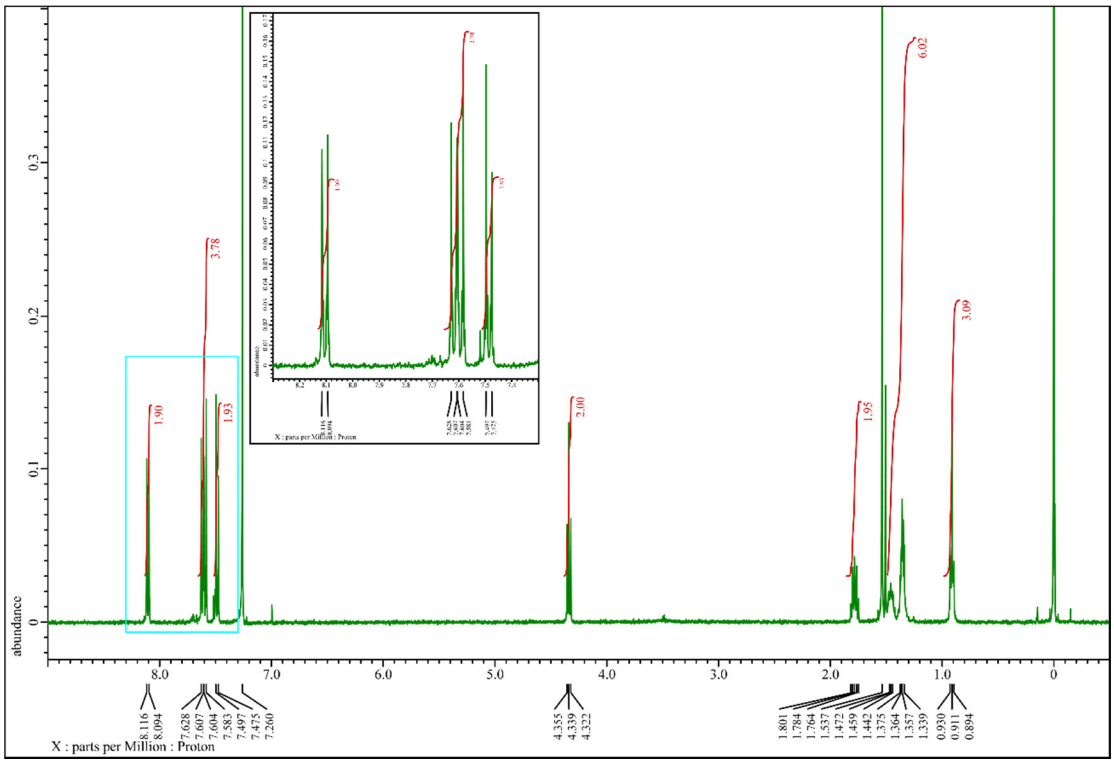

Fig. S35 ^{1}H NMR (400 MHz, $CDCl_3$) spectrum of **5**.

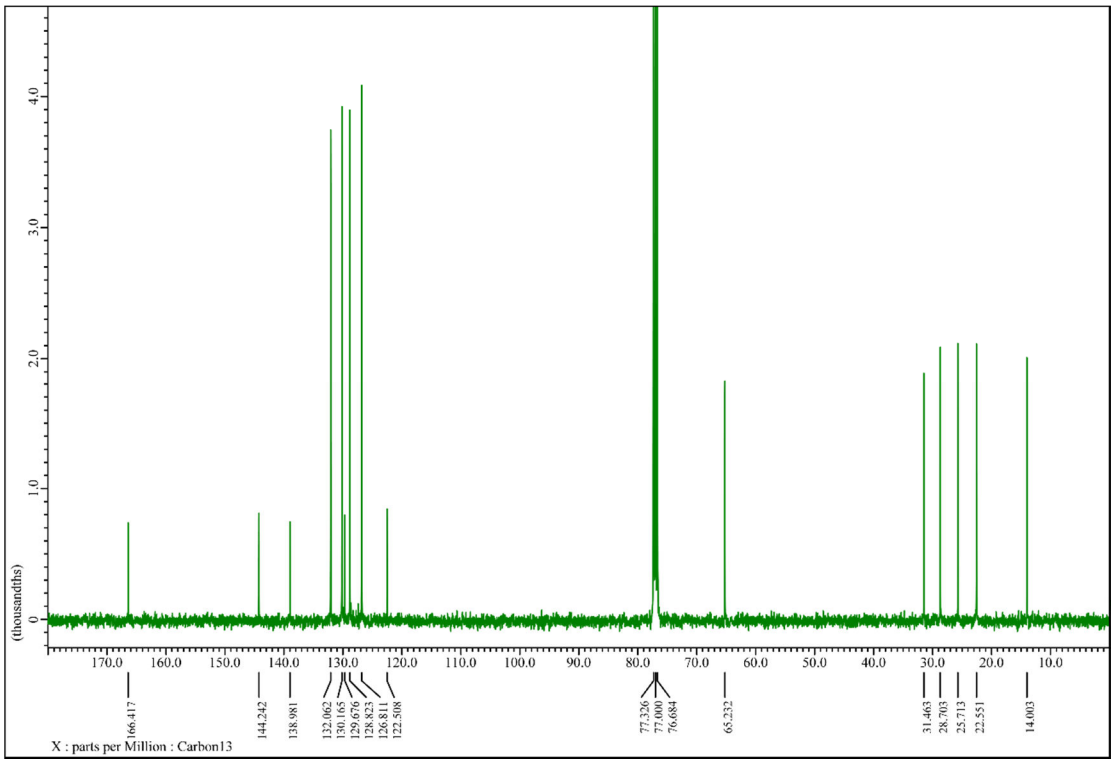

Fig. S36 ^{13}C NMR (100 MHz, $CDCl_3$) spectrum of **5**.

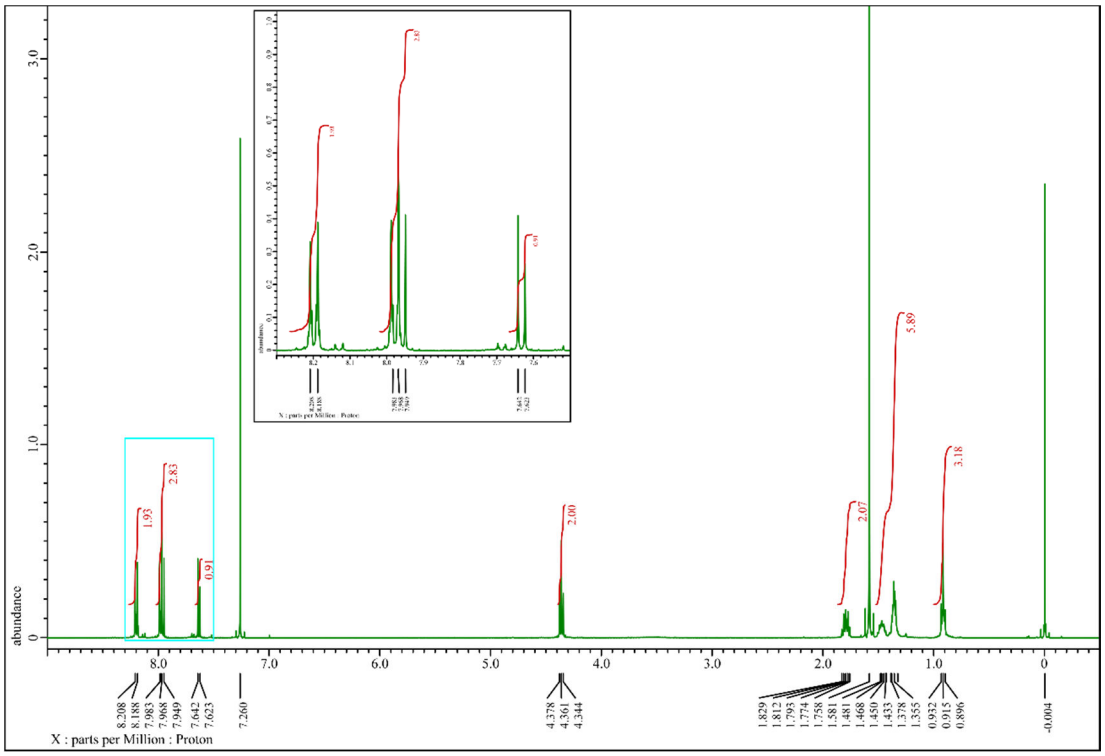

Fig. S37 ^{1}H NMR (400 MHz, $CDCl_3$) spectrum of **6**.

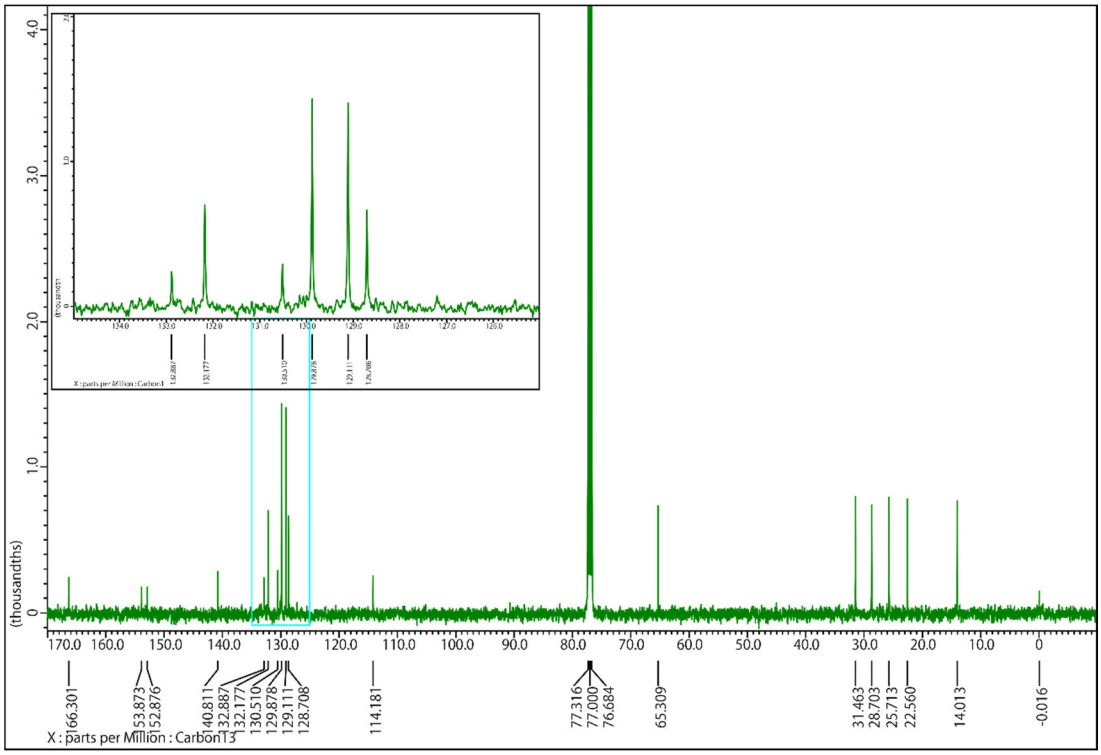

Fig. S38 ^{13}C NMR (100 MHz, $CDCl_3$) spectrum of **6**.

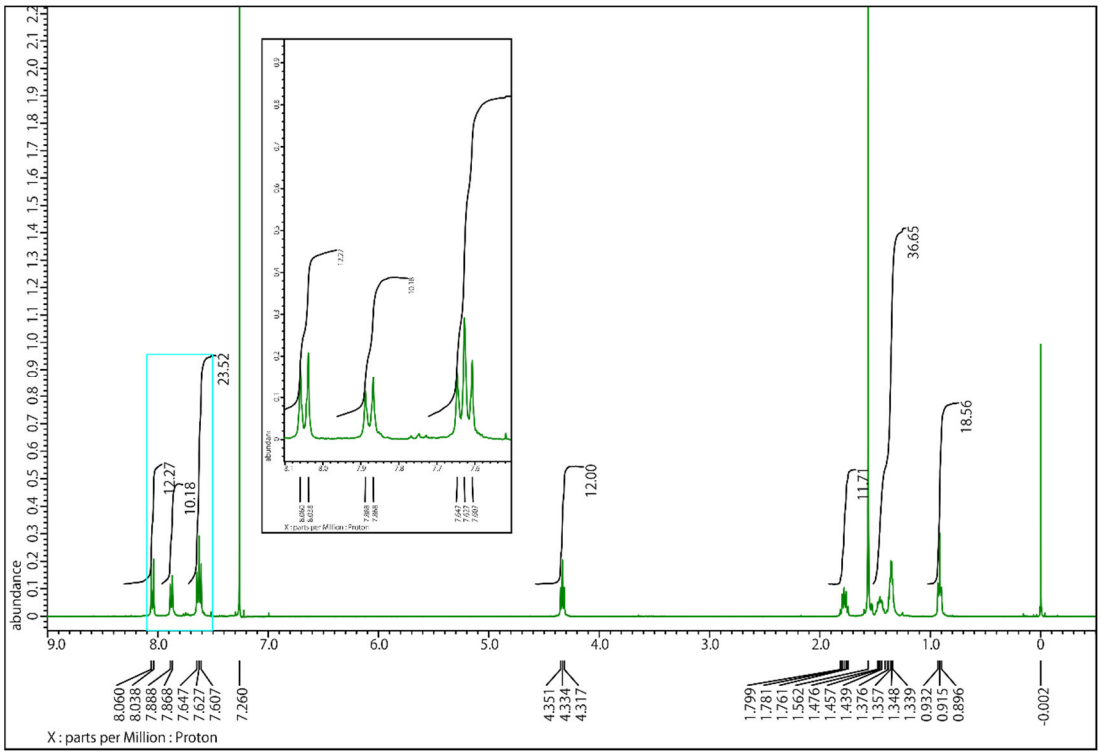

Fig. S39 ^{1}H NMR (400 MHz, $CDCl_3$) spectrum of **9a**.

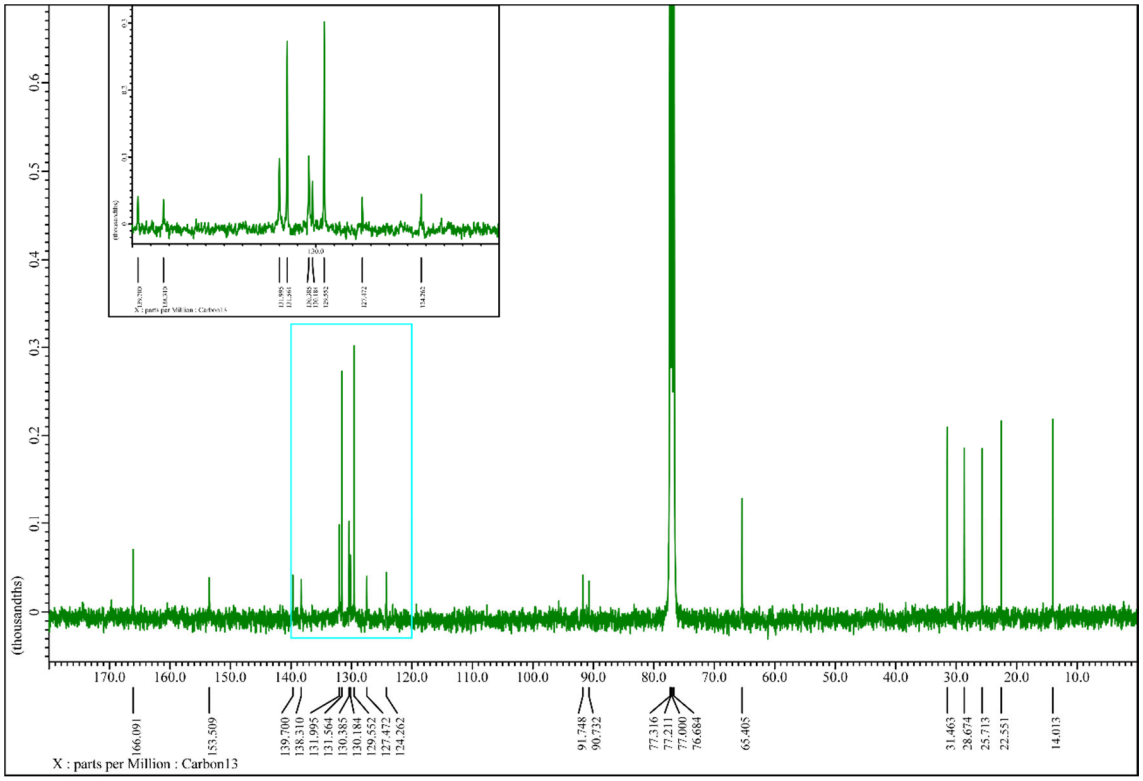

Fig. S40 ^{13}C NMR (100 MHz, $CDCl_3$) spectrum of **9a**.

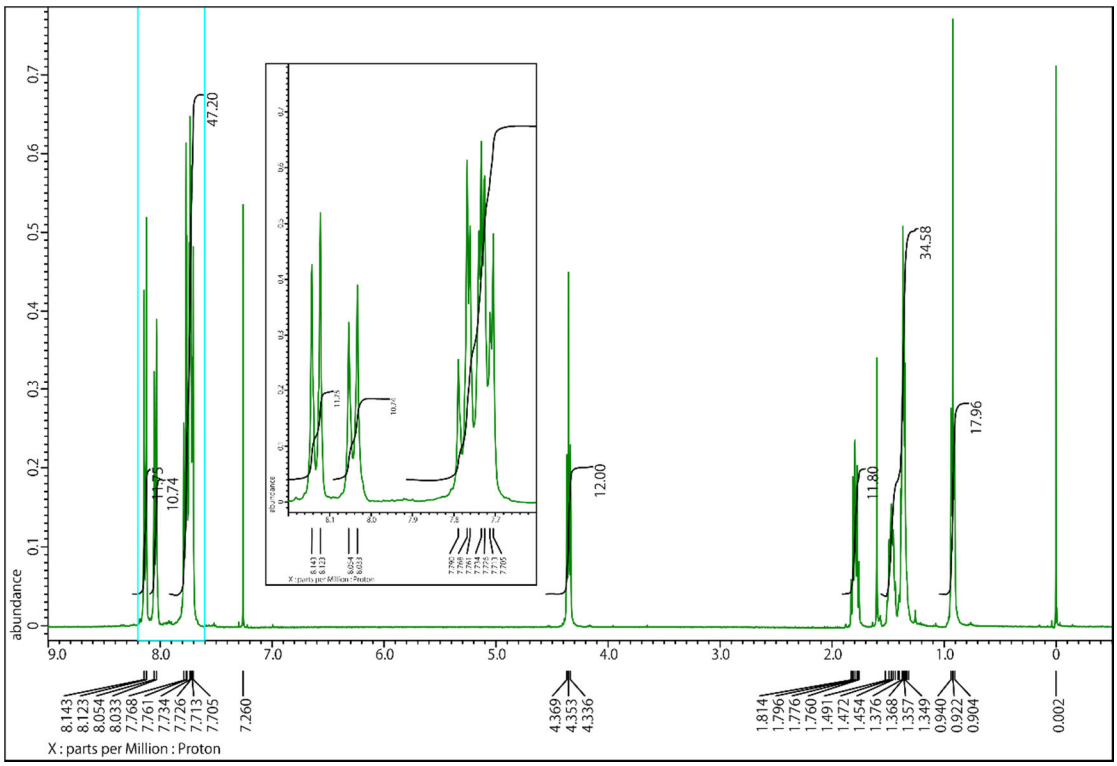

Fig. S41 ^{1}H NMR (400 MHz, $CDCl_3$) spectrum of **9b**.

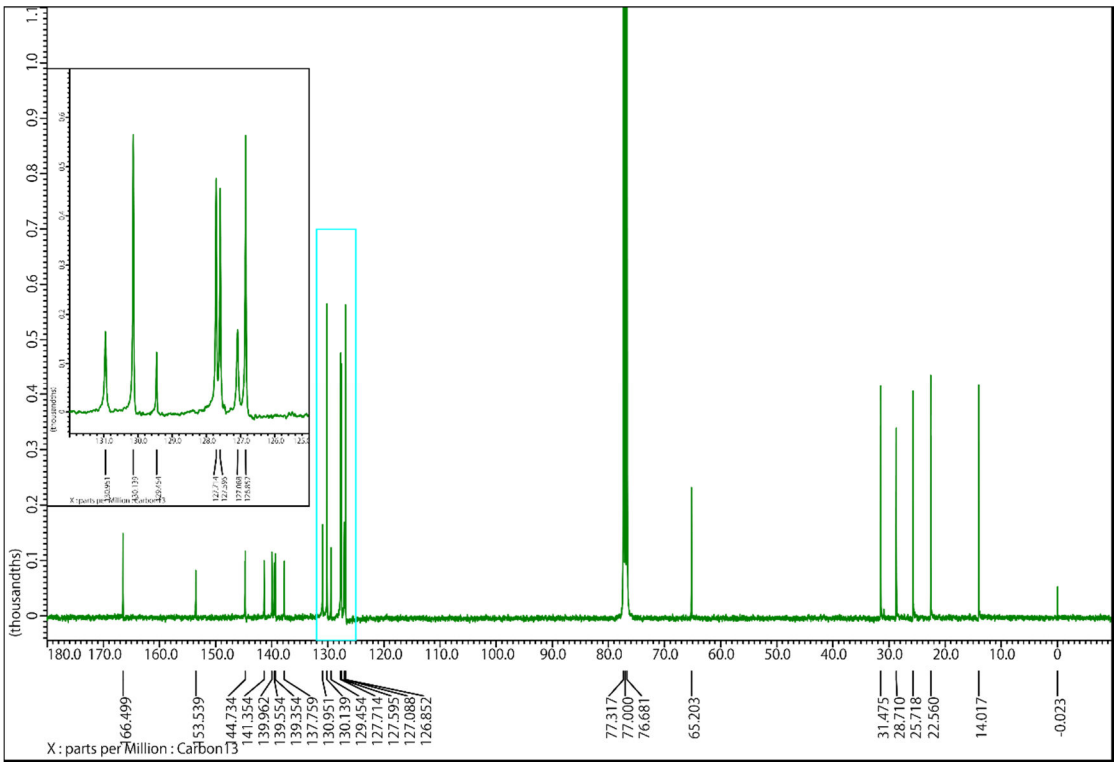

Fig. S42 ^{13}C NMR (100 MHz, $CDCl_3$) spectrum of **9b**.

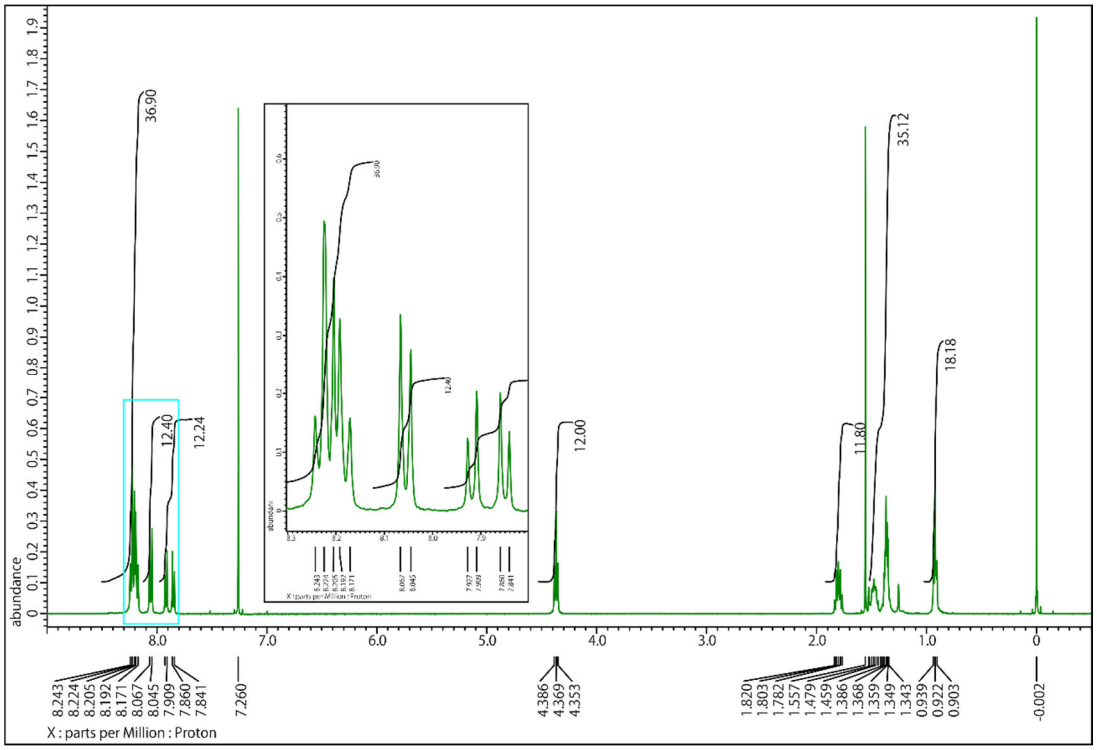

Fig. S43 ^{1}H NMR (400 MHz, $CDCl_3$) spectrum of **9c**.

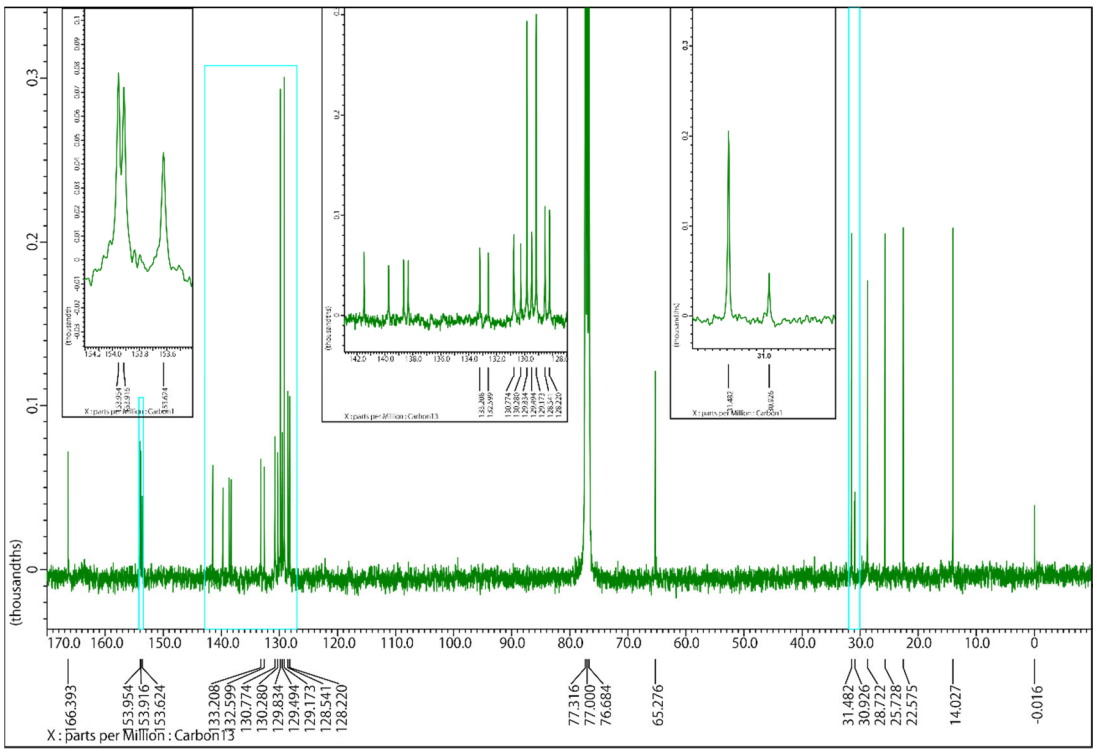

Fig. S44 ^{13}C NMR (100 MHz, $CDCl_3$) spectrum of **9c**.

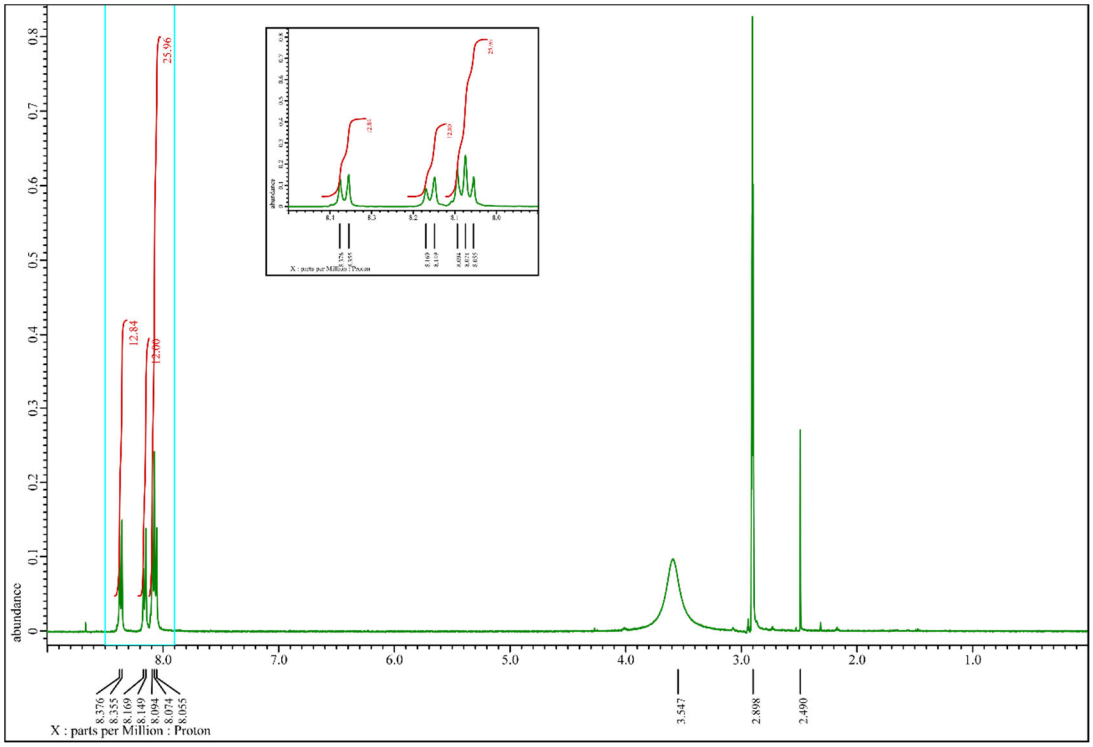

Fig. S45 ^{1}H NMR (400 MHz, DMSO-d_6) spectrum of **TolHAT**.

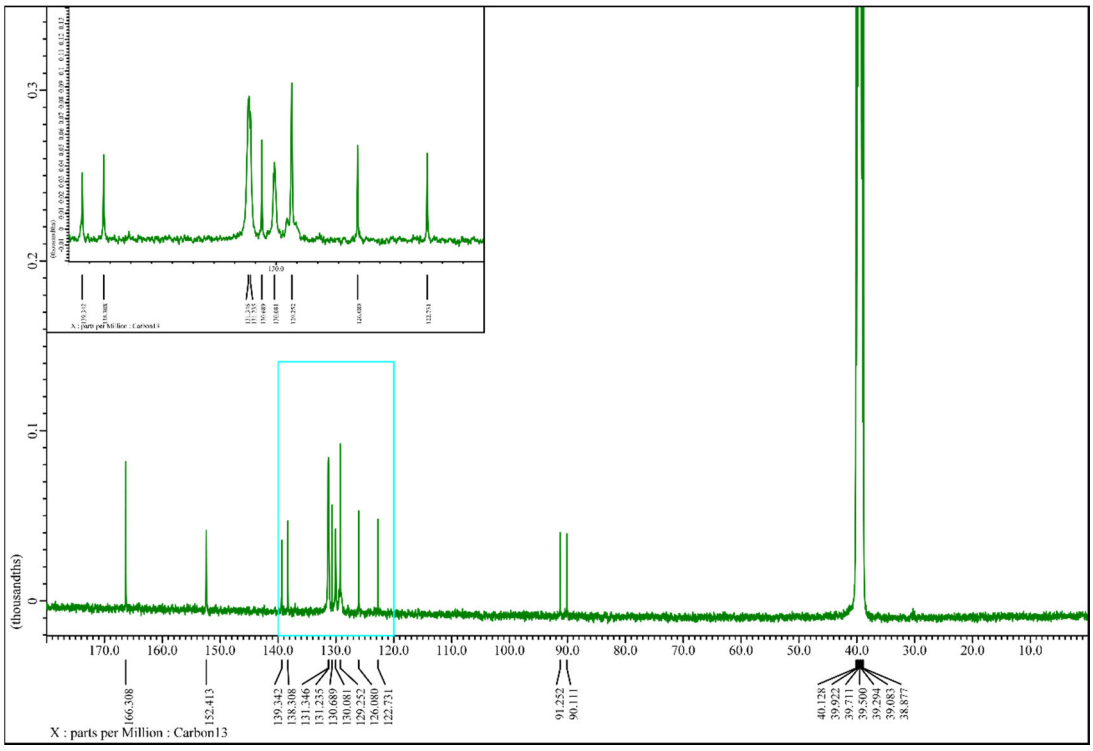

Fig. S46 ^{13}C NMR (100 MHz, DMSO-d_6) spectrum of **TolHAT**.

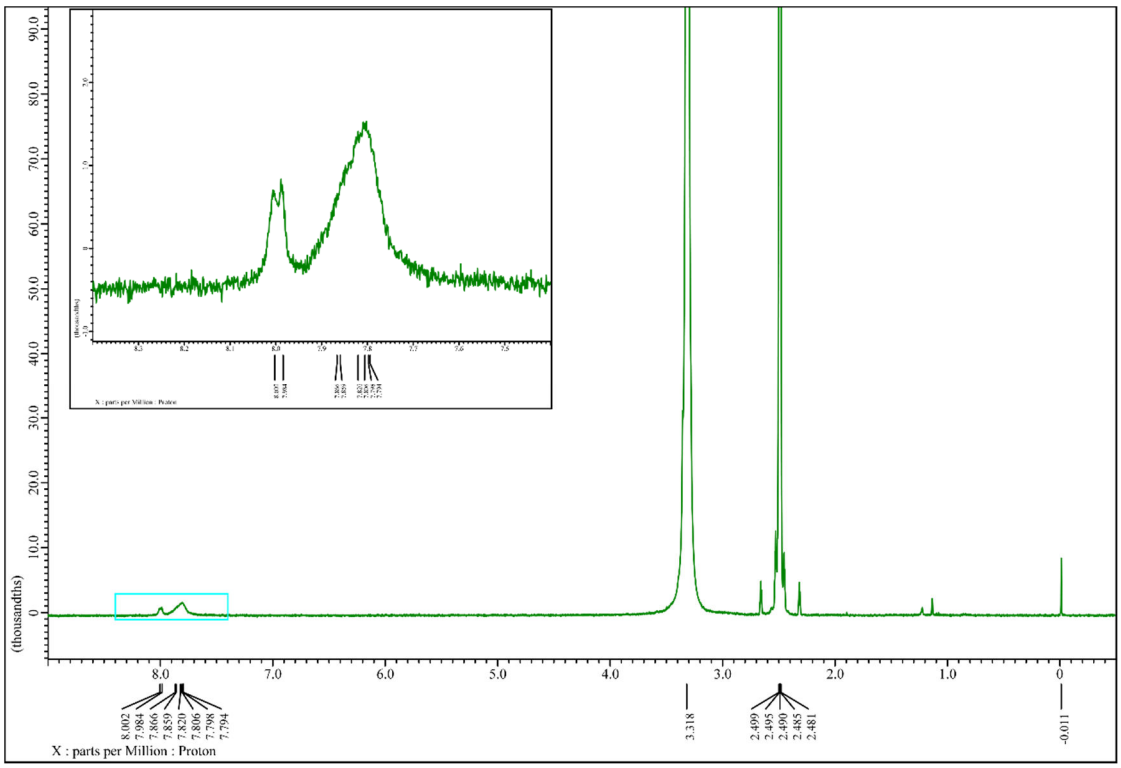

Fig. S47 ^{1}H NMR (400 MHz, DMSO-d_6) spectrum of **TPHAT**.

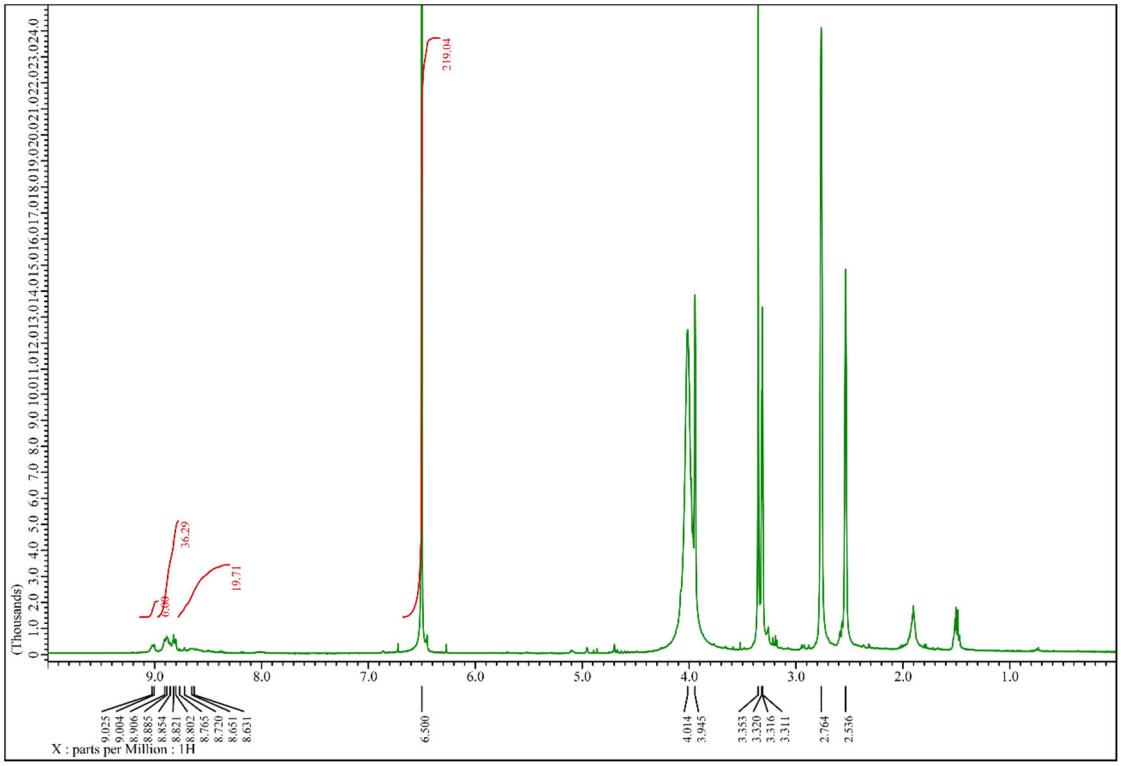

Fig. S48 ^{1}H NMR (400 MHz, NMP-d_9) of **ThiaHAT**.

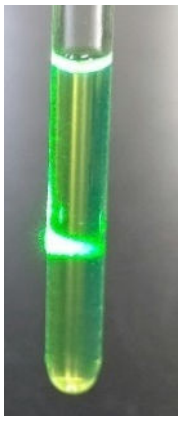

Fig. S49 Tyndall effect of a 2.6 M-NMP-d_9 solution of **ThiaHAT**. This indicates molecular aggregation forms in this concentration.

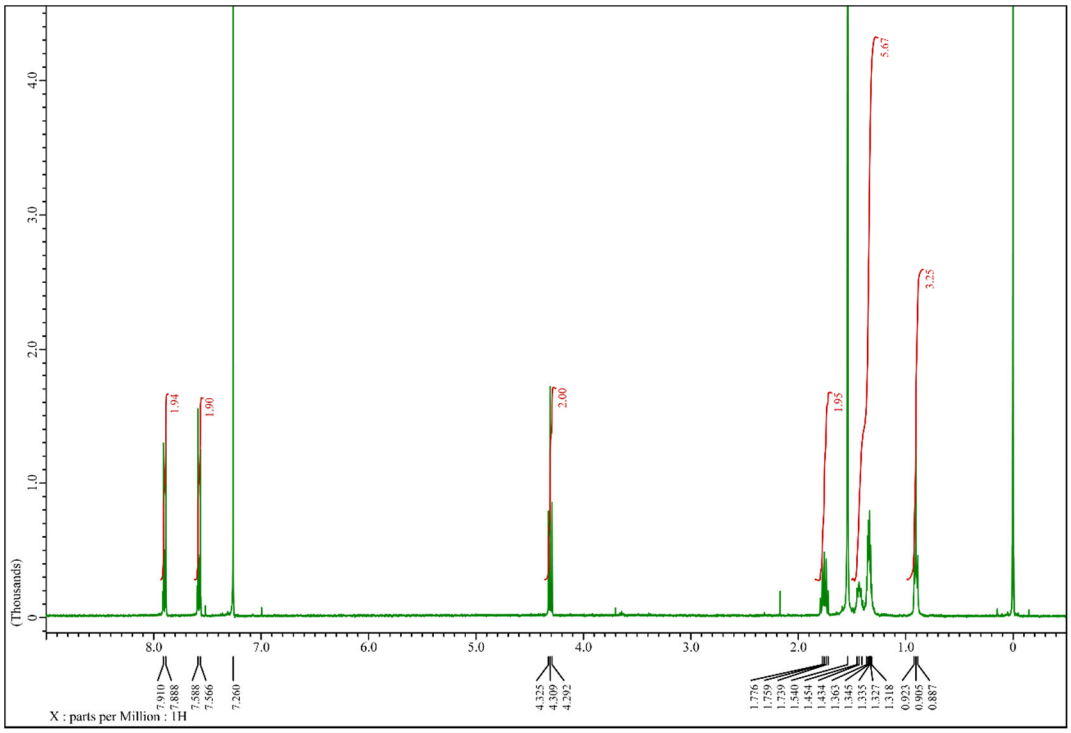

Fig. S50 ^{1}H NMR (400 MHz, $CDCl_3$) spectrum of **10**.

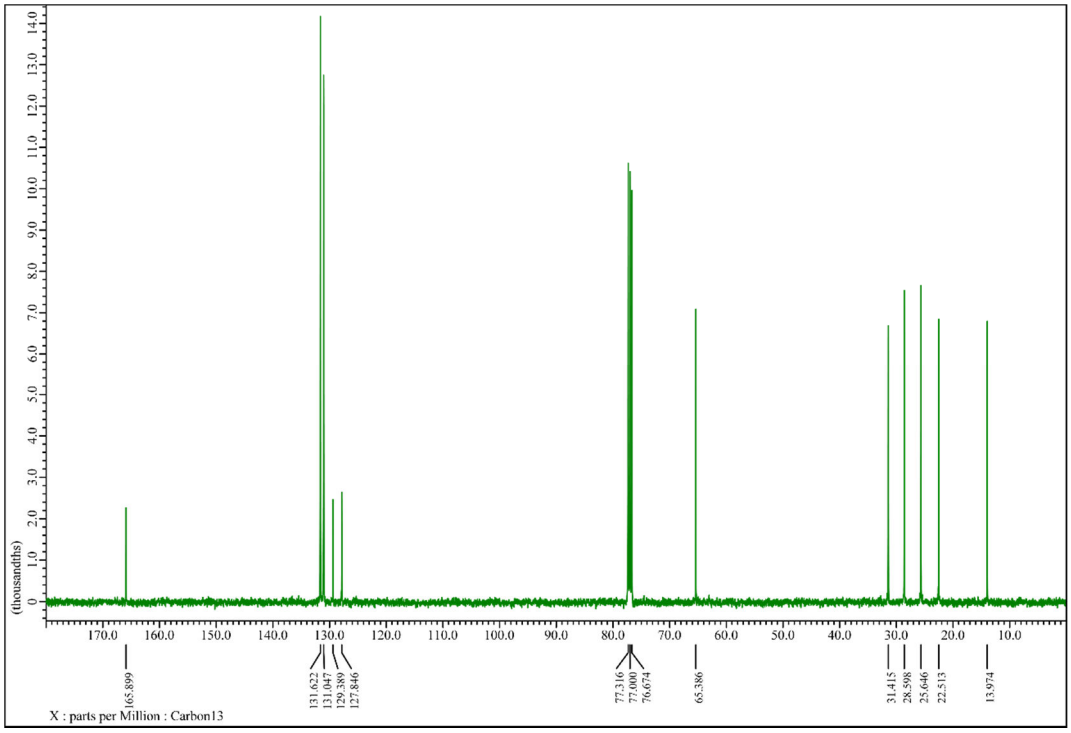

Fig. S51 ^{13}C NMR (100 MHz, $CDCl_3$) spectrum of **10**.

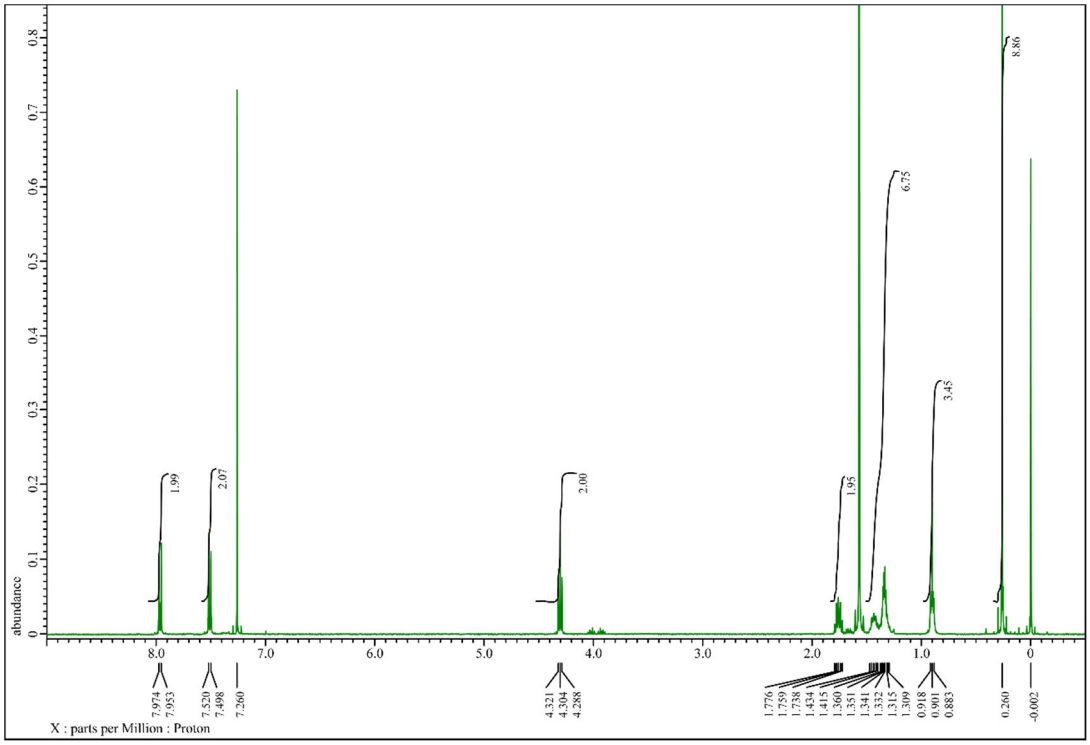

Fig. S52 ^{1}H NMR (400 MHz, $CDCl_3$) spectrum of **11**.

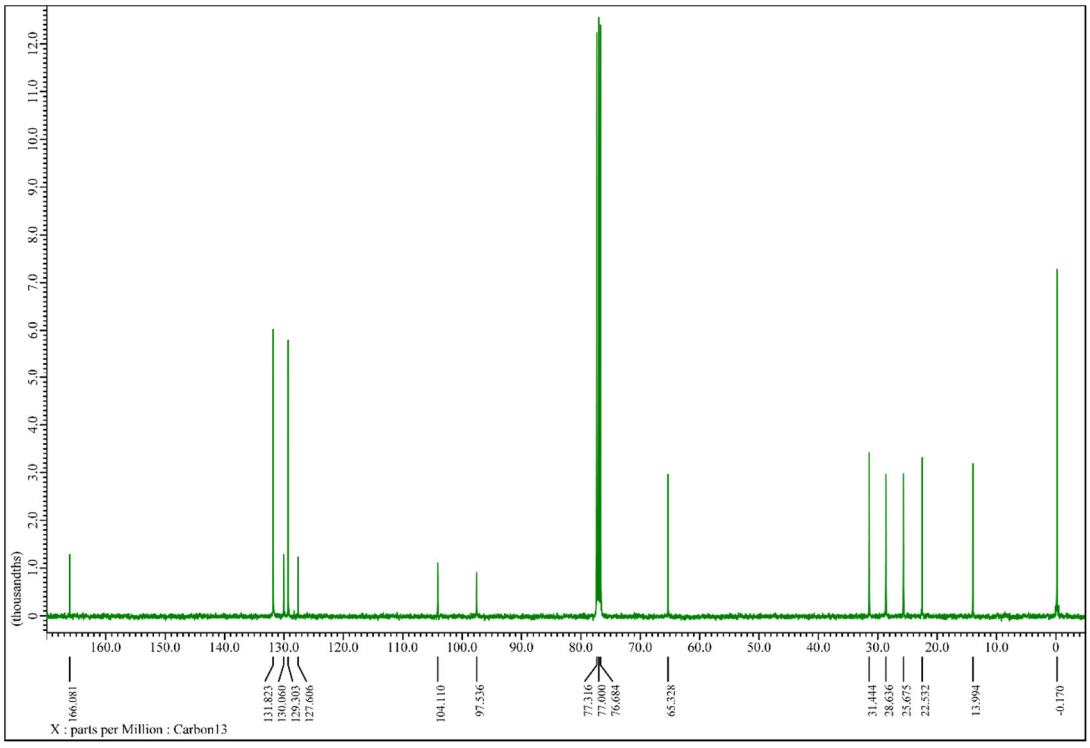

Fig. S53 ^{13}C NMR (100 MHz, $CDCl_3$) spectrum of **11**.

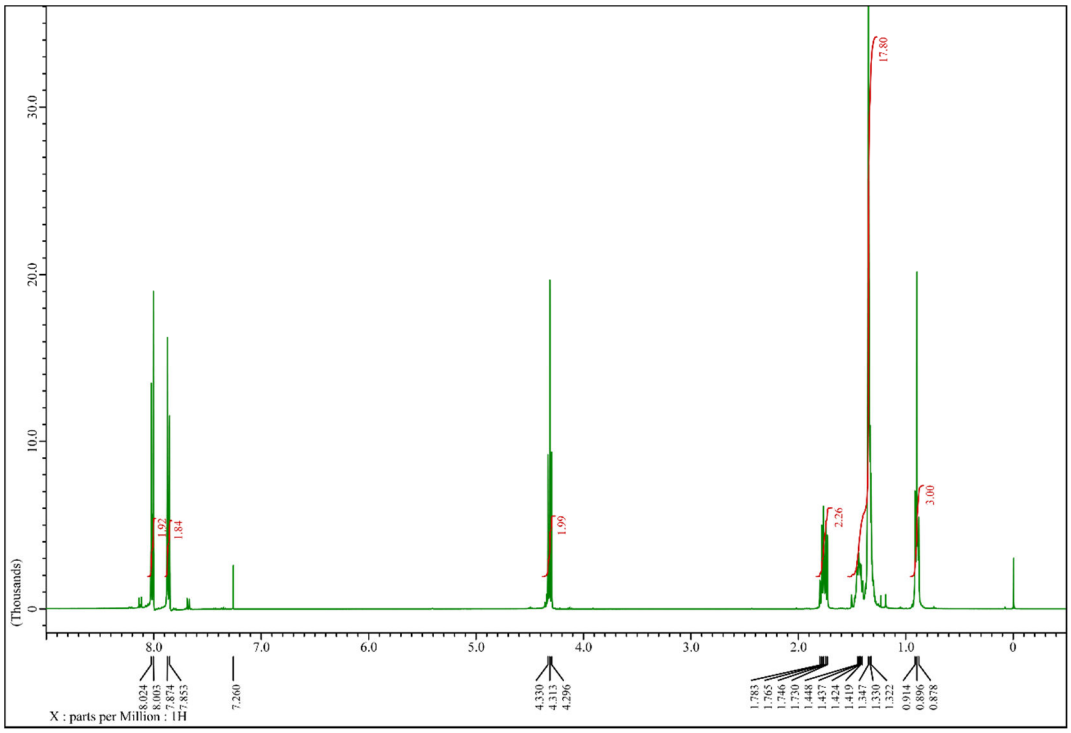

Fig. S54 ^{1}H NMR (400 MHz, $CDCl_3$) spectrum of **12**.

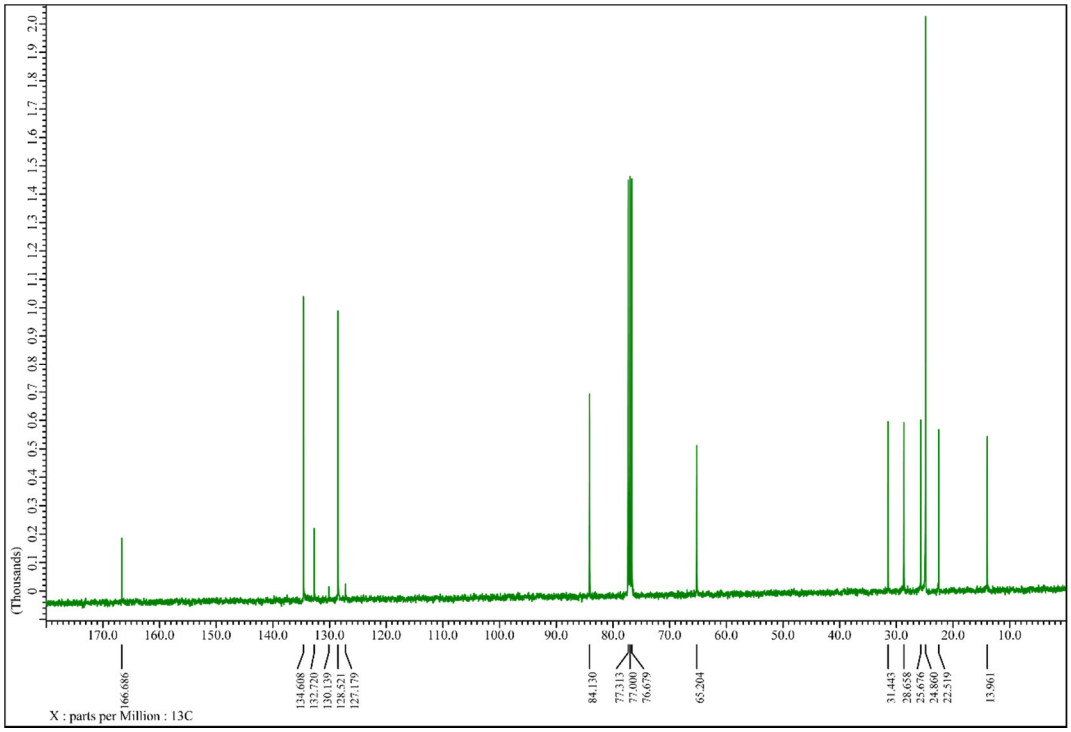

Fig. S55 ^{13}C NMR (100 MHz, $CDCl_3$) spectrum of **12**.

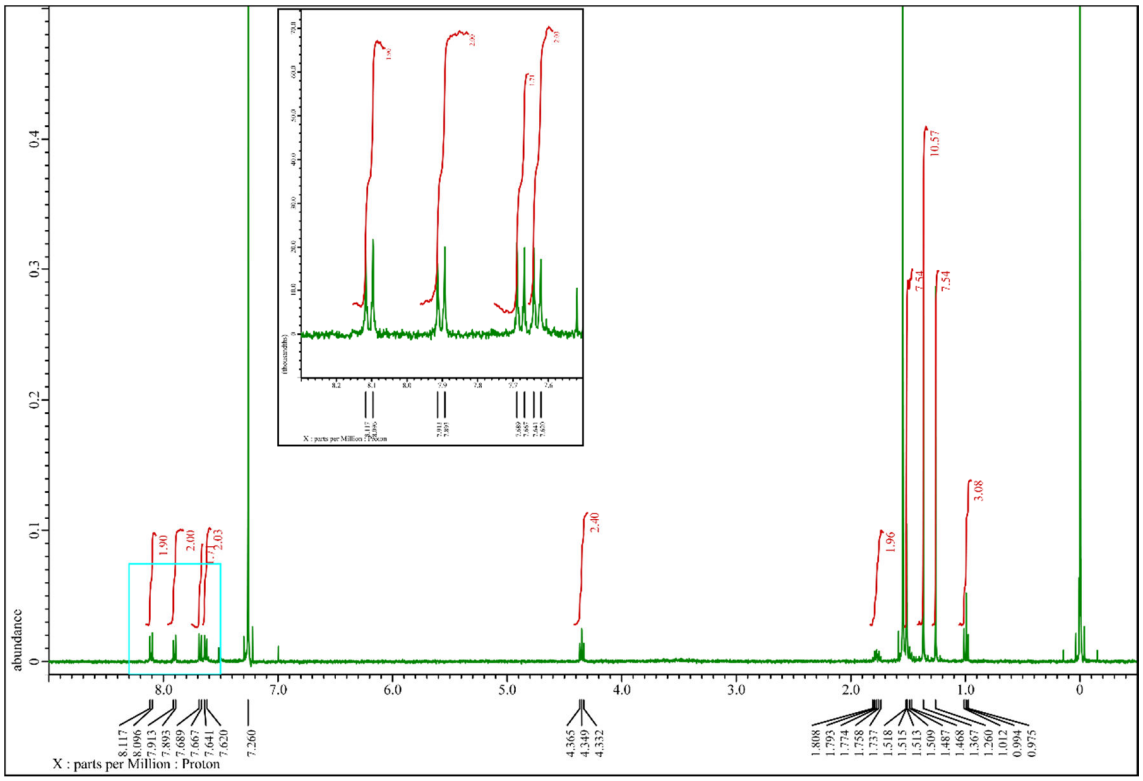

Fig. S56 ^{1}H NMR (400 MHz, $CDCl_3$) spectrum of **13**.

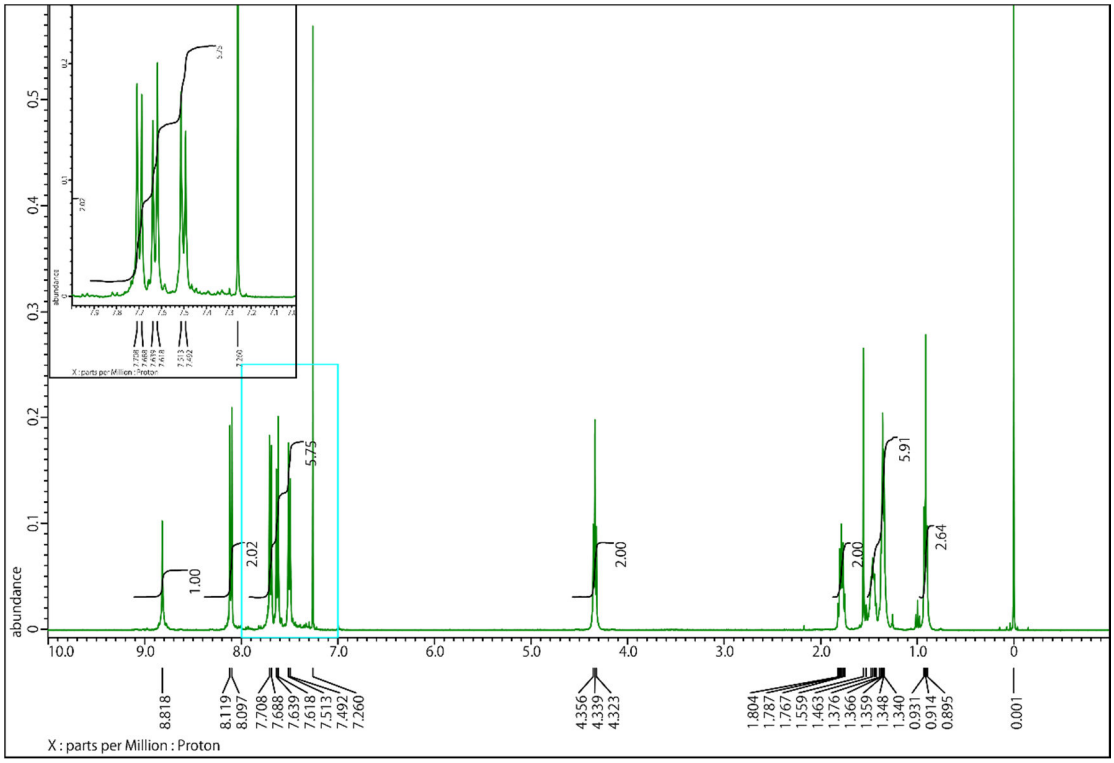

Fig. S57 ^{1}H NMR (400 MHz, $CDCl_3$) spectrum of **14**.

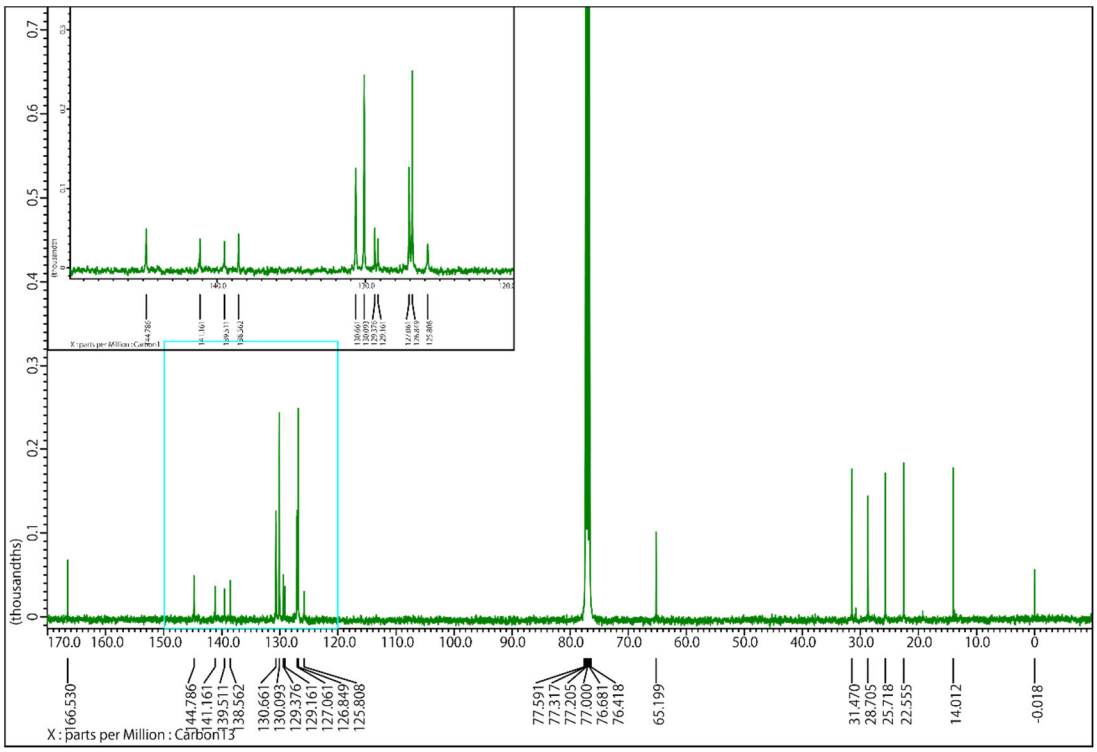

Fig. S58 ^{13}C NMR (100 MHz, $CDCl_3$) spectrum of **14**.

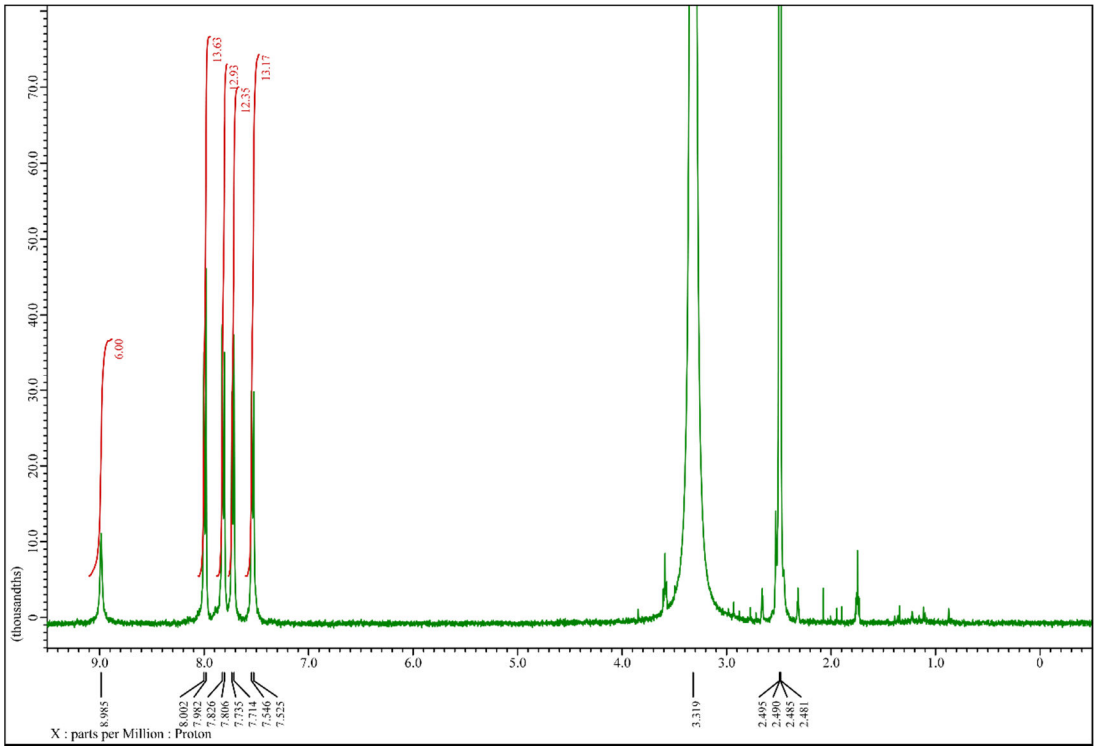

Fig. S59 ^{1}H NMR (400 MHz, DMSO-d_6) spectrum of **BPTp**.

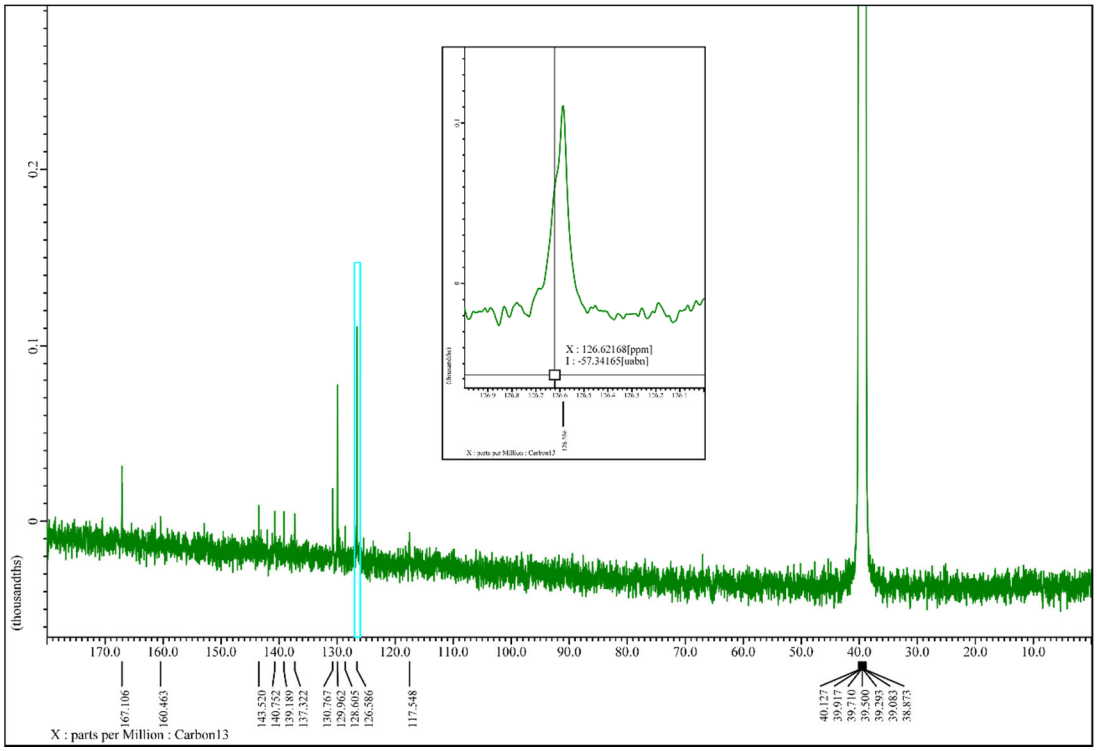

Fig. S60 ^{13}C NMR (100 MHz, DMSO-d_6) spectrum of **BPTp**.

8. References

S1. Rigaku Oxford Diffraction (2015), Software CrysAlisPro 1.171.38.41o. Rigaku Corporation, Tokyo, Japan.

S2. G. M. Sheldrick, *Acta Crystallogr. Sect. A*, 2015, **71**, 3–8.

S3. (a) Rigaku (2018). CrystalStructure. Version 4.3. Rigaku Corporation, Tokyo, Japan. (b) O. V. Dolomanov, L. J. Bourhis, R. J. Gildea, J. A. K. Howard and H. Puschmann, H. *J. Appl. Cryst*., 2009, **42**, 339–341. (c) L. J. Bourhis, O. V. Dolomanov, R. J. Gildea, J. A. K. Howard and H. Puschmann, *Acta Crystallogr*. *Sect. A*, 2015, **71**, 59–75.

S4. G. M. Sheldrick, *Acta Crystallogr. C*, 2015, **71**, 3–8.

S5. (a) P. v. d. Sluis and A. L. Spek, *Acta Crystallogr. Sect. A*, 1990, **46**, 194. (b) A. L. Spek, *Acta Crystallogr. Sect. D*, 2009, **65**, 148–155.

S6. T.-T.-T. Nguyen, D. Türp, D. Wang, B. Nölscher, F. Laquai and K. Müllen, *J. Am. Chem. Soc.*, 2011, **133**, 11194–11204.

S7. I. Hisaki, N. Ikenaka, N. Tohnai and M. Miyata, *Chem. Commun*., 2016, **52**, 300–303.

S8. I. Hisaki, Y. Suzuki, E. Gomez, B. Cohen, N. Tohnai and A. Douhal, *Angew. Chem. Int. Ed.*, 2018, **47**, 1143–1146.

S9. Gaussian 09, Revision D.01, M. J. Frisch, G. W. Trucks, H. B. Schlegel, G. E. Scuseria, M. A. Robb, J. R. Cheeseman, G. Scalmani, V. Barone, G. A. Petersson, H. Nakatsuji, X. Li, M. Caricato, A. Marenich, J. Bloino, B. G. Janesko, R. Gomperts, B. Mennucci, H. P. Hratchian, J. V. Ortiz, A. F. Izmaylov, J. L. Sonnenberg, D. Williams-Young, F. Ding, F. Lipparini, F. Egidi, J. Goings, B. Peng, A. Petrone, T. Henderson, D. Ranasinghe, V. G. Zakrzewski, J. Gao, N. Rega, G. Zheng, W. Liang, M. Hada, M. Ehara, K. Toyota, R. Fukuda, J. Hasegawa, M. Ishida, T. Nakajima, Y. Honda, O. Kitao, H. Nakai, T. Vreven, K. Throssell, J. A. Montgomery, Jr., J. E. Peralta, F. Ogliaro, M. Bearpark, J. J. Heyd, E. Brothers, K. N. Kudin, V. N. Staroverov, T. Keith, R. Kobayashi, J. Normand, K. Raghavachari, A. Rendell, J. C. Burant, S. S. Iyengar, J. Tomasi, M. Cossi, J. M. Millam, M. Klene, C. Adamo, R. Cammi, J. W. Ochterski, R. L. Martin, K. Morokuma, O. Farkas, J. B. Foresman, and D. J. Fox, Gaussian, Inc., Wallingford CT, 2016.

S10. M. J. Abraham, T. Murtola, R. Schulz, S. P´all, J. C. Smith, B. Hess and E Lindahl, *SoftwareX*, 2015, **1**–**2**, 19–25.

S11. J. Wang, R. M. Wolf, J. W. Caldwell, P. A. Kollman and D. A. Case, *J. Comput. Chem.*, 2004, **25**, 1157–1174.

S12. C. I. Bayly, P. Cieplak, W. D. Cornell and P. A. Kollman, *J. Phys. Chem*., 1993, **97**, 10269–10280.

S13. U. Essmann, L. Perera, M. L. Berkowitz, T. Darden, H. Lee and L. G. Pedersen, *J. Chem. Phys.*, 1995, **103**, 8577–8593.

S14. D. van der Spoel and P. J. van Maaren, *J. Chem. Theory Comput*., 2006, **2**, 1–11.

S15. R. W. Hockney, S. P. Goel and J. Eastwood. *J. Comp. Phys.*, 1974, **14**, 148–158.

S16. G. Bussi, D. Donadio and M. Parrinello, *J. Chem. Phys.*, 2007, **126**, 014-101.

S17. H. J. C. Berendsen, J. P. M. Postma, W. F. van Gunsteren, A. DiNola and J. R. Haak, *J. Chem. Phys.*, 1984, **81**, 3684–3690.

S18. M. Parrinello and A. Rahman, *J. Appl. Phys.*, 1981, **52**, 7182–7190.

S19. B. Hess, H. Bekker, H. J. C. Berendsen and J. G. M. Fraaije, *J. Comput. Chem.*, 1997, **18**, 1463–1472.